PFG

Photogrammetrie Fernerkundung Geoinformation

Organ der Deutschen Gesellschaft für Photogrammetrie, Fernerkundung und Geoinformation (DGPF) e. V.

Jahrgang 2011, Heft 6

Hauptschriftleiter:
Prof. Dr.-Ing. Wolfgang Kresse

Schriftleiter:
Prof. Dr. rer.nat. Carsten Jürgens, Prof. Dr. rer.nat. Lutz Plümer, Privatdozent Dr. techn. Franz Rottensteiner und Dr.-Ing. Eckhardt Seyfert

E. Schweizerbart'sche Verlagsbuchhandlung
(Nägele u. Obermiller) Stuttgart 2011

Deutsche Gesellschaft für Photogrammetrie, Fernerkundung
und Geoinformation (DGPF) e.V.
Gegründet 1909

Die *Deutsche Gesellschaft für Photogrammetrie, Fernerkundung und Geoinformation* (DGPF) e.V. unterstützt als Mitglieds- bzw. Trägergesellschaft die folgenden Dachverbände:

International Society for Photogrammetry and Remote Sensing	Deutsche Arbeits-gemeinschaft für Mustererkennung e.V.	GeoUnion Alfred-Wegener-Stiftung

Herausgeber:
© 2011 Deutsche Gesellschaft für Photogrammetrie, Fernerkundung und Geoinformation (DGPF) e.V.
Präsidentin: Prof. Dr. Cornelia Gläßer, Martin-Luther-Universität Halle-Wittenberg, Institut für Geowissenschaften, Von-Seckendorff-Platz 4, D-06120 Halle, Tel.: +49(0)345 55-26020
Geschäftsstelle: Dr. Klaus-Ulrich Komp, c/o EFTAS Fernerkundung Technologietransfer GmbH, Oststraße 2–18, D-48145 Münster, e-mail: klaus.komp@eftas.com

Published by:
E. Schweizerbart'sche Verlagsbuchhandlung (Nägele u. Obermiller), Johannesstraße 3A,
D-70176 Stuttgart. Tel.: 0711 351456-0, Fax: 0711 351456-99, e-mail: mail@schweizerbart.de
Internet: http://www.schweizerbart.de
♾ Gedruckt auf alterungsbeständigem Papier nach ISO 9706-1994

ISSN 1432-8364

Science Citation Index Expanded (also known as SciSearch®) Journal Citation Reports/Science Edition
Hauptschriftleiter: Prof. Dr.-Ing. Wolfgang Kresse, Hochschule Neubrandenburg, Fachbereich Landschaftsarchitektur, Geoinformatik, Geodäsie und Bauingenieurwesen, Brodaer Straße 2, D-17033 Neubrandenburg, e-mail: kresse@hs-nb.de
Schriftleiter: Prof. Dr. rer. nat. Carsten Jürgens, Ruhr-Universität Bochum, Geographisches Institut, Gebäude NA7/133, D-44780 Bochum, e-mail:carsten.juergens@rub.de, Prof. Dr. rer.nat. Lutz Plümer, Universität Bonn, Institut für Geodäsie und Geoinformation, Meckenheimer Allee 172, D-53115 Bonn, e-mail: pluemer@igg.uni-bonn.de, Privatdozent Dr. techn. Franz Rottensteiner, Leibniz Universität Hannover, Institut für Photogrammetrie und GeoInformation, Nienburger Straße 1, D-30167 Hannover, e-mail: rottensteiner@ipi.uni-hannover.de und Dr.-Ing. Eckhardt Seyfert, Landesvermessung und Geobasisinformation Brandenburg, Heinrich-Mann-Allee 103, D-14473 Potsdam, e-mail: eckhardt.seyfert@geobasis-bb.de

Erscheinungsweise: 6 Hefte pro Jahrgang.
Bezugspreis im Abonnement: € 198,– pro Jahrgang. Mitglieder der DGPF erhalten die Zeitschrift kostenlos. Der Online-Zugang ist im regulären Subskriptionspreis enthalten.

Anzeigenverwaltung: E. Schweizerbart'sche Verlagsbuchhandlung (Nägele u. Obermiller), Johannesstraße 3A, D-70176 Stuttgart, Tel.: 0711 351456-0; Fax: 0711 351456-99.
e-mail: mail@schweizerbart.de, Internet: http://www.schweizerbart.de
Bernhard Harzer Verlag GmbH, Westmarkstraße 59/59a, D-76227 Karlsruhe, Tel.: 0721 944020, Fax: 0721 9440230, e-mail: Info@harzer.de, Internet: www.harzer.de
Printed in Germany by Tutte Druckerei GmbH, D-94121 Salzweg bei Passau

PFG – Jahrgang 2011, Heft 6
Inhaltsverzeichnis

Originalbeiträge

Beiträge aus Wissenschaft und Praxis

Mitteilungen

Zusammenfassungen der „Originalbeiträge“ und der Beiträge „Aus Wissenschaft und Technik“ (deutsch und englisch) sind auch verfügbar unter www.dgpf.de/neu/pfg/ausgaben.htm

PFG 2011 / 6, 0405–0420
Stuttgart, December 2011

Article

Towards a National 3D Spatial Data Infrastructure: Case of The Netherlands

Jantien Stoter, Delft/Apeldoorn/Amersfoort, George Vosselman, Enschede, Joris Goos, Rotterdam, Sisi Zlatanova, Edward Verbree, Delft, Rick Klooster, Apeldoorn & Marcel Reuvers, Amersfoort

Keywords: national 3D standard, 3D GIS, 3D SDI, CityGML

Summary: This paper presents a research project in The Netherlands in which a large number of stakeholders collaborated on a 3D test bed, use cases and a test area to push ahead 3D developments and applications in The Netherlands. The pilot has realised a proof of concept for a 3D Spatial Data Infrastructure that addresses issues ranging from 3D data acquisition, definition of a 3D standard, maintenance of 3D data and use of the 3D data in specific applications. An important result is the 3D standard NL, compatible with international (i. e. CityGML) and national standards on 2D and 3D geo-information. The major contribution of this research is that the main building blocks of a 3D SDI (needs, data, test bed and standards) are studied in coherence to ultimately realise a shared approach to 3D for a whole country.

Zusammenfassung: *Auf dem Weg zu einer 3D-Geodateninfrastruktur: Der Niederländische Ansatz.* Dieser Artikel stellt ein Forschungsprojekt aus den Niederlanden vor, bei dem sich eine große Zahl von interessierten Gruppen zusammengefunden hat, um über ein 3D-Testbed, viele Anwendungsfälle und ein gemeinsames Testgebiet die Untersuchungen zu 3D-Geodaten und den darauf aufbauenden Anwendungen voranzutreiben. Das Projekt hat die Machbarkeit einer 3D-Geodateninfrastruktur nachgewiesen und dabei die 3D-Datenerfassung, die Definition von 3D Normen und Standards, Fortführung von 3D-Daten und Nutzung von 3D-Daten in unterschiedlichen Anwendungen untersucht. Ein wichtiges Ergebnis war die 3D-Norm-NL, die auf internationalen, d. h. konkret CityGML, und nationalen Normen und Standards für die 2D- und 3D-Geoinformation aufbaut. Der überragende Beitrag des Forschungsprojekts ist aber die gleichzeitige Analyse der wichtigsten Bausteine einer 3D Geodateninfrastruktur, nämlich Anforderungen, Datengrundlage, Testbed sowie Normen und Standards, um auf dieser Grundlage später die 3D-Geodaten für einen ganzen Staat aufzubauen.

1 Introduction

In the past ten years technologies for creating and managing 3D geo-information have matured while costs of generating 3D geo-information have significantly been reduced. Yet many (governmental) organisations hesitate to introduce 3D into their everyday processes. This is partly because there is no common approach for 3D geo-information and partly because knowledge of 3D technologies is still very scarce and not easily accessible to newcomers. Much relevant knowledge is only available at data providers and software vendors level which make it difficult to get an independent advice. On the other hand, the demand is not always clear which makes it hard for data providers and software vendors to offer demand-oriented products and services.

Despite the slow progress of 3D in practice, it is clear that 3D applications are important and will become even more important in the near future. The world is 3D and consequently a 3D approach has better potentials for managing and planning public spaces (for example

DOI: 10.1127/1432-8364/2011/0094 1432-8364/11/0094 $ 4.00

underground and aboveground data can be integrated). Also a 3D approach allows better environmental predictions such as flood-, air- and noise-simulations (see STOTER et al. 2008). Therefore, the Kadaster (Dutch national cadastre and mapping agency), Geonovum (the National Spatial Data Infrastructure executive committee in The Netherlands which develops and manages the geo-standards), the Netherlands Geodetic Commission (initiates fundamental and strategic research in geodesy and geo-information in The Netherlands) and the Dutch Ministry of Infrastructure and Environment initiated a pilot to advance the use of 3D in The Netherlands. In this pilot (run between March 2010 and June 2011), more than 65 private, public and scientific organisations collaborated to analyse and push ahead 3D developments in The Netherlands.

Being an absolute necessity to realise such a push-ahead, a 3D standard NL based on contributions from many different 3D experts and stakeholders was established. For this purpose use cases were defined and executed on a 3D test bed. In addition large amounts of test data were made freely available for all participants in the pilot. Finally the established Dutch 2D standardisation framework was studied for extension into 3D while aligning to the international OGC CityGML standard, driven by experiences of the use cases and the test bed.

The establishment of a national standard for 3D geo-information can be considered as one of the main results of the pilot. However, the ultimate aim was to realise a proof of concept for a 3D Spatial Data Infrastructure (SDI) by studying the main building blocks of a 3D SDI (needs, data, information architecture and standards) in coherence, to define a common 3D approach for a whole country. This is the topic of this paper. The technical details of the development of the national 3D standard are reported in VAN DEN BRINK et al. (2011). It should be noted that the research did not focus on the individual techniques for generating, handling and exchanging 3D data, which has received considerable attention in past research.

A proof of concept (POC) for a national 3D SDI may be seen as a solution limited to one specific country. However, the process that established this POC, which includes a national 3D standard extending CityGML, contains many generalities which are of interest for other countries. In particular, because experiments on CityGML extensions and on the integration with existing 2D data sets are new. Therefore, other countries can learn from the process that led to the proof of concept of the 3D SDI as described in this paper.

This paper is organised as follows. The methodology of the research is described in section 2. Section 3 summarises the main findings and conclusions per Work Package. Section 4 closes with the main findings and conclusions and formulates recommendations to further push ahead 3D developments in practice.

2 Methodology of 3D Pilot NL

The pilot had quite ambitious goals: The creation of a test bed based on use cases related to a predefined test area in order to find consensus on a 3D standard NL which should lead to a breakthrough in 3D. This required a 3D standard NL that optimally relates provided 3D information and technology to the demand. Therefore, well-defined 3D requirements were needed from the start. However, (new) users may not be aware of all potentials of 3D techniques. Therefore, they may be better capable of formulating their requirements when 'confronted' with the technical possibilities during the research process. This has been a guiding principle of the methodology of the 3D pilot, which is further described in this section.

The motivation to establish a 3D standard NL in a pilot setting is twofold. Firstly, a testing environment was required to structure the knowledge in the wide domain of 3D and to show to new users the potentials of 3D techniques. This was driven by the notion that 3D techniques are more developed than currently applied in practice. Secondly, establishing a 3D standard NL requires wide support of many stakeholders. The involvement of those stakeholders in the development process of the standard within a pilot setting would be essential to obtain this support.

In January 2010 more than 45 organisations responded to the call for participation. Because the pilot received a lot of attention during its course, the number of participating organisations grew to about 65 (the list of participants is available at GEONOVUM 2011e). Those organisations consisting of (large) municipalities, provinces, universities, main GIS and DBMS vendors, 3D data suppliers, engineering companies etc. have played a major role in the pilot. The 3D pilot participants are not limited to The Netherlands, e. g. there are participants from Germany and Belgium. In addition several organisations work beyond the Dutch borders and included their international counterparts. Also, the (interim) results of the pilot have been discussed at various international workshops. See for example STOTER et al. (2010a), VERBREE et al. (2010), and STOTER et al. (2011).

In order to realise the pilot objectives with so many contributing organisations four related work packages (WPs) were defined, each one equipped with its own WP leader (see Fig. 1). In this way all participants could contribute their expertise while pursuing their individual interests and, at the same time, jointly realising the aims of the pilot. An optimal alignment of the participants' interests was also driven by the fact that no budget was available for individual contributions. Intermediate results were exchanged and aligned during plenary sessions which were organised every six to seven weeks.

The four WPs that have run in parallel and in an integrated manner are:

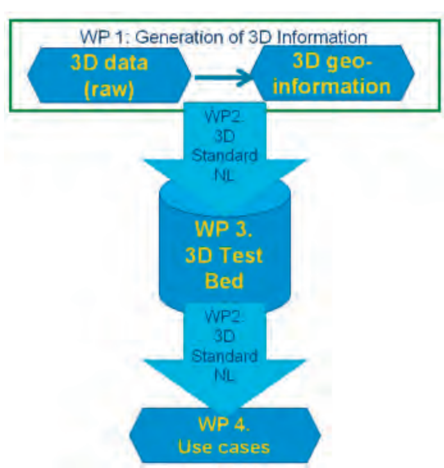

Fig. 1: Overview of the four work packages in the 3D pilot.

WP 1. Generation of 3D Information

Being the purpose of this WP, an inventory of the available 3D data as well as techniques for (automatically) generating 3D information from different sources such as 2D underground and aboveground data, laser point clouds, airborne and terrestrial measurements and 3D models created for construction applications (CAD/AEC/IFC) was created. This inventory would allow newcomers to learn what data is already available as well as how much it takes to build a 3D dataset conformant to the standard with available techniques. Furthermore, this activity made all test data on the selected test area (*Kop van Zuid, Rotterdam*) available for the other WPs.

WP 2. 3D Standard NL

The aim of the WP "3D standard NL" was the development of the national standard on 3D geo-information driven by the findings of the other WPs and also by aligning to both national and international standards. The international standards of interest are both CAD and GIS standards. The national standards of interest are the domain information models defined by the Dutch model of base geo-information (NEN3610), for example IMRO (spatial planning), IMKL (cables and pipelines), IMBOD/IMBRO (soil and subsoil), IMWA (water), TOP10NL (mid and small scale topography) and IMGeo (large scale topography), see (STOTER et al. 2010b, GEONOVUM 2011a).

WP 3. 3D Test Bed

The goal of the test bed was to provide a testing environment for conducting experiments with 3D technologies to all participants and to disseminate the experiences of the test bed within the pilot. Ultimately, the experience of the test bed should provide insight into what works, what is missing and what developments are still needed to implement 3D geo-information architectures.

WP 4. Use Cases

The core of the 3D pilot was the requirements analysis of 3D geo-information and corresponding techniques by specifying and executing use cases. This has been done in close consultation with 3D data providers (WP 1) and the 3D test bed (WP 3). The experiences of the use cases were used to further develop the 3D standard (WP 2).

3 Main findings of the work packages

This section summarises the main findings per WP.

3.1 *Generation of 3D Information*

Many data suppliers have provided their (often specifically for the pilot acquired) 2D and 3D data of the test area '*Kop van Zuid*' in Rotterdam. Examples are: 2D topographical data at scale 1:500 and 1:10k, 3D geological data of the subsurface (voxels of 100 m x 100 m x 0.5 m), two high density laser point datasets (the Height Model of The Netherlands, called *Actueel Hoogtebestand Nederland* (AHN2), with a point density of 10 pts per m^2 and a dataset with 30 pts per m^2, acquired by Fugro for the Municipality of Rotterdam), a 2.5D large scale topographical dataset contributed by Rijkswaterstaat, Cyclomedia orthophotos and panoramic imagery, high resolution point data of terrestrial laser scanners integrated with panoramic photographs (Topcon Sokkia), pan-

All 3D pilot test data integrated in one environment, by Bentley

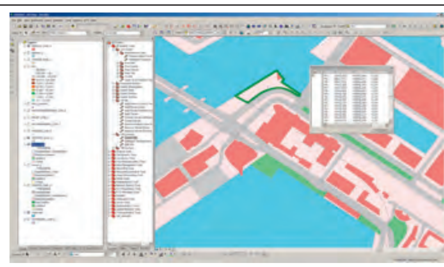

Assigning z-values to TOP10NL vertices by Kadaster

3D City model from laser point data, by IT-Pro-People (with Bentley software Terra Solid)

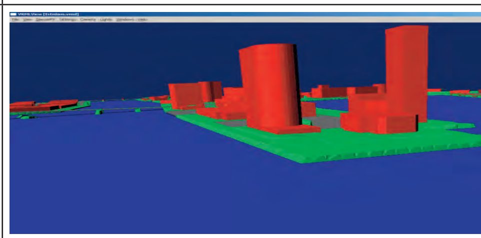

3D TOP10NL as integration of TOP10NL and laser point data, by ITC U Twente (Oude Elberink & Vosselman 2009)

CityGML buildings and trees by iDelft and Alterra

CityGML-LOD2 including trees by Toposcopie

Fig. 2: Examples of further processed data in the 3D pilot.

oramic video (Horus Surround Vision), recordings by Imagem etc.

These input datasets formed a rich starting point for 3D modelling activities of the test area. Several pilot participants have further processed these data in different types of 3D models. Some examples are shown in Fig. 2.

The main findings of this WP on 3D information generation can be summarised as follows:

- The 2D and 3D source data already available in The Netherlands in combination with data that can be obtained by additional acquisition offer rich potentials for building 3D geo-information.
- Currently no successful techniques exist for a fully automated generation of 3D information, other than using existing (2D) data and their semantics. It is expected that along with the establishment of a 3D standard the domain of 3D geo-information generation will change because people will stronger focus on the generation of 3D information.
- Laser scanning is a fast emerging technology, which contains a lot of potentials for building detailed 3D models (either in combination with existing 2D data sets or as an individual approach).
- The generation of relatively simple 3D models from 2D core spatial databases is the best starting point because of four technical reasons:
  - o connection to existing datasets means connecting to existing application domains which provides a justification for the 3D information
  - o existing datasets often contain rich semantics, which is difficult to obtain from automated acquisition techniques
  - o existing datasets contain information about objects that increases the possibilities to automatically generate 3D models
  - o the update process (or at least the update information) of existing datasets can be used for updating the 3D datasets
- From the perspective of a governmental organisation, the positioning of 3D geo-information in the organisation is not easy. The following guidelines may help:
  - o seek contact with application domains
  - o base the generation of 3D information on the intended uses which should also dictate the quality required (detailing, classification, semantics, geometry)
  - o find a balance between acquisition of new data and use of existing datasets
  - o acknowledge the file formats existing in the various application fields and realise interoperability through specific exchange formats
  - o the need for a standard exchange format is evident and makes multiple use of single-acquired 3D information possible

Tab. 1: Comparison of 3D standards in CAD and GIS domains.

Standard/Criterion	DXF	SHP	VRML	X3D	KML	Collada	IFC	CityGML	3D PDF
Geometry	++	+	++	++	+	++	++	+	++
Topology	-	-	0	0	-	+	+	+	-
Texture	-	-	++	++	0	++	-	+	+
LOD	-	-	+	+	-	-	-	+	-
Objects	0	+	+	+	-	-	+	+	+
Semantic	+	+	0	0	0	0	++	++	+
Attributes	-	+	0	0	0	-	+	+	+
XML based	-	-	-	+	-	-	+	+	-
Web	-	-	+	++	++	+	-	+	0
Georef.	+	+	-	+	+	-	-	+	+
Acceptance	++	++	++	0	++	+	0	+	++

- not supported; 0 basic; + supported; ++ extended support

3.2 *3D Standard NL*

The need for a 3D geo-information standard was evident throughout the whole pilot. This standard should align to available national and international 3D standards. After a comparison of the main 3D CAD and GIS standards (DXF, SHP, VRML, X3D, KML, Collada, IFC, CityGML and 3D PDF) the OGC standard CityGML (OGC 2008) proved to be the best starting point for a national standard on 3D geo-information, see Table 1.

CityGML provides the best support in terms of semantics, objects, attributes, georeferencing and operation via the Web. The OGC standard CityGML originated from the academia in Germany (University of Bonn, Technical University Berlin) and is often seen as an exchange format. But CityGML is also – and in particular – an information model for representing 3D spatial objects. CityGML distinguishes between thematic concepts, e. g. buildings, vegetation, water, land use, etc., at the geometric and at the semantic level. This conceptual model regards the features on every level of detail (LOD). A building object can vary from a simple block model (LOD1), a model including roof shapes (LOD2), a model

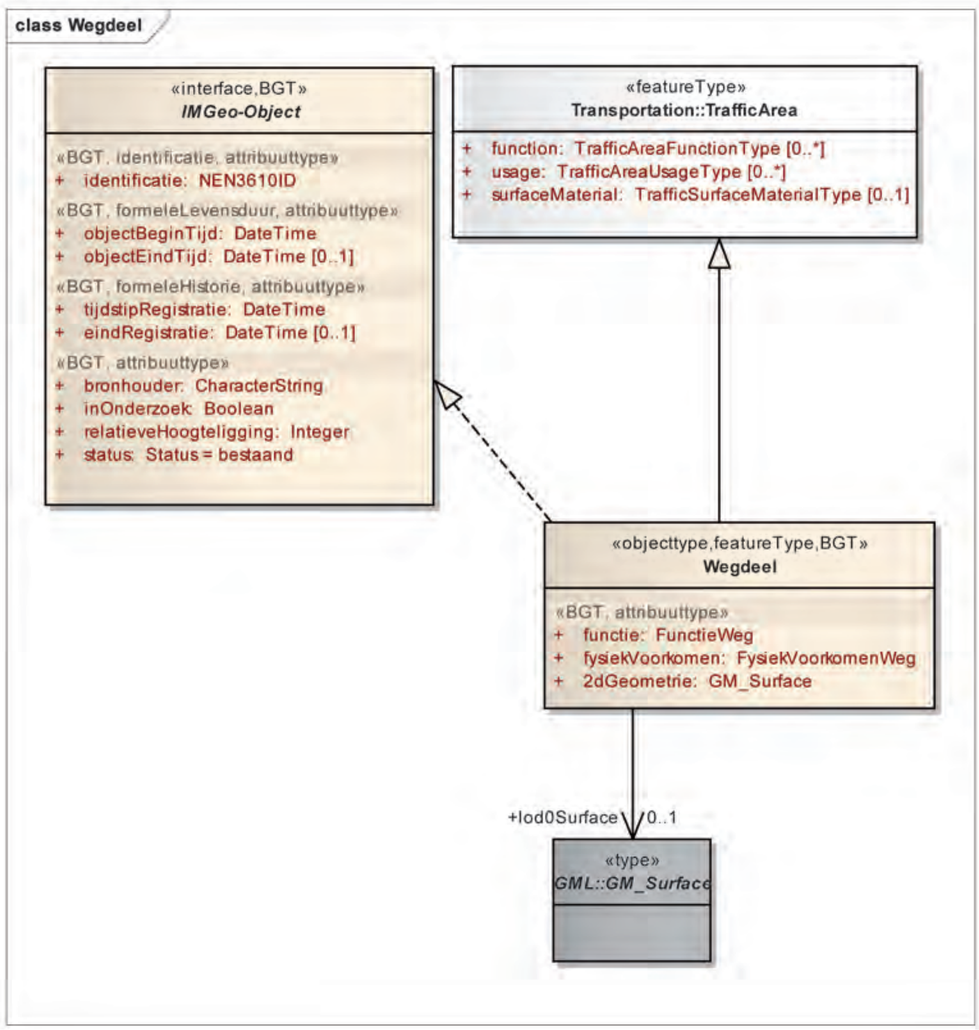

Fig. 3: Example – IMGeo modelling of *Wegdeel* as subclass of CityGML-TrafficArea (Van den Brink et al. 2011).

including windows, doors and other exterior features (LOD3) to a fully detailed interior model (LOD4) with or without texture information.

At the beginning of the pilot, participants were reluctant to use the CityGML standard. It was claimed that the standard would be too generic, that it does not contain detailed object definitions and that it does not support complex geometries supported in the CAD domain. Other problems are the focus on above ground objects, ambiguity about the LOD definitions (geometry- or semantic-based), the lack of relationship between the different LOD-representations and the lack of rules that ensure valid 3D geometry. Moreover, commercial systems had limited support for CityGML although this support improved during the pilot.

However, after a year of running the 3D pilot it became clear that, despite of these shortcomings, the connection to this standard ensures interoperability: that is, when Dutch geo-information is encoded in CityGML, this data is available to CityGML compliant clients.

Following the decision to use CityGML as a base for the standardisation of 3D geo-information in The Netherlands, the next step of this WP was to establish a CityGML implementation profile for The Netherlands. The realisation of this profile first focused on the Dutch Information Model on large scale Geo-information (IMGeo), since this model resembles CityGML the most. The main principle of the profile is the reuse of CityGML concepts as much as possible. Therefore, the agreements laid down in IMGeo were encoded in CityGML and additional classes, attributes, and attribute values were added if needed. See Fig. 3 for an example of the class *Wegdeel* (i. e. Road Parts; road segments that constitute a road*)*. IMGeo *Wegdeel* class is modelled as a specialisation of the CityGML class TrafficArea, thereby inheriting its properties. The generic attributes of IMGeo are modeled via the stereotype <<interface>>, to avoid multiple inheritance. The stereotype <<BGT>> indicates the parts that are part of the legally established authentic registry of large scale geo-information (*Basisregistratie Grootschalige Topografie, BGT*). As can be seen, the only part which is not mandatory is Wegdeel.lod0Surface. The attribute Wegdeel.functie is equivalent to TrafficArea.function; the attribute Wegdeel.fysiekVoorkomen is equivalent to TrafficArea.surfaceMaterial. Further details of the CityGML implementation profile are described in (Van den Brink et al. 2011).

The CityGML implementation profile also contains further agreements of how to use CityGML for the Dutch context. These agreements solved most of the above mentioned shortcomings of CityGML (e. g. the lack of a precise LOD-definition and the lack of rules for the object definition). The model is designed in such a way that it supports both the

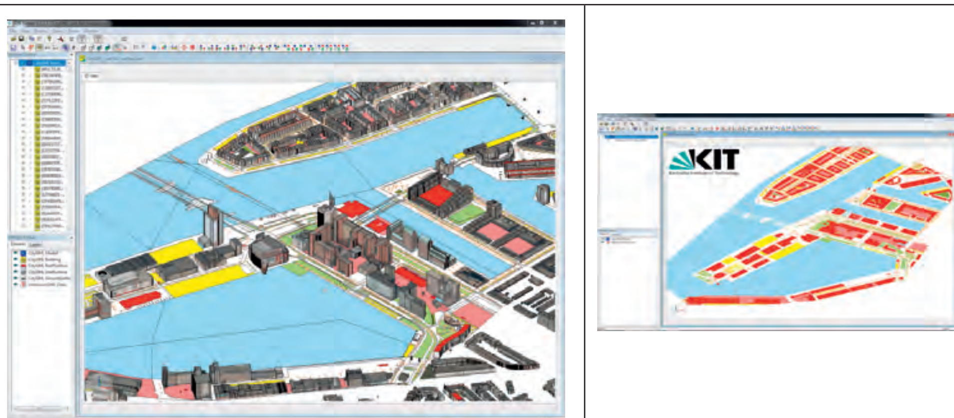

a b

Fig. 4: Visualisation of CityGML-IMGeo encoded data: LOD2 (a) and 2D LOD (b).

'2D LOD' (a term that we have introduced for the integrated model) as well as the different LODs of CityGML. In May 2011 the proposed approach has officially been approved for the information model for large scale topography in The Netherlands. This close integration between an existing information model for 2D geo-information and CityGML is a major step for the use of 3D information and a unique achievement for standardisation in 3D.

To test the CityGML-IMGeo implementation profile IMGeo data and laser point data were combined to generate CityGML-IMGeo encoded data of the pilot test area. The result is shown in Fig. 4.

During the establishment of the model and sequential testing, deficiencies were identified both for IMGeo and CityGML which were used to formulate Change Requests (CRs) for both models. Examples of CRs for CityGML (submitted in August 2011) required to model every class at least in LOD0 (in current CityGML some classes only start at LOD1 such as Building, CityFurniture, TrafficArea) and to distinguish between function and physical appearance of Land Use (the current codes for 'function' is a mixture of both) (Van den Brink et al. 2011). Also a proposal for support of voxels in CityGML is under study based on the experiences of the 3D pilot. This proposal builds on the works of Tegtmeier et al. (2009) and Zobl & Marschallinger (2008).

Besides the IMGeo specific aspects, CityGML-IMGeo contains generic aspects that can be reused for extending other Dutch domain models into 3D when appropriate. To get a feeling for the possibilities, the WP 3D standard NL finally carried out a study regarding the matching of the concepts of the other Dutch domain models with CityGML. For this matching also several Application Domain Extensions (ADE) were considered, such as the extensions for Utility Network, Tunnel and Bridge. In the future, the planned ADE for cables and pipelines may be relevant (Becker 2010, Hijazi 2010).

3.3 *The 3D Test Bed*

The 3D test bed examined the techniques to support 3D information in general and CityGML in particular, based on the data made available by the participants of the Rotterdam test area. The Section GIS technology of the TU Delft implemented a specially designed test bed environment which could be used by all participants. Apart from a file-based data server for the test data, the test bed offered a DBMS implementation, i. e. the 3DCityDB. This database is an open source 3D geo-database, developed by the TU Berlin, that implements the CityGML data model in a relational database (Oracle Spatial 11g in our case) (TU Berlin 2011). The database was (and is still) available for all pilot participants to upload, validate and export CityGML data.

The feedback of the test bed experiences to the participants during the 3D pilot led to a better understanding of CityGML, as did the free CityGML course that this WP offered in March 2011 (recorded and available at (TU Delft 2011)). Therefore, the use of the 3DCityDB increased during the 3D pilot, which was also stimulated by better CityGML support by systems provided by companies such as Bentley, Esri and Intergraph.

The experiences of the test bed confirmed that a free interpretation of the use of CityGML LODs for both geometric and semantic level is possible and that the 3D standard NL should therefore make further arrangements in a CityGML implementation profile for the Dutch context. The WP 3D standard NL has taken over this suggestion, as described above.

Because CityGML does not directly enforce the validity of the 3D geometries, the test bed also studied a geometric validation tool (developed by the TU Delft) and the validation possibilities of Oracle Spatial. The tools check whether a 3D object is valid. This means that the faces of a volume do not intersect, the volume is waterproof (no openings) etc. (Ledoux et al. 2009).

Another important activity of the WP 3D test bed was the study of methods to generate CityGML encoded data (see also examples in Fig. 2). The experience with the 3D test bed showed that CityGML is increasingly supported in commercial software. This support allows to generate and export CityGML data. Several different approaches were demonstrated by the companies participating in the pilot. For example, Bentley Map is able to export CityGML files via an FME-based interoperability component, and recently a specific mapping of CityGML to Bentley XML Feature Modelling scheme has become available. With this scheme it is possible to build semantically and geometrically valid 3D CityGML objects from scratch and to manipulate them afterwards.

Another method for generating CityGML encoded data of buildings was the extrusion of 2D building "footprints" based on a height attribute of the LOD1 objects. A good example of this approach is the 3D data conversion tool from the company iDelft that was developed during the pilot. Other examples include ArcGIS and Toposcopie that offer tools to generate 3D building block models by a combination of 2D topography (large or midscale) and point clouds from laserscan data or photogrammetry. If the footprints of the buildings connect, it is also possible to generate topologically correct CityGML LOD1 data according to the method described in (Meijers & Ledoux 2011).

Most roof types for LOD2 data could be generated (semi-) automatically from laser point data by matching laser points with predefined roof shapes (see Fig. 2, example lower left by iDelft and Alterra) or by applying surveying methods combined with images (Toposcopie). A fully automatic generation of any LOD2 and LOD3 building objects from point clouds was not shown in the test bed for two reasons: The many complex roofs require internal lines for a border-definition. Those lines are not yet available. Combined buildings such as terraced houses require an a-priori object-definition to perform a correct processing of the laser data such as merge, split, and estimation.

Models of trees for LOD2 and LOD3 could also be derived from laser point data as done by Alterra, and ITC University of Twente (for examples see Fig. 2 and 5).

Another way demonstrated to generate CityGML data (manually) was the application of SketchUp (software for creating 3D models for use in Google Earth and other systems). This software has a plugin for CityGML, although this link is still not fully operational. The validation test on CityGML structure and scheme definitions usually happens when the CityGML data is imported into one of the available viewers, for example LandXplorer of FZK (Forschungszentrum Karlsruhe) (as in Fig. 4). If this visualisation looks good, then the CityGML data is deemed acceptable. Unfortunately, our tests have shown that CityGML viewers do not check for topologically and geometrically correct CityGML data. Such data is accepted and visualised though many of it was incorrect, for example some volumes were not waterproof, meaning that, the files sometimes had overlapping planes or gaps between objects that should connect to each other.

The 2.5D representations of CityGML (LOD0), i. e. Land Use objects were also tested. They can be generated through a constrained triangulation from laser points where the polygon boundaries are used as breaklines. In this way also the height variance within the polygon surfaces are represented.

3.4 *Use cases*

The use case studies were important in the 3D pilot: What applications need 3D information? Which 3D information is needed? What is the state-of-the-art of 3D techniques in relation to 3D needs? In order to answer these questions, six use cases were defined and executed in this WP. These are:

- 3D cadastre: recording of property items located above each other (see also Stoter & Ploeger 2003, Stoter & Salzmann 2003, Stoter & Oosterom 2005),
- generation, maintenance and distribution of 3D topography,
- applying voxel data for GIS analyses,
  - integration of voxels (3D grids) with 3D objects,
  - integration of surface and subsurface data,
- 3D data integration in construction processes: How to use design data (IFC/CAD/Collada) in GIS applications and how to use 3D geo-information in building information models (BIM)?
- 3D for spatial planning: generating 3D virtual environments based on architectural models for communication with citizens,
- 3D change detection (see also Vosselman et al. 2005).

Several 3D pilot participants have experimented with the use cases, see Fig. 5. To make the use cases easily available for the wide public, demos of the use cases are published on YouTube (see GEONOVUM 2011b).

Experience with the use cases confirmed that lacking knowledge about generating and using 3D data and techniques is often a bigger problem for 3D applications than the lack of technology itself. Technical problems did oc-

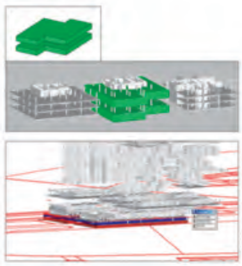	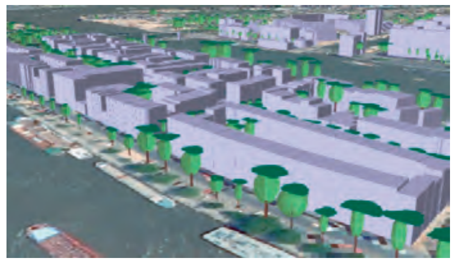
3D Kadaster (Dutch Kadaster and Bentley)	Tree model generated by Alterra for use case 3D topography
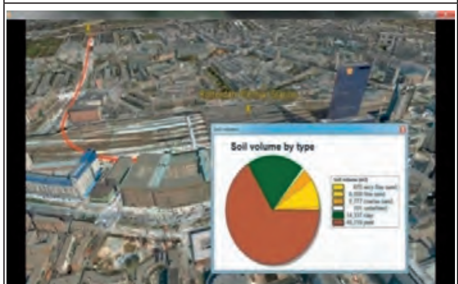	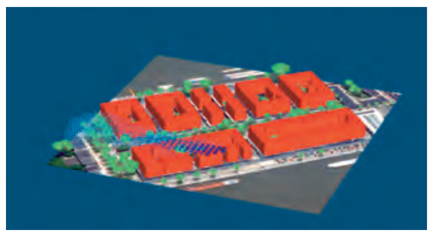
Calculation of soil volumes (voxels) at the location of a planned tunnel, by Esri and TNO	Realtime interactive airstream simulation with voxels, Alterra
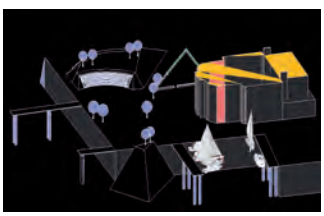	
Spatial planning objects in CityGML, Crotec	3D change detection, NEO BV
	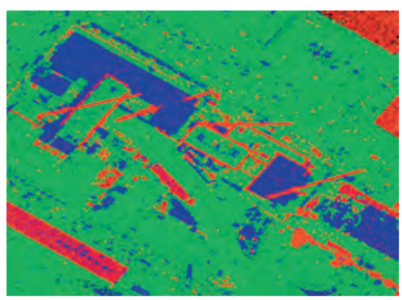
Integrating design models in virtual environments , Gemeente Apeldoorn	3D Change detection based on differences between two point clouds, U Twente

Fig. 5: Selection of the executed use cases.

cur during the exchange of 3D data between software, because not always the original information (geometry and semantics) was maintained. Thus, the importance of an exchange format for 3D geo-information again proved to be evident.

Many of the use cases addressed the conversion from BIM information to 3D geo-information and vice versa (not shown in Fig. 5). These conversions go beyond the technical conversions as studied in Berlo & De Laat (2010), Bormann (2010) and El-Mekawy (2010). Instead, the efforts were focussed on the semantic issues of the conversions: How do concepts from the BIM domain relate to concepts in the GIS domain? Which information is specific for the two domains? How can the relevant characteristics be preserved in the conversion? How shall differences in the conceptual models in both domains be dealt with? How shall the different geometries in both domains, i. e. simple geometries in GIS and complex, parameterized geometries in BIM, be dealt with? These questions extend the work of Isikdag & Zlatanova (2009).

The experiences of the use cases on the BIM/GIS topic reinforced the different characteristics between BIM and GIS data. The integration of both types of data via a common exchange format is beneficial because BIM data can feed GIS data and GIS can serve as a reference for BIM data. However, integration should acknowledge the differences between both types of data. To start with, the object description of BIM and GIS, e. g. CityGML LOD4, differs significantly. In addition, GIS is characterised by the coverage of large areas, e. g. a complete city, and lower precision, while BIM is characterised by its local and very detailed approach, a limited number of construction models usually available in a city and high precision necessary for reliable construction calculations. Assuming that original BIM files may serve specific applications in the future, it is important to maintain both the original BIM source file and the simplified CityGML representation of the BIM file (in the city model).

4. Conclusions, main findings and recommendations

The aim of the research project presented in this paper was the advancement of 3D developments in The Netherlands by studying and applying 3D technologies on use cases and using these experiences to establish a national 3D standard to support a 3D SDI. After a year of collaboration with many stakeholders it can be concluded that the objective is achieved. The 3D pilot has shown the added value of 3D and what it takes to exploit this value. A typical example is the integrated planning and management of space above and under the surface. The findings of the pilot have shown that it is no longer the question if, but how 3D in The Netherlands should be organised and implemented in a 3D SDI. These conclusions can be drawn from several main findings. These will be summarised in Section 4.1. Section 4.2 formulates recommendations that follow from these findings.

4.1 *Main findings of the 3D pilot*

3D is needed and feasible

The 3D pilot has accomplished a focus on 3D geo-information developments in The Netherlands. At the beginning of the 3D pilot a small group of experts was aware that 3D technology is further developed than currently used in practice. But specific knowledge on how 3D could be applied in common applications was lacking. The extensive exchange of 3D knowledge and experiences between a large number of participants resulted in the consciousness of the feasibility of 3D within a wide public. The field of 3D geo-information has therefore become tangible and manageable, which is important for further 3D developments. The changing perception of the standard CityGML over time may illustrate the strong increase of awareness. The 3D pilot participants considered this standard as exotic at the start; at the end of the pilot there was a widely supported 3D CityGML-IMGeo profile. Also it became clear that 3D geo-information not only belongs to the traditional field of geo-information. Instead it requires close cooperation with other disciplines such as planning, design, and construction management to make 3D feasible and use its added value.

3D standard NL is important and has been realised

According to another finding the lack of a 3D standard considerably inhibits the use and exchange of 3D geo-information. Therefore, formalised agreements on a standard such as CityGML are essential. Even if this standard is not being considered 100% optimal it equips governmental organisations with the kind of 3D geo-information that they can build upon. At the same time it provides private industry a stable platform for innovative developments. The pilot provided a suitable environment to formulate user specific requirements for a diverse group of users which eventually led to the CityGML-IMGeo standard. This standard solved some of the issues of the generic standard CityGML. Without the pilot it would have been much harder to establish such an extended 3D standard.

3D base dataset is required and feasible

The pilot has shown the need for a nationwide 3D base (or reference) dataset. This dataset is needed for referencing (new) 3D information in the virtual model of the world and for providing a basis for 3D planning and management of public space. Many large municipalities have 3D datasets, which unfortunately are often restricted to the territory of the city and available in different formats and resolutions. Currently, only Google Earth is available on a country-wide scale, but has a limited representation of subsurface features - among other restrictions such as an unknown update status and an undisclosed accuracy. The pilot achieved promising results for generating 3D topography to be used as such a reference dataset, i. e. by a combination of 2D IMGeo data with AHN2 (both soon available nationwide) a 3D topographic base dataset can be quite easily generated. Also, a combination of TOP10NL and AHN2 showed potentials to rapidly and efficiently build a nationwide 3D base dataset at midscale.

3D NL is organised

One of the main results of the 3D pilot is the generation of an informal network in The Netherlands. This is valuable because further 3D developments ask for wide support as well as for an integrated approach of various expertises. The network is active on Twitter and LinkedIn (more than 400 members) which makes it easy to exchange and publish specific and generic 3D achievements within the 3D network of The Netherlands. This networking environment has appeared to be very powerful.

The pilot approach was successful

The collaboration of a large number of participants without any financial compensation can be considered as a good indication of the success of the pilot. It was also valuable that companies with more or less the same, and therefore competing, “businesses” were willing to share their knowledge. A major reason for the strong commitment of the participants was the overall goal being beneficent for all participants: pushing ahead 3D developments in The Netherlands. The result-oriented approach led to a close connection with practitioners and to a stimulating and motivating environment for collaboration.

The 3D pilot also received national and international attention, e. g. OGC has awarded the 3D Pilot NL with the OGC 3D award in September 2010. This was partly due to the various national and international publications and presentations.

The lack of 3D knowledge is the severest bottleneck

The execution of the use cases showed that a lack of 3D knowledge is a bottleneck for applying 3D. This is true for governmental organisations because they suffer from a lack of knowledge in the new domain of 3D. In addition, the pilot showed that 3D has many different fields of expertise. Structuring the knowledge within the broad field of 3D has been important for a wide support of 3D in The Netherlands. The intensive knowledge exchange resulted in several small partnerships among pilot participants (sometimes behind the 3D pilot scenes). Those partners have evoked 3D innovations (such as a better support of CityGML in commercial GISs and improved automatic object construction options).

In line with this finding, the five final reports of the pilot (one for each WP and an additional executive summary, see GEONOVUM 2011c) specifically aimed at filling knowledge gaps within the wider public. The reports are intended both to inform outsiders about what has been achieved in the pilot, but also to make various aspects of 3D accessible for newcomers to the field of 3D. In addition the pilot closed with a national symposium on 3D at which the acquired knowledge was presented to a wide public (GEONOVUM 20011d).

Besides generating new knowledge and merging existing knowledge, the findings of the 3D pilot identified a number of issues for further research. Examples include further developments in automatic generation of 3D information, updating 3D datasets, and maintaining 3D information. However, 3D topology and validation of 3D geometry needs further research attention. More attention should be drawn to the kind of 3D spatial operations that should be implemented, and to the broader use of the 3D information. As mentioned above, most of the use cases were focussed on the integration of data.

4.2 *Recommendations*

An important next step is the search for further agreements about the way of implementing and organising 3D in The Netherlands. In line with the findings and conclusions, some recommendations have been formulated. On one hand they cover aspects that can be picked up by the initiators of the 3D pilot (Kadaster, Geonovum, Ministry of I&M and NCG). On the other hand, some topics need further investigation and therefore require a similar collaborative and experimental environment as the 3D pilot.

Recommendations for the initiators of the pilot to take over the results and findings are:

- The established 3D standard NL needs maintenance and further testing on usability and technical aspects. In addition, experience with 3D IMGeo should be used to extend also other domain models with a notion of 3D if appropriate.
- The extention of the existing national 2D large and midscale reference datasets towards 3D requires further attention. This covers both, the implementation of successful 3D pilot results into practice as well as a business case study for providing such a 3D reference dataset supporting the Dutch SDI.
- The commercial companies should be encouraged to provide importers/exporters for the 3D standard NL.
- The accomplished network is important for further 3D developments in The Netherlands. Therefore, the network should be maintained and further expanded by a continued facilitation of the 3D test bed, maintenance of the Twitter and LinkedIn environment and organisation of regular knowledge sessions (as was done during the pilot).

The issues that require further elaboration in a pilot environment were derived directly from the observation that relevant knowledge is often lacking at the relevant organisations and that this hinders 3D developments. Therefore, more knowledge is needed to let governmental organisations as well as data-, technology- and service-providers better direct their 3D developments. Sometimes, this includes existing knowledge that still requires structuring in a collaborative environment. Sometimes it involves (new) knowledge that needs to be built in an experimental setting.

For several aspects the 3D pilot has built new capacities and organised existing knowledge, e. g. regarding the generation, management and implementation of 3D geo-information. But the pilot also identified capacity gaps that require additional knowledge building. Some topics that need further research attention in a pilot setting are:

Successful 3D strategies for governmental organisations

The introduction of 3D in governmental organisations is relatively new. The study of successful (technical) 3D strategies based on "good practices" may support the introduction of 3D in those organisations. These strategies regard the generation, update and management of the 2.5D and 3D data. In addition, example specifications for outsourcing 3D geo-information generation may be helpful as well as (more) examples of added value of 3D in governmental processes.

Aligning to other disciplines
An important part of a successful 3D strategy is the technical alignment with other disciplines such as design-, construction- and facility management-domains. Insight is required on how to balance between strict agreements on one hand and sufficient flexibility in the separate domains on the other hand.

Organisational issues of 3D geo-information
It is obvious that 3D requires a specific organisational approach within a governmental organisation, but the way how this best can be achieved remains open. Defining and executing use cases for municipal tasks may provide guidance how to best organise a 3D information infrastructure in such an organisation. How can optimal collaboration be accomplished between disciplines such as geo-information, planning, design, management and BIM? Often the benefits of 3D occur in other departments than those where the bill has to be paid. This causes another obstacle for organisations which plan to introduce 3D. This uncertainty about costs-benefits may be an obstacle and thus requires organisational solutions that can be studied with the help of dedicated use cases.

A new project group is currently working on these topics in a next phase (planned for September 2011 till June 2012). More than 100 participants have subscribed. The new project group will further work on the results of the first phase to make them ready for use in practice. Addressing the still open 3D issues in a collaborative and experimental setting where expertise of universities, industries and governmental parties are brought together, offers the optimal conditions for 3D being actually picked up by practice, as it was shown by the 3D pilot presented in this paper.

Acknowledgements

This research is supported by the Dutch Technology Foundation STW, which is part of The Netherlands Organisation for Scientific Research (NWO) and by the Ministry of Economic Affairs, Agriculture and Innovation. (Project number: 11300).

References

Becker, T., Nagel, C. & Kolbe, T.H., 2010: Integrated 3D modeling of multi-utility networks and their interdependencies for critical infrastructure analysis. – 5th International 3D GeoInfo Conference, November **2010**, Berlin.

Berlo, L. & de Laat, R., 2010: Integration of BIM and GIS: The development of the CityGML GeoBIM extension. – 5th International 3D GeoInfo Conference, November **2010**, Berlin.

Borrmann, A., 2010: From GIS to BIM and back again – A Spatial Query Language for 3D building models and 3D city models. – 5th International 3D GeoInfo Conference, November **2010**, Berlin.

El-Mekawy, M.S., Östman, A. & Shahzad, K., 2010: Towards Interoperating CityGML and IFC Building Models: A Unified Model Based Approach. – 5th International 3D GeoInfo Conference, November **2010**, Berlin.

Geonovum, 2011a: www.geonovum.nl/geostandaarden/informatiemodellen (14.9.2011).

Geonovum, 2011b: Demonstrations of the 3D pilot use cases on Youtube. – www.youtube.com/user/GeoReport (14.9.2011).

Geonovum, 2011c: Final reports of 3D pilot. – www.geonovum.nl/dossiers/3dpilot/resultaten (14.9.2011).

Geonovum, 2011d: Report of the national 3D symposium, 16 June 2011. – www.geonovum.nl/dossiers/3dpilot/congres/english (14.9.2011).

Geonovum, 2011e: List of Participants 3D Pilot 2010/2011. – www.geonovum.nl/dossiers/3d/aanpak/deelnemers (14.9.2011).

Hijazi, I., Ehlers, M., Zlatanova, S., Becker, T. & van Berlo, L., 2010: Initial investigations for modeling interior Utilities within 3D Geo Context: Transforming IFC-interior utility to CityGML/UtilityNetworkADE. – 5th International 3D GeoInfo Conference, November **2010**, Berlin.

Isikdag, U. & Zlatanova, S., 2009: Towards defining a framework for automatic generation of buildings in CityGML using Building Information Models. – In: Lee, J. & Zlatanova, S. (eds.): 3D Geo-Information Sciences **2009:** 79–96, Springer.

Ledoux, H., Verbree, E. & Hang, Si, 2009: Geometric Validation of GML Solids with the Constrained Delaunay Tetrahedralization. – In: De Mayeer, Neutens & De Rijck (eds.): Proceedings of the 4th International Workshop on 3D Geo-Information, November **2009**: 143–148, Ghent.

LEDOUX, H. & MEIJERS, M., 2011: Topologically consistent 3D city models obtained by extrusion. – International Journal of Geographical Information Science **25** (4): 557–574, doi:10.1080/13658811003623277.

OUDE ELBERINK, S. & VOSSELMAN, G., 2009: 3D information extraction from laser point clouds covering complex road junctions. – The Photogrammetric Record **24** (125): 23–36.

OGC, 2008: OpenGIS® City Geography Markup Language (CityGML) Encoding Standard, version 1.0.0, document # 08-007r1. – http://portal.opengeospatial.org/files/?artifact_id=28802 (14.9.2011).

OGC, 2011: www.citygmlwiki.org/index.php/CityGML-ADEs.

STOTER, J.E. & SALZMANN, M., 2003: Towards a 3D cadastre: Where do cadastral needs and technical possibilities meet? – Computers, Environment and Urban Systems **27** (4): 395–410.

STOTER, J.E. & PLOEGER, H.D., 2003: Property in 3D registration of multiple use of space: current practice in Holland and the need for a 3D cadastre. – Computers, Environment and Urban Systems **26** (6): 553–570.

STOTER, J.E. & VAN OOSTEROM, P.J.M., 2005: Technological aspects of a full 3D cadastral registration. – International Journal of Geographical Information Science IJGIS **19** (6): 669–696.

STOTER, J.E., DE KLUIJVER, H. & KURAKULA, V., 2008: 3D noise mapping in urban areas. – International Journal of Geographical Information Science (IJGIS) **22** (8): 907–924.

STOTER, J.E., REUVERS, M., VOSSELMAN, G., GOOS, J., VAN BERLO, L., ZLATANOVA, S., VERBREE, E. & KLOOSTER, R., 2010a: Towards a 3D geo-information standard in The Netherlands. – 5th International 3D GeoInfo Conference, November **2010**, Berlin.

STOTER, J.E., VISSER, T., VAN OOSTEROM, P., QUAK, W. & BAKKER, N., 2010b: A semantic-rich multi-scale information model for topography. – International Journal of Geographical Information Science, iFirst: **2010**: 1–25, doi: 10.1080/13658816.2010.490218.

STOTER, J.E., VAN DEN BRINK, L., VOSSELMAN, G., GOOS, J., ZLATANOVA, S., VERBREE, E., KLOOSTER, R., VAN BERLO, L., VESTJENS, G., REUVERS, M. & THORN, S., 2011: A Generic approach for 3D in the Netherlands. – 6th International 3D GeoInfo Conference, June **2011**, Wuhan.

TEGTMEIER, W., ZLATANOVA, S., VAN OOSTEROM, P. & HACK, R., 2009: Information management in civil engineering infrastructural development: with focus on geological and geotechnical information. – In: KOLBE, T.H., ZHANG, H. & ZLATANOVA, S. (eds.): Proceedings of the ISPRS workshop, Volume **XXXVIII (**3–4/C3) July **2009**: 68–73, Vancouver.

TU DELFT, 2011: 100% CityGML course. 15 March 2011. – http://collegerama.tudelft.nl/mediasite/SilverlightPlayer/Default.aspx?peid=7b440617cd1342b0b5b006fc0f6563ef1d (14.9.2011).

TU BERLIN, 2011: http://opportunity.bv.tu-berlin.de/software/projects/3dcitydb (14.9.2011).

VERBREE, E., STOTER, J.E., ZLATANOVA, S., DE HAAN, G., REUVERS, M., VOSSELMAN, G., GOOS, J., VAN BERLO, L. & KLOOSTER, R., 2010: A 3D model for geo-information in the Netherlands. – In: MADDEN, M. & USERY, L. (eds.): Geospatial data and geovisualization: environment, security and society (1–5). Orlando, USA.

VOSSELMAN, G., KESSELS, P. & GORTE, B.G.H., 2005: The Utilisation of Airborne Laser Scanning for Three-Dimensional Mapping. – International Journal of Applied Earth Observation and Geoinformation **6** (3–4): 177–186.

ZOBL, F. & MARSCHALLINGER, R., 2008: Subsurface GeoBuilding Information Modelling GeoBIM, GEOinformatics **8** (11): 40–43.

VAN DEN BRINK, L., STOTER, J.E. & ZLATANOVA, S., 2011: Establishing a national 3D standard compliant to CityGML. – Submitted to International Journal of Geographical Information Science (August 2011).

Addresses of the authors:

Dr. JANTIEN E. STOTER, OTB Research Institute for the Built Environment, Delft University of Technology, Jaffalaan 9, 2628BX Delft, The Netherlands, e-mail: j.e.stoter@tudelft.nl & Kadaster, Product and Process Innovations, Postbus 9046, 7300 GH Apeldoorn, The Netherlands, jantien.stoter@kadaster.nl & Geonovum, Barchman Wuytierslaan 10, 3818 LH Amersfoort, The Netherlands, e-mail: j.stoter@geonovum.nl

Prof. dr. ir. GEORGE VOSSELMAN, Faculty of Geo-Information Science and Earth Observation (ITC), University of Twente, Postbus 217, 7500 AE Enschede, The Netherlands, e-mail: vosselman@itc.nl

Ir. JORIS GOOS, Department of Surveying, Public Works, City of Rotterdam, Galvanistraat 15, Europoint III 9th floor, 3029 AD Rotterdam, The Netherlands, e-mail: j.goos@rotterdam.nl

Dr.-Ing. SISI ZLATANOVA, OTB Research Institute for the Built Environment, Delft University of Technology, Jaffalaan 9, 2628BX Delft, The Netherlands, e-mail: s.zlatanova@tudelft.nl

Ir. E. Verbree, OTB Research Institute for the Built Environment, Delft University of Technology, Jaffalaan 9, 2628BX Delft, The Netherlands, e-mail: e.verbree@tudelft.nl

Ing. Rick Klooster, Municipality of Apeldoorn, Marktplein 1, 7311 MJ, Apeldoorn, The Netherlands, e-mail: r.klooster@apeldoorn.nl

Ing. Marcel Reuvers, Geonovum, Barchman Wuytierslaan 10, 3818 LH Amersfoort, The Netherlands, e-mail: m.reuvers@geonovum.nl

Manuskript eingereicht: Juli 2011
Angenommen: August 2011

PFG 2011 / 6, 0421 – 0434
Stuttgart, December 2011

Article

Antarctic Coastline Detection using Snakes[1]

Tobias Klinger, Marcel Ziems, Christian Heipke, Hannover; Hans Werner Schenke & Norbert Ott, Bremerhaven

Keywords: Automation, snakes (active contours), coastline, Antarctica, classification, model selection

Summary: In this paper we present an approach for automatic coastline detection from images based on snakes (parametric active contours) and apply it to Landsat images from Antarctica. Snakes require the definition of an energy functional that reflects the underlying coastline model. For Antarctica the coastline appearance in the images is heterogeneous. Therefore, it is not possible to use a single model only. After inspecting the images to be used we formulate three different transition models that match a large part of the Antarctic coastline: (a) from ice shelf to water, (b) from ice shelf to sea ice and (c) from rocky terrain to water. For each of the three models the energy terms are optimised based on the radiometric properties of the adjacent regions as well as the curvature and the potential change-rate of the coastline itself. A supervised classification for the three classes *ice*, *water* and *rocky terrain* controls the whole process by selecting the most applicable model for a given image region along the coastline. We present results for the extraction of approximately 12 % of the Antarctic coastline from an up-to-date Landsat mosaic.

Zusammenfassung: *Küstenliniendetektion in der Antarktis mit Hilfe von Snakes*. In diesem Artikel präsentieren wir einen Ansatz zur automatischen Erfassung von Küstenlinien mit Hilfe von Snakes (parametrische aktive Konturen) und verwenden diesen für die Detektion der Antarktischen Küstenlinie in Landsat-Bildern. Snakes erfordern die Definition eines Energiefunktionals, welches das zugrunde liegende Küstenlinienmodell beschreibt. In der Antarktis ist die Erscheinung der Küstenlinie in optischen Bildern inhomogen. Daher ist es nicht hinreichend, mit einem einzelnen Modell zu arbeiten. Wir formulieren drei verschiedene Übergangsmodelle, die einen großen Teil der Antarktisküste abdecken: (a) von Schelfeis zu Wasser, (b) von Schelfeis zu Meereis und (c) von felsigem Gelände zu Wasser. Für jedes dieser Modelle optimieren wir die Energieterme auf Grundlage der speziellen radiometrischen Eigenschaften im Bereich der Küstenlinie sowie deren jeweils zu erwartender Kurvigkeit und Veränderungsrate. Eine überwachte Klassifizierung dieser Regionen für die Klassen Eis, Wasser und Felsen kontrolliert den Prozess. Wir zeigen Ergebnisse der Extraktion aus einem aktuellen Landsat-Mosaik für circa 12 % der antarktischen Küstenlinie.

1 Introduction

Mapping a coastline is a comprehensive task, traditionally carried out by manual digitization from images. Exploiting remotely sensed imagery by means of automatic image-processing techniques is an increasingly important approach, especially where the need for frequently updated coastline data is high. Considering the coastline in a temporal sense, the update cycle of the coastline data is limited by the revisit time of the imaging sensor, and the accuracy of the coastline is influenced by the ground sample distance of the images. The availability of space borne imagery has increased in recent decades due to a larger number of related satellites, including Radarsat-1, Landsat ETM+ or MODIS on board Aqua/Terra.

[1] Extended version of a paper published in The International Archives of the Photogrammetry, Remote Sensing and Spatial Information Sciences, Vol. XXXVIII, Part 4, 2010, 7 p. (on CD-ROM).

 www.schweizerbart.de
DOI: 10.1127/1432-8364/2011/0095 1432-8364/11/0095 $ 3.50

In Antarctica, the coastline attains particular attention, as it constitutes the border of the vast ice sheet, influencing our climate and significantly contributing to sea level rise when melting (Houghton et al. (eds.) 2001). The mass balance of the Antarctic ice sheet changes due to surface and basal melting related to climate change, resulting in many floating ice shelves around the periphery of the continent. The link between the break-up of ice shelves and climatic effects such as global warming and sea level rise is discussed e.g. in (Bindschadler 1998, Scambos et al. 2000). In order to quantify such effects accurate and up-to-date coastline information is necessary.

During the last 15 years, imagery of three high/medium resolution satellites has been used to create image mosaics of the Antarctic continent. Two SAR image mosaics have been generated from Radarsat-1 data in 1997 and 2000, i.e. the Radarsat Antarctic Mapping Mission 1 (AMM-1) and its modified counterpart (MAMM-2) (Jezek et al. 2002). The MODIS Mosaic of Antarctica (MOA) has been derived from images of the MODIS sensors acquired from 2003–2004 (Scambos et al. 2007). A Landsat Image Mosaic of Antarctica (LIMA) with a ground sample distance of 240 m, with images taken from 1999 to 2003, has been released in support of the International Polar Year in 2007/2008 (Bindschadler et al. 2008). Due to orbit inclination, LIMA covers Antarctica only from 82.5° southern latitude northwards. Two coastlines have been extracted from the Radarsat Antarctic Mapping Project (RAMP) mosaic in a semiautomatic way and another one from MOA completely manually. To our knowledge, no complete coastline has been extracted yet on the basis of LIMA.

With respect to the fractal nature of coastlines (Mandelbrot 1967), the length of the Antarctic coastline as detected in modern high resolution satellite imagery reaches the size of the Earth's equator (cmp. Liu & Jezek 2004), thus frequently mapping the coastline is a formidable task. As mentioned before, visual interpretation of the imagery is still often being applied in modern mapping projects (e.g. Scambos et al. 2007). This process yields a seamless and unique realization of the coastline, but suffers from the immense time consumption and the subjectivity of the observer. In the spirit of map updating we consider the existing coastline as an additional input when automatically creating an up-to-date version. Fig. 1 visualizes our idea of taking advantage of a given coastline for detecting the up-to-date position. We employ snakes (active contours) introduced by Kass et al. (1988), with the extended external force field by Xu & Prince (1997), referred to as Gradient Vector Flow (GVF) snakes.

The remainder of the paper is structured as follows. In the next chapter we discuss related approaches that deal with coastline detection

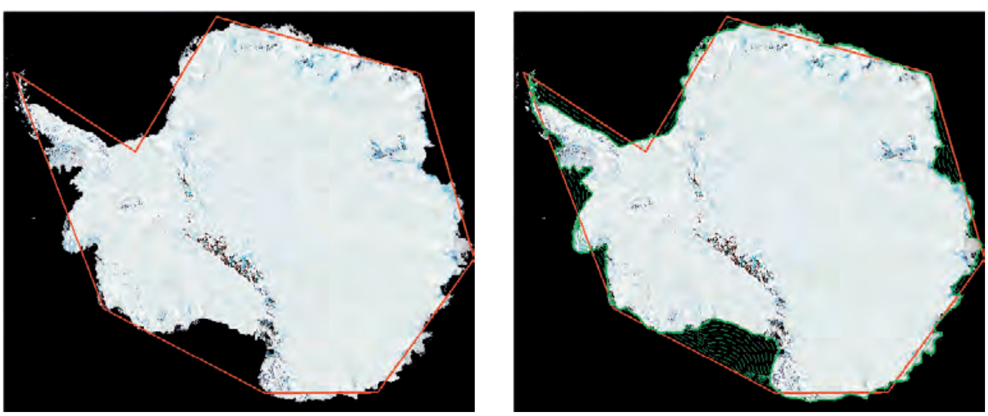

Fig. 1: Coastline detection for the Antarctic context. Initialisation of the snake with a polygon of eight supporting points connected by the red line (left); result of the coastline detection using snakes: the result is shown as a green line and every 10th iteration is symbolized by a green dashed line (right).

in digital imagery. Chapter 3 specifies our model definition for the different types of coastlines we deal with. In chapter 4 we describe the incorporation of these different model types into our snake algorithm. Chapter 5 contains some results of our approach including a quantitative evaluation of completeness, correctness and geometric accuracy. We conclude the paper in chapter 6.

2 Related Work

In the following, we give an overview of approaches that have been proposed towards automated coastline extraction in remotely sensed images. Basically, the methods can be divided into region-based classification techniques and methods based on edge detection.

Ryan et al. (1991) applied texture classification to scanned aerial photographs based on a neural network. The coastline is defined as the boundary between different homogeneous regions. Templates for the calculation of the neighbourhood information of the selected texture features lead to smoothed results but reduce the geometric accuracy. Muslim et al. (2006) utilize soft classification methods in coarse resolution images for predicting the proportion of land and water coverage in a super-resolution mapping step. Soft classification yields sub-pixel accuracy, but may fail for land-cover classes excluded from the training sites. Liu & Jezek (2004) classify regions adjacent to the Antarctic coastline based on grey values of Radarsat-1 images, which usually provide better contrast for the Antarctic context than available optical sensors. The classification strategy exploits the bimodal character of the SAR image histogram in coastal regions. Locally adaptive contrast ratio thresholds are determined to separate image regions. After the classification step several shape descriptors are employed to generate plausible regions, whose boundaries are the basis for coastline extraction. The practical applicability of the approach was proven when the complete Antarctic coastline was extracted from a SAR image mosaic of 25 m and 100 m resolution with a relative precision of approximately one pixel.

Methods based on automatic edge detection have been applied to detect coastlines in remotely sensed images, but to the best of our knowledge not yet for the Antarctic context. Mason & Davenport (1996) presented a hierarchical strategy that combines a region-based classification and an edge-based strategy. In a first step a SAR image of reduced resolution is used to detect an approximate position of the coastline by classification of the adjacent regions. Subsequently, an active contour model (Kass et al. 1988) is applied to find a geometrically accurate solution in the image of original resolution. A further development of this idea is described in Della Rocca et al. (2004) where the initial contour is derived from the output of a wavelet operation. Niedermeier et al. (2000) detect edges in SAR images by segmenting the image into land, water and coastal areas using a block tracing algorithm. The vectorized water-coastal region boundary of the blocktracing is utilized as initialisation of a snake algorithm.

Region based techniques for coastline detection in Antarctica using optical imagery is stated to be less appropriate due to lower contrast than in SAR imagery. In fact, it remains difficult to separate regions like annual sea ice and ice shelf by classification because of their spectral similarity. Therefore, none of the region based methods can be expected to handle the occurrence of the ice-to-ice constellation as frequently observed in Antarctica with optical images as input. It was also found that using global statistics for training may provide an inappropriate description of the classes to be distinguished locally and hence decrease the accuracy of coastline prediction (Muslim et al. 2006). When using the traditional snake approach, the initialisation must be very close to the salient feature for obtaining the correct result. Furthermore, without local adaptation the snakes would fail in the Antarctic context, since the coastline appearance varies broadly from one area to the next.

3 Model Definition

The spectral and geometric characteristics of the Antarctic coastline in optical imagery are heterogeneous, so that no single coastline model can adequately reflect the different appearance. On the basis of the Landsat mosaic LIMA we therefore formulate three different models that match a large part of the Antarctic coastline, i.e. the transition from ice shelf to water, from ice shelf to sea ice and from rocky terrain to water (Fig. 2), where "ice shelf" includes grounded as well as floating ice shelf, and "sea ice" is not older than one year, and is frequently covered by snow, which makes it hard to distinguish from ice shelf. The fourth model in this row would be the transition from rocky terrain to sea ice. This model, however, is not regarded further, since it appears only very seldom. The following characteristics are considered with regard to the definition of the snake energy terms (see also chapter 4).

3.1 *Ice Shelf to Water*

The transition from ice shelf to water is expected to always show a clear contrast due to the much lower albedo of water than the one of snow or ice. The adjacent regions are mostly homogeneous, except for the existence of floes preloaded to the offshore side. Hence, for this model a high edge response in the image indicates the location of the coastline. Except for rifts, the shape of the coastline is mostly smooth. Floating and calving ice shelves can cause planimetric movements of the coastline of up to 1 km per year (Brunt et al. 2010).

3.2 *Ice Shelf to Sea Ice*

The transition from ice shelf to sea ice exhibits little contrast in intensity, colour and texture (see Fig. 2, centre). Sharp changes of slope perpendicular to the coastline direction often causes the thick ice shelf fronts to cast shadows on the sea ice or to appear very bright, especially at low sun angles. In the image these effects result in a thin line that usually does not exceed a width of one pixel. Shadows cause the coastline to appear as a dark line while the illumination at low sun angles results in a bright line. The coastline is mostly smooth and undergoes the same geometric changes over time as the *ice shelf to water* coastline.

3.3 *Rocky Terrain to Water*

The transition from rocky terrain to water is difficult to recognise in the image (see Fig. 2, right), while the contrast between rock and ice further inbound the continent, which often occurs in the vicinity of rocks, is rather high. Nevertheless, there is a noticable difference in terms of colours between the rocks and the water, which results in characteristic differences in the HSI (hue, saturation, intensity) space (see Fig. 3). The coastline is not expected to significantly change its geometric position over time. In contrast to the previously discussed models, the coastline is rather curvy due to rifts and bays.

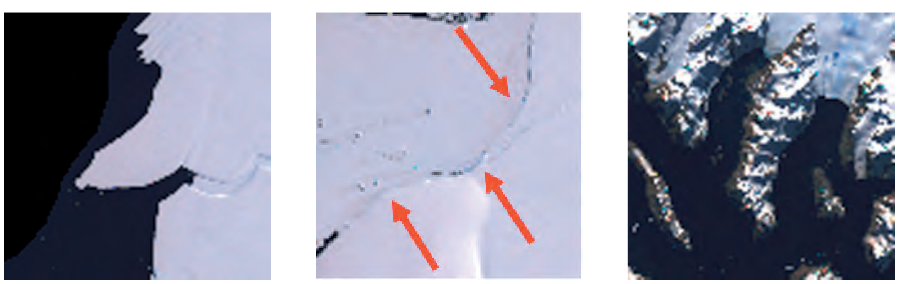

Fig. 2: LIMA subsets with instances of the transitions from ice shelf to water (left); ice shelf to sea ice (centre; the coastline extends from bottom left to the upper right corner as pointed out by the red arrows); and rocky terrain to water (right).

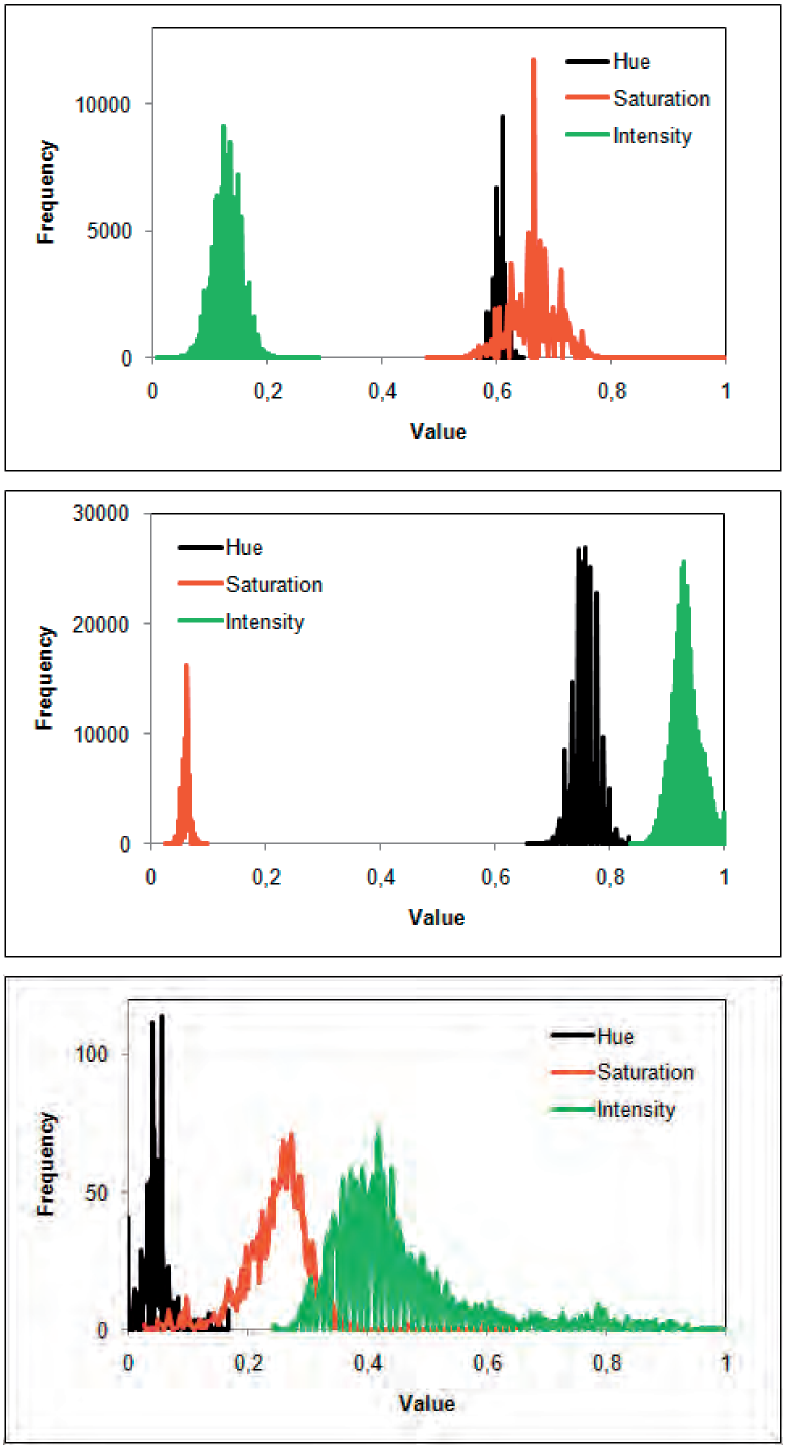

Fig. 3: Histograms of normalised hue, saturation and intensity values for the classes water (top), ice (centre) and rock (bottom).

4 Strategy

We follow Mason & Davenport (1996) and present a method which uses snakes as the core algorithm. It is known that snakes require a sufficiently good initialisation to yield an accurate and reliable solution. In our approach the initialisation is derived from the RAMP coastline, which is represented as a polygon. We define a new coastline model for optical data consisting of three individual and different snake models. For this purpose representative regions on both sides along the initial coastline are classified so that the appropriate snake model can be selected automatically. The related snake algorithm then computes the position of the coastline. By incorporating the Gradient Vector Flow (GVF) into our image energy description, we achieve a higher attraction range for initialisations further away from the final coastline. In the following the automated selection of the model and the strategy for employing the model within a snake algorithm are described in detail.

4.1 *Pre-processing*

Due to the heterogeneous coastline characteristics as well as the immense data volume it is not reasonable to process the complete Antarctic coastline simultaneously. Instead, the Landsat mosaic is segmented into a number of tiles of equal size (here: 460 tiles of 240^2 km^2 each), and snakes are placed over each tile that contains a section of the given coastline. Out of the 460 tiles, only those are considered further, which overlap with the given RAMP coastline.

4.2 *Model Selection*

An automated analysis is carried out for each image tile to find the best-matching model. For this task we subdivide the coastline into line-segments with an equal number of polygon points. This idea seems to be more promising than choosing equally long sections since the distance between the polygon points is smaller where the coastline is more structured leading to more frequent transitions within different object types. The line-segments are classified into one of the three models described in chapter 3 using features from regions on both sides of the line-segment, shifted by a certain offset in off- and onshore direction (see Fig. 4). We set the offset with respect to the highest speed expected for the floating ice shelf (1km per year) and the time interval between the acquisition of the previously and currently used imagery (two years in our case) to be 2 km.

For classification we used a simple nearest neighbour algorithm. We trained the classifier using features from manually selected areas from different tiles of the LIMA mosaic (Note that for mosaic generation the different original images were radiometrically adjusted to each other. Therefore it was possible to select

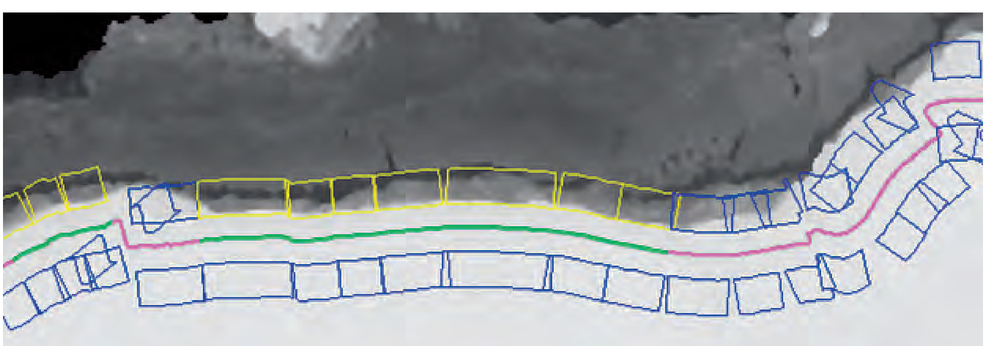

Fig. 4: Classification results: line segments coloured in relation to the classification result, i.e. green for water-ice and magenta for ice-ice boundary. The analysed regions are coloured in accordance with the detected object type: yellow for water and blue for ice.

the training areas from different parts of the coastline without problems due to multi-temporal data acqusition etc.). First tests with features from RGB space yielded unsatisfactory results. We therefore used features from HSI space. In this colour space water has a characteristic distribution of saturation values compared to ice and rock (see Fig. 3 and discussion above), whereas ice is significantly brighter than the other classes with regard to the intensity channel and rock appears slightly redish/brownish leading to a low angle of hue. We found the best classificaton results with the following three features: the average region values of saturation and intensity and the percentage of pixels with hue values in the range of [0;π/2]. The last feature is able to detect rocks also in the presence of ice (see again Fig. 3). The classification results for the corresponding regions on either side of the given coastline are then combined to select the correct snake model. Hence, we consider the coastline types according to the corresponding regions as *ice shelf to water*, *ice shelf to sea ice* or *rocky terrain to water* and select the related snake model for further processing.

4.3 *Parameterisation of Snakes*

Snakes require the definition of an energy functional that reflects the underlying coastline model. For each of the three different models the energy terms and related parameters are optimised based on the radiometric properties of the adjacent regions as well as the curvature and the potential change-rate of the considered coastal region. Traditionally, a snake is considered as a curve $\mathbf{v}(s) = (x(s),y(s))$ parameterised with the arc length $s \in [0,1]$, that iteratively moves in the image domain $I(x,y)$ until its energy functional E^*_{Snake} is minimised (Kass et al. 1988):

$$E^*_{snake} = \int E_{\text{int}}(\mathbf{v}(s)) + E_{con}(\mathbf{v}(s)) + E_{img}(\mathbf{v}(s))ds \qquad (1)$$

The internal energy E_{int} controls the shape of the snake and thus varies with every deformation of the curve. Typically the bending and stretching of **v** are the considered internal snake characteristics, modelled by the first and second derivatives of **v** with respect to s:

$$E_{\text{int}}(\mathbf{v}(s)) = \frac{1}{2} \cdot \left[\alpha \cdot \left|\mathbf{v}'(s)\right|^2 + \beta \cdot \left|\mathbf{v}''(s)\right|^2 \right] \qquad (2)$$

where E_{int} = internal energy
$\mathbf{v}', \mathbf{v}''$ = derivations of v with respect to s
α = elasticity parameter
β = rigidity parameter

The elasticity and rigidity parameters α and β act as weighting factors of the first and second order term of eq. 2. The first term controls the length of the snake. Large values for α stretch the coastline and smooth the effect of local disturbances in the image energy. The second term controls the snake curvature: β allows to adapt the shape properties of the coastline models, e.g. large values for β lead to a straighter coastline while small values allow a high curvature coastline.

The constraint energy E_{con} and the image energy E_{img} of eq. 1 are considered as context dependent external influences that affect the snake's position, being responsible for iterative movements and deformations. E_{con} can make the snake move towards or away from fixed points or lines. In our current implementation constraints are not considered, however, they could be easily added, e.g. for pulling the snake towards manually selected points.

The image energy affects the position of the snake with respect to the features in the image. E_{img} can be considered as a scalar potential energy that is defined for each pixel as a function of the grey value $I(x,y)$ so that it adopts smaller values at salient features. E_{img} can hence be calculated once in advance before starting the iterative optimisation procedure.

Since for the present approach we distinguish different types of coastline, we use different image energy definitions that attract the snake to lines or edges in the image according to the associated model. In the literature, the image energy for lines is often simply the image function itself (Kass et al. 1988), with the sign indicating if the snake is to be attracted to light (-) or dark lines (+). As explained above, for the detection of coastlines that match the line model, the snake must be attracted to both, light and dark lines. For line detection we employ the Steger line operator (Steger 1998). The image energy for the line model results from a binary decision as

$$E_{img}^{line}(x,y)=\begin{cases}1, if\ (x,y)\in(L_{-}\vee L_{+})\\ 0 \qquad otherwise\end{cases} \tag{3}$$

with L_- being the set of light lines and L_+ the set of dark lines, respectively, detected by the line operator. For edges, the energy term is traditionally defined as the negative squared magnitude of the gradient image. We apply the Canny operator (Canny 1986) for edge detection yielding image gradients ∇(x,y) and binarisation with respect to an edge threshold t as

$$E_{img}^{edge}(x,y)=\begin{cases}1,\ if\ \ |\nabla(x,y)|>t\\ 0\ \ otherwise\end{cases} \tag{4}$$

The capture range of the traditional image energy is limited with respect to the width of the template of the gradient operator (see Fig. 5a). As soon as the distance to the initialisation is only slightly larger than the capture range of the image energy, convergence is not assured. To overcome this limitation, Xu & Prince (1997) have extended the energy field by applying a generalised diffusion equation to the response of the image energy term called Gradient Vector Flow (GVF) field. The increased capture range is visualized in Fig. 5b. Moreover, the capture range of the GVF related snake also enables the contour to progress into concave parts of the boundary.

In order to minimise the snake energy E^*_{snake} the related Euler equation (eq. 5) must be solved:

$$\alpha\cdot\mathbf{v}''(s)-\beta\cdot\mathbf{v}''''-\nabla E_{img}=0 \tag{5}$$

which leads to:

$$\mathbf{v}(t)=(\mathbf{A}+\gamma\cdot\mathbf{I})^{-1}\cdot\left[\gamma\cdot\mathbf{v}(t-1)-\kappa\cdot f_{\mathbf{v}}(\mathbf{v}(t-1))\right] \tag{6}$$

where **v**(t) = snake representation at time t
A = design matrix
γ = step size (viscosity factor)
I = identity matrix
κ = weight factor for external energy
$f_{\mathbf{v}}$ = gradient values from image energy

In eq. 6 the snake is made dynamic by describing **v** as a function of time. The matrix A+γ•I is a pentadiagonal banded matrix and γ controls the step size that influences the viscosity of the snake (for details of snake optimisation see Kass et al. (1988), Fua (1995), and Butenuth (2008)).

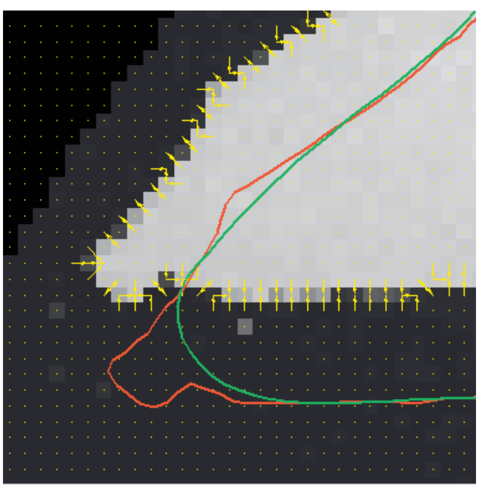

a)

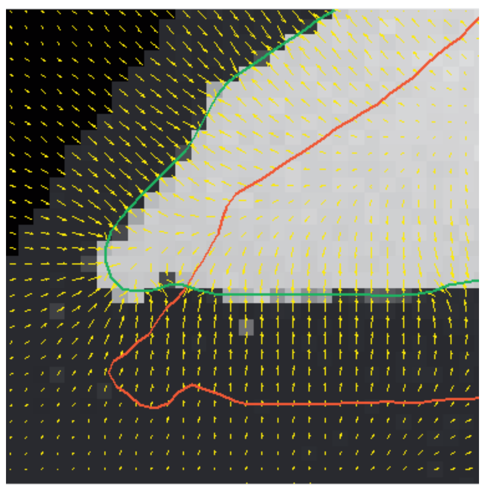

b)

Fig. 5: Vector field marked by yellow arrows: a) standard vector field with vectors pointing towards the edges; the snake cannot converge to the correct solution from a poor initialisation (red) yielding a wrong result (green); b) GVF field, where the snake can be initialized anywhere in the GVF field for being pulled towards an edge, thus the result is correct.

5 Experiments and Results

In this chapter we report the results achieved with the described coastline extraction approach. Until now, we have processed approximately 5000 km or 12 % of the Antarctic coastline around the Weddell Sea (see Fig. 6). As data source we use the ETM+ true-colour composite LIMA, the RAMP coastline (acquired shortly before the images) was used as initialisation for the snakes. The coastline was subdivided into 703 sections for classification out of which 353 were labeled as water-to-ice, 338 as ice-to-ice and 12 as water-to-rock. Upon visual inspection we found 659 sections (94 %) to be correctly classified, only 44 sections (6 %) had to be manually corrected prior to further processing. The classification of adjacent regions may lead to false decisions for the type of coastline, if the initialisation is fur-

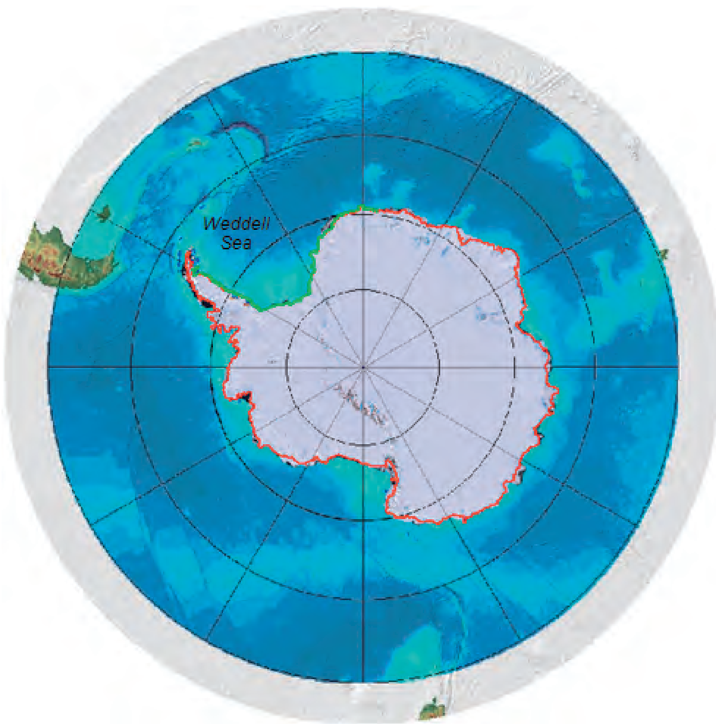

Fig. 6: Chart of the Southern Ocean sea bed topography from the General Bathymetric Chart of the Oceans (GEBCO) in the background and LIMA (centre filled with MODIS data). We have processed the green part of the coastline.

Tab. 1: Parameter settings for the different coastline models.

Parameter		Ice shelf to water	Ice shelf to sea ice	Rocky terrain to water
Internal Energy:	α	0.01		
	β	0.1		0.01
Image Energy:	image pre-processing	Canny edge detection	Steger line detection	HSI transformation Canny edge detection
Optimization Term:	γ	1.0		0.1
	κ	1.0		10
	max. iterations	40		

ther away from the correct solution than approx. 2 km (see section 4.2). With regard to a practical application we found a manual inspection and correction of the classification results to be a reasonable solution for this problem, since checking is very fast, especially within the interactive software environment we had created for this task.

According to our model description (see chapter 3) we applied a set of default parameters for the snake optimisation. A qualitative explanation of the selected parameters is given in the following subsections. The whole list of default parameters is shown in Tab. 1.

5.1 *Ice Shelf to Water*

Fig. 7 depicts a subset of LIMA that contains a coastline of the type water-to-ice. The red line marks the initial RAMP coastline. For the displayed example the initial line differs by up to 6 pixels (1.4 km) from the position indicated by the image. The high intensity contrast between the adjacent object types led to the selection of the edge model (eq. 4) as image energy. We applied the default parameters specified in Tab. 1: an intermediate value for β and a small value for κ that both lead to a relatively smooth coastline without harsh bendings still

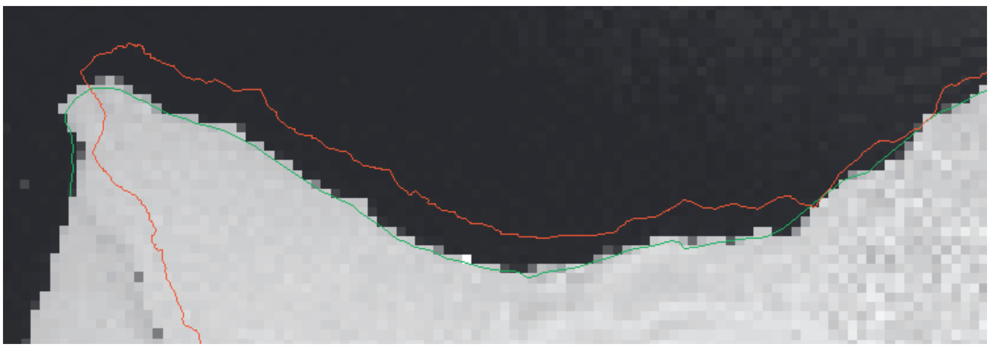

Fig. 7: Ice shelf to water model: a 28•10 km^2 subset of LIMA showing an ice shelf next to open water with the corresponding RAMP coastline (red) and the result of the coastline detection (green).

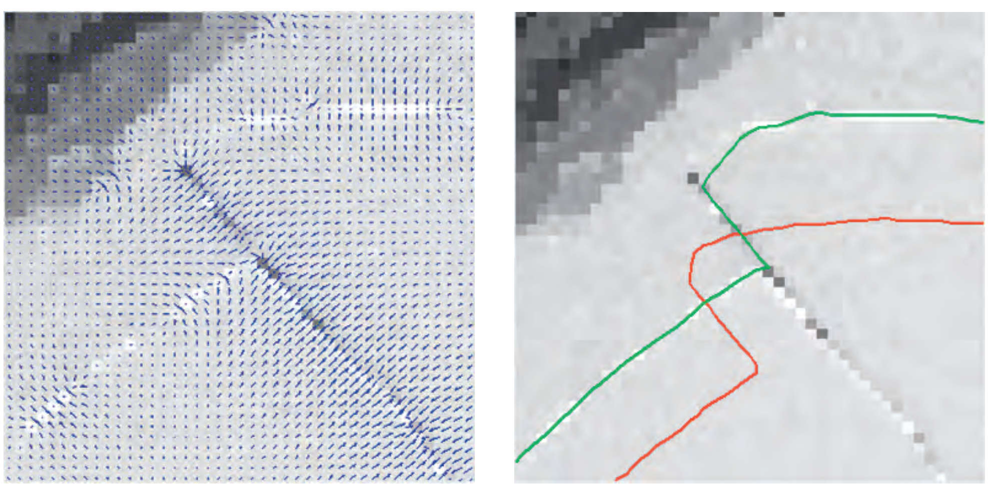

a) b)

Fig. 8: Ice shelf to sea ice model: a 10•10 km^2 subset of LIMA showing ice shelf next to sea ice with a) the energy field based on Steger line detection; b) the corresponding RAMP coastline (red) and detection result (green). This result is identical to what we consider as ground truth.

allowing the snake to manoeuvre into concave regions. The effect of an adeqate parameter β is also notable in the extraction result of (Fig. 5b) where at the tip the upper side of the initialisation is placed below the lower side of the ice shelf, and still correctly pulled towards the upper side, kept in shape by the internal energy. The optimisation term is parameterised by a large value for γ (step size) that leads to a fast convergence of the snake.

5.2 *Ice Shelf to Sea Ice*

Fig. 8 shows a typical constellation of annual sea ice on the upper left above an ice shelf on the lower right of the green line. The initial coastline differs by up to 10 pixels (2.4 km) from the coastline in the image, visible partly as a bright line and partly as a dark line along the rift (centre part). The parameter settings for the energy terms and the snake optimisation are set similarly to those for the separa-

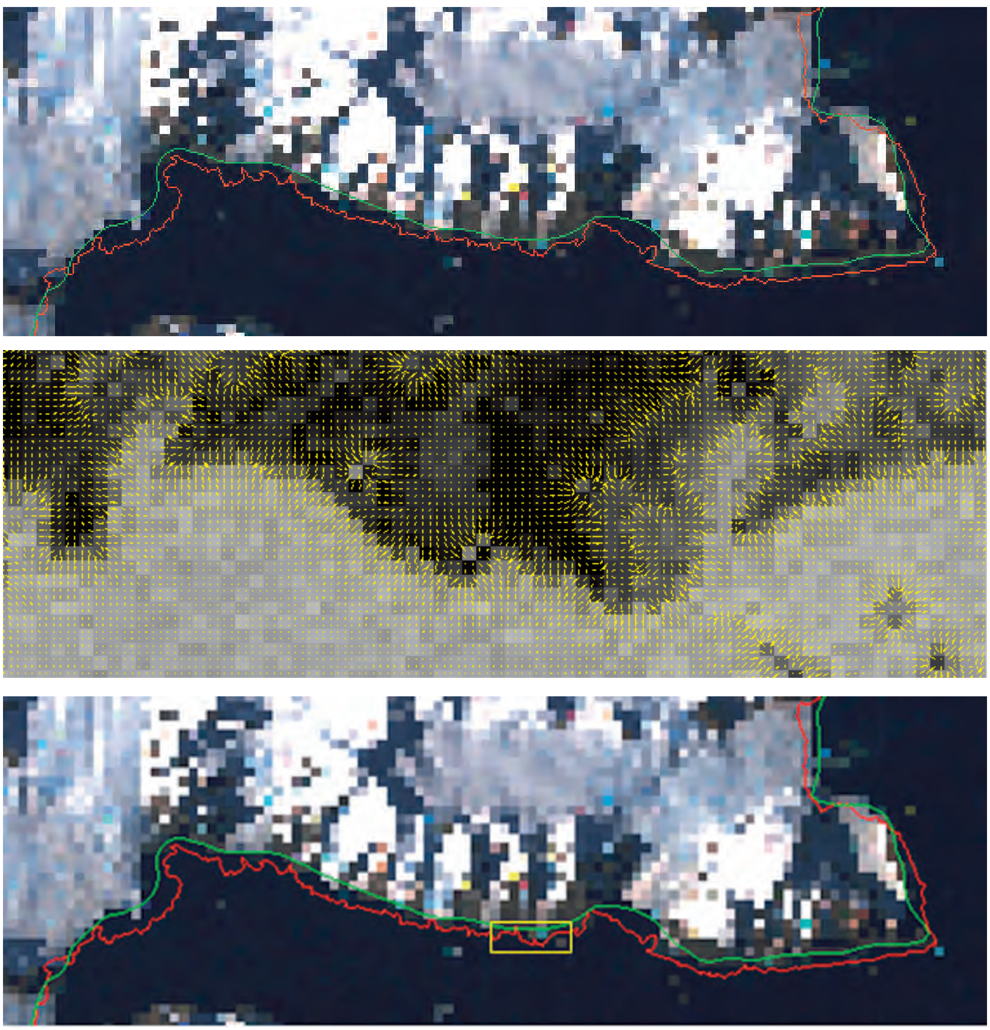

Fig. 9: Rocky terrain to water model: example shown in a 20•8 km² subset of LIMA (top); 2•0.8 km² ETM+ saturation image superimposed with the derived energy field (centre) and in RGB representation with the corresponding RAMP coastline (red) and the result of the coastline detection (green, bottom). The yellow box in the top image indicates the position of the ETM+ subset.

tion of ice and water, see section 5.1. For the image energy the line model is chosen.

Most of the problems that arise in this configuration are related to the lack of line-like appearance of the border line. Smaller gaps can be successfully bridged by the internal energy of the snake. Such an example can be seen in the lower left corner of Fig. 8.

5.3 *Rocky Terrain to Water*

Based on the model defined in section 3.3 the initialisation does not differ much from the coastline in LIMA. In fact, using the medium resolution image mosaic possibly downgrades the accuracy of the given coastline acquired from higher resolution data, if the coastline position has not changed over time. For the LIMA test scene (Fig. 9, top) we achieved a convergence of the snake towards the rocky coast. The coastline has moved by 1-2 pixels from the initial position, which is in fact a degration of the positional accurancy for the major parts of that coastline type. However, the result is still within the accuracy requirements for the task.

For demonstrating the payoff of the model definition we repeated this experiment with the original Landsat ETM+ image with 30 m ground resolution (see Fig. 9, bottom). Here, the initialisation (red) and detection result (green) show differences of up to 10 pixels (0.30 km), which could be removed by our method. The rocks that only show a weak contrast to the water in the intensity channel appear in a high contrast in the saturation channel, which was used in this model for defining the image energy. The saturation channel of the test area is depicted in Fig. 9 (middle), superimposed with the energy field that is oriented well towards what we consider ground truth. We assign a small value to β and a higher weight for κ due to the potentially high curvature of the coastline.

5.4 *Quantitative Evaluation of the Results*

For the evaluation of the proposed method, a reference dataset was extracted manually from the LIMA imagery for the coastline segment shown in Fig. 5. We then calculated the correctness (the percentage of extracted data matching the reference) and completeness (the percentage of the reference data matching the extracted data) in accordance with Heipke et al. (1997). With an expected geometrical accuracy for the processed coastline of 1000 m

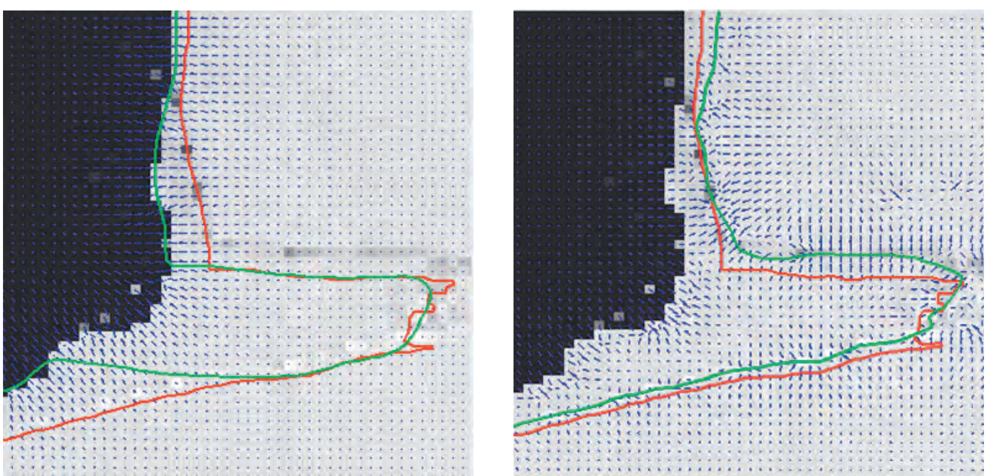

a) b)

Fig. 10: Detection results using a) the edge model and b) the line model. The underlying image energy is depicted as blue vector field. The red line indicates the initialisation (identical in both cases), the green line the result. The correct choice for the final result consists of a combination of the individual results with the solution from a) for the coastal parts and from b) for the onshore.

we achieved a completeness of 87.9 % and a correctness ratio of 86.3 %. In other words, 12.1 % of the manual reference cannot be detected by the approach (false negative) and 13.7 % of the obtained result is incorrect (false positive). Thus, interactive post processing is still necessary, but the human effort is significantly reduced compared to a completely manual digitisation of the coastline. The RMS error of the true positives accounts for 380 m or approximately 1.5 pixels, which is sufficient for our purpose.

Three major issues explain the 12.1 % of omitted detection. Firstly, the image energy that is selected in accordance with a local classification result may not be adequate if the initialisation lies further away from the solution than expected in the model definition due to special coastline geography like long narrow bays. Hence the snake is not assured to converge to the correct solution. Secondly, in case of ice-to-ice transition, the line response is not high along the entire scenario (see Fig. 8). This is related to the large pixel size which dampens some of the information content required for our model assumption. Thirdly, problems occur if the coastline type changes within one of the polygon segments used for classification. A scenario as in Fig. 10 requires processing with the edge model where the initial coastline (red) runs from the upper side downwards closely along the correct result in a) (green), and with the line model further down where the actual coastline is visible as a sequence of dark and bright pixels, heading towards the inbound of the ice shelf. If the sampling interval of the classification segments is too large, an inappropriate snake model might be applied within that segment leading to partially wrong solutions.

6 Conclusions

The developed approach is capable of extracting the Antarctic coastline with a high degree of automation. Satisfying quality values can be achieved if the set of free parameters is optimised for each employed model. The proposed method of coastline extraction combines classification and updating of a given coastline in a combined scheme. The classification supports the model selection by analysing the spectral properties of the local vicinity of the coastline and significantly reduces the effort of manually assigning the correct snake model to each section of the coastline. Up to now, our classifier was based on manually selected training areas and the snake parameters were chosen empirically. We strive to incorporate more sophisticated parameter selection schemes from machine learning in future work.

In order to achieve a higher detection rate one has to further investigate the issues discussed in section 5.4. That is, on one hand, if a larger absence of image energy is encountered within the area that we consider as relevant (using an offset of 2 km in section 4.2), one could improve the classification strategy for finding the next appropriate model, e.g. by applying a stepwise increasing search radius instead of using regions at constant distance from the initialisation. On the other hand, the impact of inappropriately chosen snake models that we experienced around transitions between different coast types, can be reduced by further decreasing the sampling intervals or by incorporating additional knowledge about land cover from other sources. Lastly, the absence of image energy encountered for the ice-to-ice model can often be circumvented by using higher resolution imagery, which already proved promising results for the rocky-terrain-to-water-model.

References

Bindschadler, R., 1998: Future of the West Antarctic ice sheet. – Science **282:** 428.

Bindschadler, R., Vornberger, P., Fleming, A., Fox, A., Mullins, J., Binnie, D., Paulsen, S.J., Granneman, B. & Gorodetzky, D., 2008: The Landsat Image Mosaic of Antarctica. – Remote Sensing of Environment **112** (12): 4214–4226.

Brunt, K.M., King, M.A., Fricker, H.A. & MacAyeal, D.R., 2010: Flow of the Ross Ice Shelf, Antarctica, is modulated by the ocean tide. – Journal of Glaciology **56** (195): 157–161.

Butenuth, M., 2008: Network Snakes. – PhD Thesis, University of Hannover, DGK-C 620.

Canny, J., 1986: A computational approach to edge detection. – IEEE Transactions on Pattern Analysis and Machine Intelligence **8:** 679–698.

Della Rocca, M.R., Fiani, M., Fortunato, A. & Pistillo, P., 2004: Active Contour Model to Detect Linear Features in Satellite Images. – International Archives of Photogrammetry, Remote Sensing and Spatial Information Sciences **35** (B3): 446–450.

Fua, P., 1995: Parametric Models are Versatile: The Case of Model Based Optimization. – International Archives of Photogrammetry and Remote Sensing **XXX** (III/2): 236–246.

Heipke, C., Mayer, H., Wiedemann, C. & Jamet, O., 1997: Evaluation of automatic road extraction. – International Archives of Photogrammetry Remote Sensing **XXXII** (3–4,W2): 151–160.

Houghton, J.T., Ding, Y., Griggs, D.J., Noguer, M., van der Linden, P.J., Dai, X., Maskell, K. & Johnson, C.A. (eds.), 2001: The Scientific Basis. Contribution of Working Group I to the Third Assessment Report of the Intergovernmental Panel on Climate Change (IPCC). – 881 p., Cambridge University Press, Cambridge, United Kingdom and New York, NY, USA.

Jezek, K. & RAMP Product Team, 2002: RAMP AMM-1 SAR Image Mosaic of Antarctica. – Fairbanks, AK: Alaska Satellite Facility, in association with the National Snow and Ice Data Center, Boulder, CO. Digital media.

Kass, M., Witkin, A. & Terzopoulos, D., 1988: Snakes: Active contour models. – International Journal of Computer Vision **1** (4): 321–331.

Liu, H. & Jezek, K.C., 2004: A complete high resolution coastline of Antarctica extracted from orthorectified Radarsat SAR imagery. – Photogrammetric Engineering & Remote Sensing **70** (5): 605–616.

Mandelbrot, B.B., 1967: How long is the coastline of Britain? Statistical self-similarity and fractional dimension. – Science **156:** 636–638.

Mason, D.C. & Davenport, I.J., 1996: Accurate and efficient determination of shoreline in ERS-1 SAR images. – IEEE Transactions on Geoscience and Remote Sensing **34:** 1243–1253.

Muslim, A.M., Foody, G.M. & Atkinson, P.M., 2006: Localized soft classification for super resolution mapping of the shoreline. – International Journal of Remote Sensing **27:** 2271–2285.

Niedermeier, A., Romaneessen, E. & Lehner, S., 2000: Detection of coastlines in SAR images using wavelet methods. – IEEE Transactions on Geoscience and Remote Sensing **38:** 2270–2281.

Ryan, T.W., Sementilli, P.J., Yuen, P. & Hunt, B.R., 1991: Extraction of shoreline features by neural nets and image processing. – Photogrammetric Engineering & Remote Sensing **57:** 947–955.

Scambos, T.A., Hulbe, C., Fahnestock, M. & Bohlander, J., 2000: The link between climate warming and break-up of ice shelves in the Antarctic Peninsula. – Journal of Glaciology **46** (154): 516–530.

Scambos, T.A., Haran, T.M., Fahnestock, M., Painter, T. & Bohlander, J., 2007: MODIS-based Mosaic of Antarctica (MOA) datasets: Continent-wide surface morphology and snow grainsize. – Remote Sensing of Environment **111:** 242–257.

Steger, C., 1998: An unbiased detector of curvilinear structures. – IEEE Transactions on Pattern Analysis and Machine Intelligence **20** (2): 311–326.

Xu, C. & Prince, J.L., 1997: Gradient Vector Flow: a new external force for snakes. – IEEE Conference on Computer Vision and Pattern Recognition: 66–71.

Addresses of the authors:

Dipl.-Ing. Tobias Klinger, Dipl.-Ing. Marcel Ziems, Prof. Dr.-Ing. Christian Heipke, Leibniz Universität Hannover, Institut für Photogrammetrie und GeoInformation, Nienburger Str. 1, D-30167 Hannover, Tel.: +49-511-762-2482, Fax: +49-511-762-2483, e-mail: <nachname>@ipi.uni-hannover.de.

Dr.-Ing. Hans Werner Schenke, Dr. Norbert Ott, Alfred-Wegener-Institut für Polar- und Meeresforschung, Van-Ronzelen-Str. 2, D-27568 Bremerhaven, Tel.: +49-471-4831-1222, Fax: +49-471-4831-1977, e-mail: hans-werner.schenke@awi.de, norbert.ott@awi.de.

Manuskript eingereicht: Juli 2011
Angenommen: August 2011

PFG 2011 / 6, 0435–0446
Stuttgart, December 2011 **Article**

MACS – Modular Airborne Camera System for Generating Photogrammetric High-Resolution Products

Frank Lehmann, Ralf Berger, Jörg Brauchle, Daniel Hein, Henry Meissner, Sebastian Pless, Bernhard Strackenbrock & Alexander Wieden, Berlin

Keywords: Airborne Camera, Modular Camera System, Photogrammetry

Summary: This article describes a Modular Airborne Camera System (MACS), which is based on industrial grade components. The camera system has been developed by the Department of Optical Information Systems of the German Aerospace Center (DLR). Several versions have been in use since 2009 in order to acquire experimental aerial image data.

The aim was to develop a system capable of acquiring image data with ground resolutions in the centimeters range easily and at low costs. These data should help to develop and to define photogrammetric methods and products. High emphasis was put on high frame rates as well as on short integration times in order to achieve a high overlap and low motion blur. This is essential for exact 3D modeling, especially when using fast airplanes flying at low altitudes.

The article describes the principles and the layout of the camera system together with its flight-specific accessories as well as the software developed for operating the system. Finally, the article delineates current and future fields of application.

Zusammenfassung: *MACS – Modulares Luftbildkamera-System für die Erzeugung hochauflösender photogrammetrischer Produkte.* Der Artikel beschreibt den Aufbau eines Modularen Luftbild-Kamerasystems (MACS) auf Basis von Industriekameramodulen und Industrieoptiken. Dieses System wurde in der Einrichtung Optische Informationssysteme des Deutschen Zentrums für Luft- und Raumfahrt e.V. (DLR) entwickelt und wird in verschiedenen Ausbaustufen und Varianten seit 2009 zur Erhebung experimenteller Luftbilddaten verwendet.

Zielstellung war die einfache und kostengünstige Erzeugung von umfassend verarbeitbaren Bilddatensätzen mit Bodenauflösungen im Zentimeterbereich. Damit sollen photogrammetrische Verfahren und Produkte weiterentwickelt und demonstriert werden. Besonderer Wert wurde auf hohe Aufnahmefrequenzen und kurze Integrationszeiten der Kameramodule gelegt. Die damit erzielbaren hohen Überlappungen und geringen Bewegungsunschärfen sind Voraussetzung für exakte 3D-Modellierungen, auch aus schnell fliegenden Trägerflugzeugen sowie aus geringen Flughöhen.

Prinzip und Aufbau des Kamerasystems mit den flugspezifischen Zusatzgeräten werden ebenso vorgestellt, wie die selbst entwickelte Software zum Betrieb der Kamera. Eine abschließende Betrachtung zeigt die derzeitigen und zukünftigen Einsatzmöglichkeiten.

1 Introduction

This article introduces a set of photogrammetric cameras (MACS) which were developed at the German Aerospace Center (DLR) in Berlin since 2009. Although already used successfully, the camera system is still being under development. The article gives a general overview of the camera system.

1.1 *Motivation*

The output from commercial aerial cameras is not always suitable for developing and enhancing photogrammetric concepts. These cameras are often turnkey systems designed for standard applications. This leads to less flexibility when configuring them for the acquisition of experimental aerial image data.

DOI: 10.1127/1432-8364/2011/0096 1432-8364/11/0096 $ 3.00

Therefore a camera system – based on matrix image sensors – was needed which provides high flexibility at low costs. This includes the architecture of the camera system as well as its capability to deliver optimal results under various operating conditions.

The goal of the development is not a replacement of common aerial imaging systems but the creation of a tool for developing new concepts and methods. The camera system is intended to be a prototype version but can be developed further for commercial or industrial applications.

1.2 *Requirements*

The key requirement for the system is to deliver aerial image data which can be processed into high-quality 3D data. Experience in 3D processing of images from commercial aerial cameras (Lehmann et al. 2011) has shown that if the frames overlap 80 % and more in flight direction, accurate 3D information can be derived efficiently. In order to gain this overlap when flying at low altitudes and using fast aircraft the camera system had to deliver high frame rates and thus handle large amounts of data.

Another requirement was the flexibility of the camera system. In order to set different configurations the camera modules had to work autonomously and be compact. Besides being used in especially equipped aircraft, the camera system should also be usable in external pods, which means that volume and weight of the system had to be as low as possible.

The costs for each camera system configuration had to be significantly below the costs for commercial systems. This was achieved by re-using key parts – including camera modules and lenses – for different system layouts.

Because of these requirements industrial-grade camera modules, lenses, and peripheral equipment were used as basic components for the set of cameras described.

2 System Layout

In the following paragraphs the layout, components and features of the camera system

Fig. 1: MACS 50/70.

will be described. The focus will be put on the MACS 50/70 configuration (Fig. 1), which is set for the acquisition of aerial image data in the centimetres range when using commercial airplanes and helicopters.

Six MACS configurations including the MACS 50/70 have been successfully used in different projects so far. Examples are given below and some will be described in detail in following publications.

MACS 50/70 consists of three camera modules and three lenses connected by a body structure. When configuring this system version, our aim was to test its suitability as an aerial imaging camera in low flying altitudes and to test the processing methods of combined image fields of several camera modules as described below. The key technical specifications of the MACS 50/70 configuration are shown in Tab. 1.

Other camera systems using standard components have also been brought to the market over the last years (Grenzdörffer 2008). Most of the medium format camera back-plains developed for high-quality photography are combined with mechanical shutters and off-the-shelf optics. Sometimes standard photographic cameras and lenses are used for mapping applications, for instance CAIMS (McCarthy et al. 2008), or for oblique imaging like MIDAS by Track'Air (2011). The MACS concept mainly differs from these systems in its flexibility of the configuration and its focus on high frames rates rather than on pixel quantity.

Tab. 1: MACS 50/70 camera head data sheet.

Geometric resolution	5084 × 4008 Pixels true colour (RGB, Bayer pattern) 4008 × 2672 Pixels near infrared (NIR)
Pixel Size	9 µm
Focal length / Aperture	70 mm (RGB) / f : 5.6 (open) 50 mm (NIR) / f : 5.6 (stopped down)
Field of view	app. 40° × 27° (RGB) app. 35° × 29° (NIR)
Radiometric resolution	14 bit
Frame rate	max. 5 Hz
Operational conditions	0 °C to 35 °C ambient air temperature
Ground resolution	10 cm at 780 m flight altitude (RGB)
Weights and measures	app. 45cm × 25cm × 40cm (length × width × height), 8 kg

2.1 *Camera Modules*

The pco.4000 camera modules, which have been used for the Modular Airborne Camera System, were developed by PCO AG Kehlheim (PCO 2011). Originally designed for industrial applications like traffic and quality control, the modules were adapted for aerial imagery applications. The features of these modules are relatively high geometric and radiometric resolutions, high frame rates, high sensitivity as well as short integration times, which are realized electronically. A mechanical shutter, which is prone to wear, is omitted.

The PCO modules are equipped with KODAK Interline CCD image sensors (KAI-11002) (Kodak 2011). The light sensitive area is about 36 mm × 24 mm and has 4008 × 2672 active pixels with a pixel size of 9 µm. Each photo diode is equipped with an additional microlens, which expands the photo effective area up to 80 % of the surface of one pixel.

A special characteristic of the sensor is an asymmetric peripheral light fall-off. This is caused by the Interline principle in connection with the microlens structure. In order to minimize the general light loss of the camera system the camera modules of the MACS 50/70 were arranged in a way that the long sides of the sensor planes are aligned.

Due to thermoelectrical cooling down to 45 °C below ambient temperature the camera module features low noise down to 11 electrons (RMS at 8 MHz, manufacturer information) and has therefore an excellent signal-to-noise ratio.

The pco.4000 modules are available with or without colour filters. Sensor modules with Bayer RGB filters have been used for the MACS 50/70. An integrated primary image memory guarantees data rates of up to 128 MB/s and enables the system to transfer this amount of data to the measuring computer via 'Camera Link'.

The exposure times of the electronic shutter can be set as short as 5 µs. In the field of aerial imaging integration times between 500 µs and 3 ms are common.

2.2 *Lenses*

The lenses for the MACS cameras were chosen according to the field of view needed for each individual application. So far lenses with focal lengths of 35, 50, 70 and 100 mm have been used. The requirements for the image diagonal and resolution are given by the camera modules' specifications.

For the MACS 50/70 two different types of industrial-grade lenses are used. As two of the lenses are shifted in relation to the sensor, a longer image circle is needed for these modules. This is why large format lenses (Rodenstock Digaron-W 70 mm, 1:5.6) have been selected. For the third module with a concentrically arranged lens, a Zeiss Planar T* 50 mm, 1:1.4, has been used.

The Digaron lenses were especially developed for the application with digital sensors and are available in the required range of focal lengths (Qioptiq 2011). Because of its shorter image diagonal the construction of Zeiss SLR lenses (Zeiss 2011) is more compact.

2.3 *Camera Layout*

The core of the camera head is a body which is customized for each application. The body of the MACS 50/70 is milled from aluminium. The camera modules and lenses are attached to this structure. The shift of the sensor planes in relation to the optical axes is realized by the way the modules and lenses are attached to the body. The body structure also provides space for required filters as well as suspension points for attaching the camera to the aircraft. When changing the configuration for a different application the body has to be newly constructed. After each modification, the interior orientation of each camera module has to be re-calibrated.

Two of the MACS 50/70 modules are equipped with identical 70-mm-lenses. Their optical axes are shifted in relation to the centre of the respective image sensor. Fig. 2 shows the 70-mm-lenses and RGB camera modules in the foreground. The sensors are arranged alongside on one plane. This results in two image fields with only minor overlap.

In the standard application configuration they point in nadir direction. As the sensor plane and the image plane are parallel, the geometry of the image is orthogonal despite of the oblique viewing angle. This results in a constant ground sample distance as opposed to systems with tilted camera modules like the Z/I Imaging Digital Modular Camera (Tang et al. 2000).

The lens of the third module is arranged concentrically to the centre of the image sensor. Because of its shorter focal length it has a wider angle of view. Thus, this sensor approximately covers the combined image field of the other two camera modules (see Fig. 3).

In contrast to common aerial imaging systems it is not intended to generate a 'virtual negative' from the individual image fields, as described in Ladstädter & Gruber (2011). The generation of a 'virtual negative' would have tightened up the requirements for the geometric stability of the camera layout, limited its flexibility and resulted in higher costs.

In order to guarantee correct colour rendition by the sensors, infrared band-elimination filters are used for the other two modules, which – due to the narrower angle of view – have a higher ground resolution. For the third module a band-elimination filter for visible light is used. The module therefore provides a near infrared image.

2.4 *Control and Data Acquisition Unit*

The image data from the camera modules is transferred to one or several computers, which store the data and control as well as synchronize the cameras with GNSS or GNSS/INS-Systems. A 'Flight Image Acquisition Panel' (Fig. 4) is used with the MACS 50/70 which comprises all components needed to operate the camera system.

The panel is equipped with a PCO proprietary interface, which controls power and event handling. Up to four camera modules can be connected. The image data is obtained via 'Camera Link' interfaces. In addition, data from two gigabit Ethernet interfaces can be processed. A server board provides capacity for minor pre-processing and stores the data on a removable hard disk RAID. Important information such as error messages or status information is displayed on a graphic touch display.

UTC time is the basis for synchronizing the sensor data with further information, e.g. navigation data, temperature and flight protocols. The panel is equipped with a timer board which enables flexible handling of the synchronisation. By (temporarily) connecting a

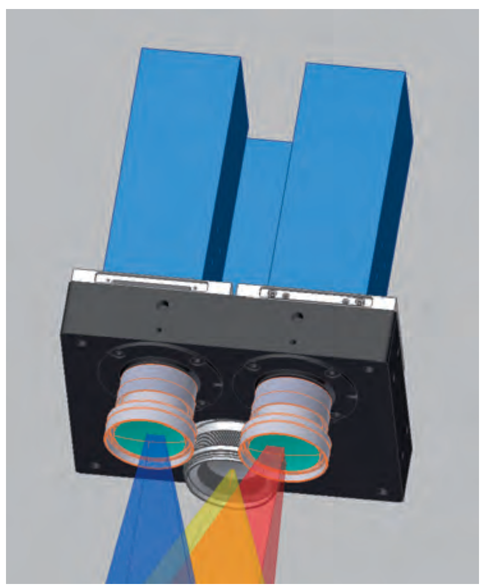

Fig. 2: Layout of the MACS 50/70 (sensor modules and lenses).

GPS antenna, an absolute time reference can be established within the board. Thus, sensors can be triggered and events can be time stamped. Whereas in common approaches a navigation system with GNSS receiver is necessary for triggering and event logging – due to the timer board – the MACS can be configured and tested without a navigation system.

Fig. 3: Image fields of the MACS 50/70 showing Santiago de Chile (right image semi-transparent).

Fig. 4: Flight Image Acquisition Panel.

2.5 *Position and Orientation Measurement*

As there are no relevant space and weight restrictions imposed by the aircraft operated for aerial imaging, for most applications an IGI AEROcontrol system is used as the combined inertial and GNSS system for the MACS 50/70. The horizontal attitude determination of the INS has a specified RMS of 0.004 degrees. The positioning data has RTK quality, which is common for aerial imaging applications.

The Modular Airborne Camera System enables scalability and modularity also with respect to geo-referencing. In all MACS layouts one camera module is included that points in nadir direction. This module does not only generate image data, but it also produces approximations of the exterior orientation for all camera modules. Therefore, in contrast to the orientation of e.g. laser scanners or linear sensor cameras, high accuracy in direct georeferencing is not necessary. This is also a major advantage when using pods, which have space and weight restrictions, or when processing low-grade navigation data (non-replaceable L1 GPS antenna, 'low grade' or no IMU).

Fig. 5: MACS 50/70 on board an aircraft with data acquisition unit, GNSS/INS system, stabilized platform and peripheral equipment (without wiring).

2.6 *Peripheral Equipment*

A modular set of electronics made of several 19-inch rack cartridges was developed for the use in aerial imaging aircraft. Each cartridge can be operated individually. The cartridges consist of different auxiliary devices such as GNSS receivers, antenna splitters and amplifiers, computer and network hardware. A 'Flight Power Distribution Panel' converts and stabilizes the electrical power provided by the aircraft.

Thus different configurations of camera systems and external sensors can be realized. For most cases application-specific solutions are no longer necessary. Fig. 5 shows a layout with camera system, IMU, gyro-stabilized mount and specially modified 19-inch rack with cartridges.

2.7 *Other MACS configurations*

Besides the MACS 50/70, other configurations using one to five camera modules have been tested to date. Four variants have been used in specialized aircraft for aerial imaging. They mainly differ in the configuration of the camera head. Two highly integrated camera systems have been designed for the use inside pods.

The MACS that will be described in the following was successfully used in 2010 and 2011. Its camera head layout is similar to the one of the MACS 50/70. However, different optics are used. It was configured for use inside a pod without GPS signal. The functionality of the 'Flight Image Acquisition Panel' had to be integrated into the pod as well.

For initializing the system a GPS antenna was connected and then removed shortly before take-off. Thus an integrated timer board was synchronized to GPS time. It had a specified free-run time accuracy of ±1.6 s/a. Even if, due to non-ideal conditions, the time varies by ±10 s/a, the variation in event time is as low as 2.3 ms during a two-hour flight. The images were time-stamped during the flight using the timer board. After the flight 10 Hz navigation data from an external GPS pod was assigned to the image data through temporal interpolation. The expected time stamp error of the timer board thus was below the resolution limit of the navigation data by a factor of 43, which is considered to be acceptable.

This configuration, which was used with a high-speed aircraft flying at 750 km/h, produced images with a ground sample distance of 15 cm. These images were successfully processed to 3D models.

Another MACS has been used in a pod carried by a motor glider (Fig. 6). It is equipped with a relatively inexpensive INS Novatel SPAN-CPT (specified horizontal accuracy RMS = 0.02 deg., L1/L2 GPS). Image data from this Modular Airborne Camera System has been processed successfully, too.

In order to meet the environmental conditions when flying at high altitudes partly heated casings have been constructed for some MACS configurations, especially for those used in pods.

3 Camera Software

The software operates the camera as well as peripheral devices. It was especially developed for the camera modules used and meets the requirements for different applications. The modular design of the software is a prerequisite to the adjustments that have to be made for the different versions of the Modular Airborne Camera System.

3.1 *Software Architecture*

The MACS software is based on a client-server architecture (Fig. 7). Essential functionality – communication, operating and monitoring the camera, frame grabbing as well as storing the image data on a hard disk – can be found in the server, the so called MACSServer. This software module is implemented as a service. When booting the computer, the operating system boots and monitors the service automatically. One MACSServer instance can operate up to four PCO cameras.

Several layers of buffers provide the basis for consecutive data storage even at high data rates (over 300MB/s). This requires special provisions concerning the responsiveness of the concurrent subsystems. All image data is stored as raw data with 16 bit colour depth.

3.2 *Control Software*

The MACSServer is equipped with a remote control interface (based on TCP/IP) via which the service can be configured and operated. The respective client software MACSRemoteControl (MRC) can operate and monitor one or more MACSServer instances and is the main control module of the camera system. The MRC has the following functions:

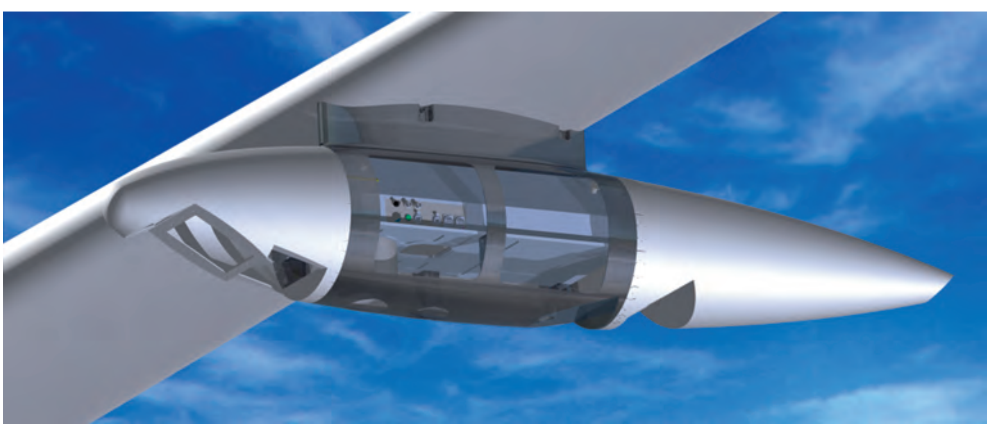

Fig. 6: MACS variant inside a glider pod (CAD model).

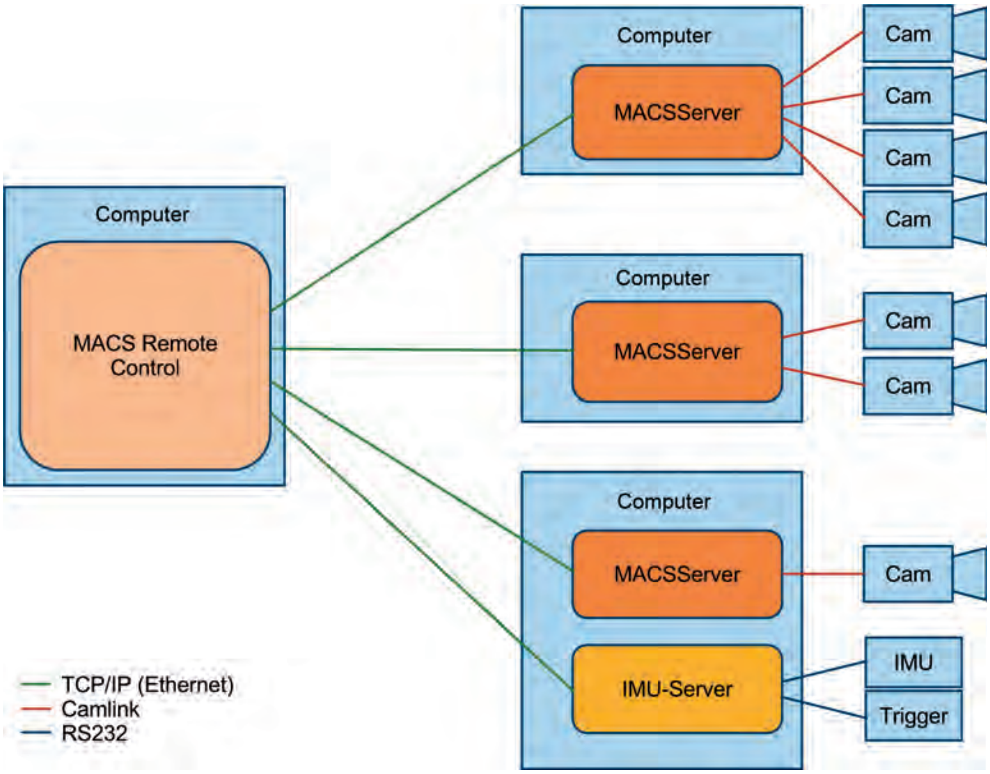

Fig. 7: Client-server architecture of the MACS software (sample configuration).

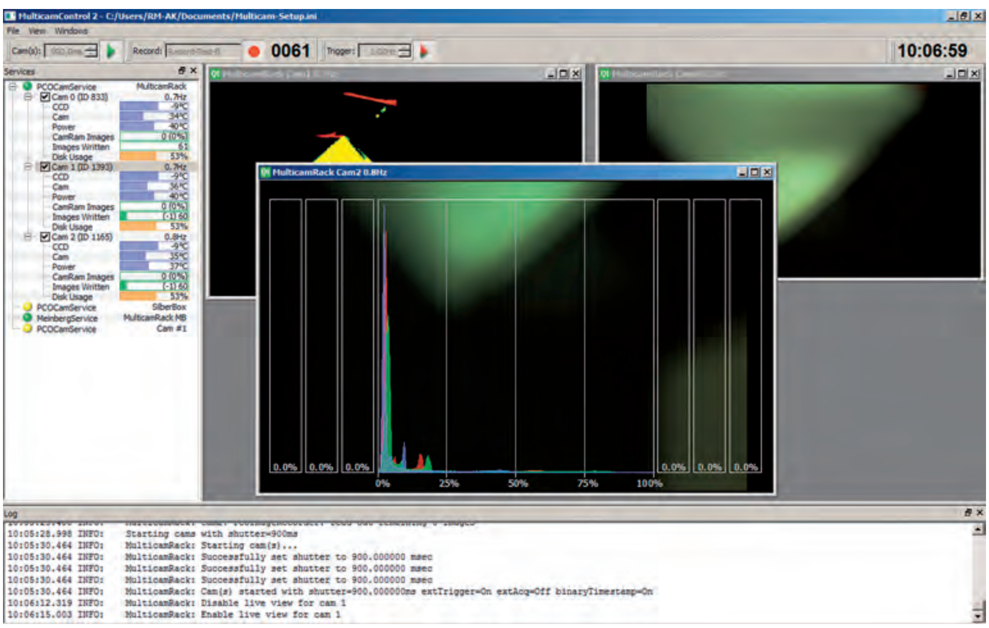

Fig. 8: MACSRemoteControl (MRC) interface.

- Display connected camera modules
- Display temperatures (CCD, camera casing, power supply)
- Set and display frame-rates of each camera
- Control parameters necessary for data acquisition (integration time in ms, recording files)
- Display live images of all cameras (incl. indication of under- and overexposure)
- Display buffer space of all buffers
- Display used/free hard disk space (for each data folder)
- Optional: Controlling further services (GNSS/INS sensors, trigger generators, etc.)

Furthermore, the MRC is built in this modular way in order to be able to operate and monitor other remote services, too. Services that control different GNSS/INS sensors and timer boards already exist.

The modular client-server architecture enables cascading of any sensor service, e.g. the MACSServer. With this any number of cameras can be connected and controlled as well as monitored simultaneously by the MRC as the central unit (Fig. 8).

4 Data Products

The direct output of the Modular Airborne Camera System comprises the individual images of the camera modules. They are in raw integer format with the 14 actual bits per pixel expanded to 16 bits, and contain – in addition to the image information – an image number and a time stamp.

For photogrammetric processing each individual image is converted into baseline TIFF format using an advanced raw converter – developed in-house at the DLR – that retains the images' original colour depth. Using this software, radiometric corrections (Dark Signal Non-Uniformity and Photo Response Non-Uniformity) are applied adaptively to each Bayer component (red, green and blue). Then, in order to obtain true RGB triplets, the pixels are passed on to the de-mosaicking algorithm. Subsequently, remaining geometric errors, particularly radial and tangential distortion, are eliminated using high-quality subpixel interpolation.

Calculations are executed in floating-point space throughout preprocessing in order to minimize the influence of round-off errors. The result is a set of homogeneous images that comply with the pinhole camera model and can therefore be directly used for further high-level processing.

By adding orientation information to the preprocessed images – in form of geographic coordinates – an instant product for time-dependant applications can be generated.

4.1 *Photogrammetric Products*

After image orientation, for which usually photogrammetric standard software is used, the individual images can be processed into different photogrammetric products. Among other applications, the image data is also used to test new approaches to automated orientation.

Subsequently, a digital surface model (DSM) is processed using the 'Semi-Global Matching' approach (Hirschmüller 2008). An accurate DSM with only minor gaps is the basis for creating a homogenous true ortho image mosaic from the high resolution image data (Hirschmüller & Bucher 2010). Samples of a DSM and true ortho image are shown in Fig. 9.

Because of the camera system's flexibility it is possible to generate more products than the standard true ortho image and digital surface model, for example point clouds, geometrically corrected oblique aerial photos or 3D models (Fig. 10). Current developments will lead to fully texturised 3D models.

4.2 *Sample Project*

The science and technology park in Berlin-Adlershof has been used as a test field and sample area for image flights. Hundreds of check points have been geodetically surveyed with an accuracy of about 2 cm in planimetry and height.

One image flight over Berlin-Adlershof was carried out in March 2011. Altogether, data for seven parallel strips and two cross tracks at a flight altitude of about 700 m above ground

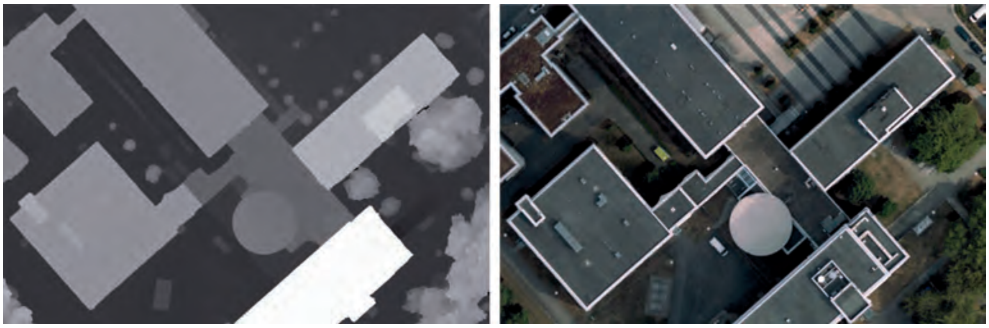

Fig. 9: Digital surface model and true ortho image processed from MACS data (showing the German Aerospace Center site in Berlin-Adlershof).

Fig. 10: Interactive 3D model without façade textures (Furth im Wald).

were acquired. A nominal ground sample distance of about 13 cm and 9 cm for the NIR and RGB camera modules, respectively, were acquired.

An overlap of approximately 98 % along-track and 78 % across-track was achieved for all images. Fig. 11 depicts each fifth image – respectively its outline – of one RGB camera module.

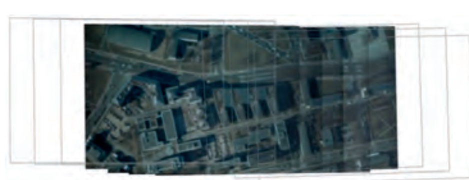

Fig. 11: Overlap along-track of one RGB camera module (reduced to 88 % for visualization).

The triangulation of the image data acquired by the NIR and RGB camera modules

Tab. 2: Height differences between check points and DSM generated from MACS image data.

Sensor	GSD [cm]	DSM grid [cm]	RMS [cm]*	Mean [cm]	Max/Min [cm]		Check Points [#]
NIR	13	15	8.8	5.0	13.9	−17.5	87
RGB 1	9	10	7.2	0.3	11.4	−9.1	54
RGB 2			5.7	−0.7	9.1	−10.7	53
*) gross error elimination							

was carried out separately. For the RGB modules a high resolution DSM and true ortho image was generated by Semi-Global Matching.

Subsequently, the accuracy of the generated DSM was checked by comparing DSM pixels with check points located in the target area. Tab. 2 lists the height differences between the height values of the check points and the respective DSM pixels. The results show that the MACS 50/70 can generate high-resolution data that meets current photogrammetric requirements with respect to accuracy.

5 Conclusion and Outlook

The Modular Airborne Camera System is mainly used for large scale experimental image flights. One of the key interests is high-resolution and high-accuracy 3D modelling of urban areas. Many campaigns thus focus on densely built-up urban areas. In contrast to existing camera systems as described in Jacobsen (2007) current MACS configurations are not intended for small-scale mapping.

The key difference between the MACS and other digital camera systems is the high frame rate of up to 5 images per second. Because of this frame rate and the resulting high overlap along flight of up to 98 %, complete and precise models of narrow structures, e.g. in urban areas, can be processed using Semi-Global Matching. Gapless surface models in particular enhance the classification of three-dimensional structures, for example when detecting corners and other attributes of buildings automatically (Fig. 12).

Another distinction to similar camera systems is the electronic shutter of the camera modules. It adds to the flexibility of the MACS and ensures stable radiometry and very short integration times.

Because of its small outline and low weight the camera system can be used in small aircraft or in pods. It is also possible to use the system for oblique aerial imaging. The MACS 50/70 layout, for example, was used in a helicopter to acquire oblique aerial photos (Günthner 2010).

For the use in pods, control concepts have been developed so that adaptations during the

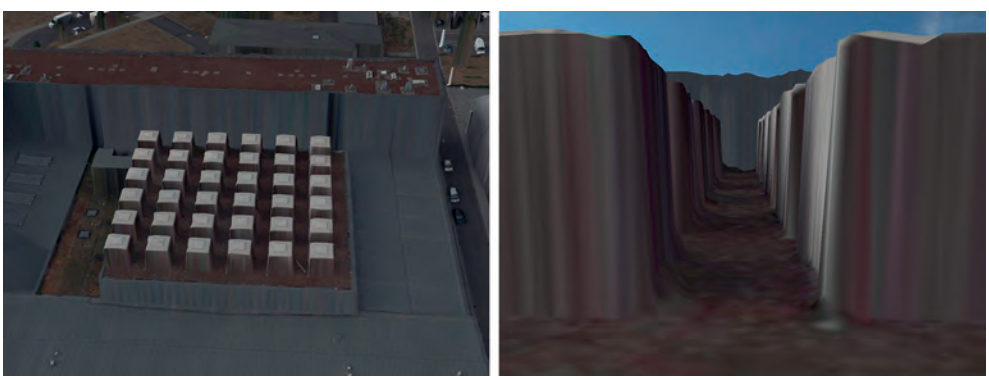

Fig. 12: High overlap reduces obscured areas and minimizes interpolation artefacts around elevated objects. The roof structures are 2 m apart, 3.7 m high and cover 4 × 4 m.

flight are unnecessary if the system is configured before take-off.

By using a camera module which is equipped with a matrix image sensor and points into nadir direction, the requirements for direct orientation measurement techniques can be reduced. The use of high-quality INS systems can therefore be avoided; the results are still of high quality. However, when high-quality orientation is available in real-time, on-board processing is possible.

The camera system is constantly being optimized. Because of its modular layout new and updated sensor modules can be integrated into the Modular Airborne Camera System. The camera system is not limited to panchromatic, RGB and NIR sensors. This opens up new fields of work, for example multi-frame thermography (Luhmann et al. 2011), as well as data fusion.

Publications on various aspects of the camera system and its products, for instance about the orientation of the images of the camera modules, the use of the system for special applications or regarding derived products are currently under preparation.

References

Günthner, W.A. (ed.), 2010: Bayerischer Forschungsverbund “Virtuelle Baustelle” (ForBAU): Abschlussbericht 2010. – TU München, Germany.

Grenzdörffer, G., 2008: Medium format digital cameras – a EuroSDR project. – IAPRS **XXXVII** (B1): 1043–1050, Beijing, China.

Hirschmüller, H. & Bucher, T., 2010: Evaluation of Digital Surface Models by Semi-Global Matching. – DGPF Proceedings **2010** (19): 571–580, Vienna, Austria.

Hirschmüller, H., 2008: Stereo Processing by Semi-Global Matching and Mutual Information. – IEEE Transactions on Pattern Analysis and Machine Intelligence **30** (2): 328–341, Los Alamitos, CA, USA.

Jacobsen, K., 2007: Comparison of Large Size Digital Airborne Frame Cameras with Analogue Film Cameras. – In: Gomarasca, M.A. (ed.), 2007: GeoInformation in Europe. – Proceedings of the **27th** EARSel Symposium: 89–95, Millpress, Rotterdam, The Netherlands.

Kodak, 2011: Product Summary Kodak KAI-11002 Image Sensor. – www.kodak.com:80/global/plugins/acrobat/en/business/ISS/productsummary/Interline/KAI-11002ProductSummary.pdf (25.07.2011).

Ladstädter, R. & Gruber, M., 2011: Optimales Stitching-Verfahren für Multi-Sensor basierte Luftbildkameras. – DGPF Proceedings **2011** (20): 91–100, Vienna, Austria.

Lehmann, F., Bucher, T., Pless, S. & Wieden, A., 2011: Hochauflösende Oberflächenmodelle und True Ortho Photos aus digitalen Luftbildkameras: Die Entwicklung anhand von Beispielen der letzten 10 Jahre. – DGPF Proceedings **2011** (20): 101–108, Mainz, Germany.

Luhmann, T., Ohm, J., Piechel, J. & Roelfs, T., 2011: Geometrische Kalibrierung von Thermographiekameras. – Photogrammetrie-Fernerkundung-Geoinformation **2011** (1): 5–15.

McCarthy, T., Fotheringham, A.S. & O’Rian, G., 2007: Compact Airborne Image Mapping System (CAIMS). – IAPRS **XXXVI** (5/C55): 198–202, Padua, Italy.

PCO AG, 2011: pco.4000 Cooled Digital 14 bit CCD Camera System. – www.pco.de/de/sensitive-kameras/pco4000/ (25.07.2011).

Qioptiq, 2011: Rodenstock – Objektive für die digitale Fachfotografie – www.rodenstock-photo.com/de/main/products/lenses-for-digital-photography/ (25.07.2011).

Tang, L., Dörstel, C., Jacobsen, K., Heipke, C. & Hinz, A., 2000: Geometric accuracy potential of the Digital Modular Camera. – IAPRS **XXXIII** (4): 1051–1057, Amsterdam, The Netherlands.

Track’Air, 2011: MIDAS – Multi-cameras Integrated Digital Airborne System. – http://82.141.26.35/wp-content/uploads/2010/11/TrackAir_MIDAS_brochure.pdf (25.07.2011).

Zeiss, 2011: Carl Zeiss Planar T* 1.4/50 mm. – www.zeiss.com/C12578B8004E8E1D/0/19ECDA719620FACCC12578CD0035C432/$file/flyer_planar_t_14_50_ger.pdf (25.07.2011).

Address of the Authors:

Dipl.-Geol. Frank Lehmann, Dipl.-Inf. Ralf Berger, Dipl.-Ing. Jörg Brauchle, Dipl.-Inf. Daniel Hein, Dipl.-Ing. Henry Meissner, Dipl.-Ing. Sebastian Pless, Dipl.-Ing. (FH) Bernhard Strackenbrock, Dipl.-Ing. (FH) Alexander Wieden, German Aerospace Center, Optical Information Systems, D-12489 Berlin, Germany, Tel.: +49-30-67055-425, -572, -274, -276, -540, -350, -512, -467, Fax: +49-30-67055-385, e-mail: firstname.lastname@dlr.de

Manuskript eingereicht: Juli 2011
Angenommen: September 2011

PFG 2011 / 6, 0447–0455
Stuttgart, December 2011

Short paper

INSPIRE Data Specification for harmonised Orthoimageries

Markus Seifert, Munich

Keywords: INSPIRE, orthoimagery, data specification, spatial data infrastructure

Summary: Orthoimageries may have a specific role which comprises the extraction of thematic information, as well as mapping and monitoring of the environment. Therefore, the related data theme has been included in the Annex II of the INSPIRE directive. Data specifications are currently developed for 34 INSPIRE data themes. Based on the data specifications INSPIRE will develop legally binding implementing rules. A review process has been launched to allow stakeholders to submit comments to the drafts in order to achieve reasonable requirements for implementation (INSPIRE 2011). The review process ended at the end of October 2011. This paper briefly introduces the main principles and objectives of the INSPIRE initiative. Then, the data specification for the data theme Orthoimagery is explained in detail.

Zusammenfassung: *INSPIRE Datenspezifikation für Orthophotos.* Orthophotos spielen eine wichtige Rolle beim Extrahieren von thematischen Informationen, zur Aktualisierung von topographischen Karten und zum Monitoring der Umwelt. Aus diesem Grund wurde dieses Datenthema in den Annex II der INSPIRE Rahmenrichtlinie aufgenommen. Derzeit werden zu insgesamt 34 Themen die entsprechenden Datenspezifikationen erarbeitet. Auf Grundlage der Datenspezifikationen werden rechtlich verbindliche Durchführungsbestimmungen erstellt. Um praxisnahe und umsetzbaren Vorgaben festzulegen, wurde im Rahmen eines Reviews die Fachöffentlichkeit zur Kommentierung der Datenspezifikationen aufgerufen (INSPIRE 2011). Das Reviewverfahren lief bis Ende Oktober 2011. Dieser Beitrag erläutert kurz die Grundlagen und Ziele von INSPIRE. Anschließend wird die Datenspezifikation für Orthophotos im Detail vorgestellt.

1 Introduction

Currently most of the high quality spatial information is available at local and regional level and is therefore difficult to exploit in a broader context for a variety of reasons. The situation on spatial information in Europe is characterized by fragmentation, gaps regarding the availability of geographical information, duplication of data collection and problems of identifying, accessing or using the data that is available.

The data often has unsatisfactory or undefined quality, is based on proprietary geographic information systems and not accessible to the public or other users at the local, regional, national or international level. Policies need to be put in place to reduce the duplication of data collection, to promote harmonisation efforts and to facilitate a wide dissemination of the data. By passing the INSPIRE directive, also orthoimagery are addressed in order to establish interoperable datasets across Europe.

2 The European Spatial Data Infrastructure (INSPIRE)

Good policy relies on quality information. The increasing complexity and interconnectedness of issues that affect the quality of life today is recognized by the policy-makers and influences the way new policies are being prepared today. INSPIRE (Infrastructure for Spatial Information in Europe) (INSPIRE 2007) is a Eu-

DOI: 10.1127/1432-8364/2011/0097 1432-8364/11/0097 $ 2.25

ropean directive currently being implemented by the EU member states to support the availability of spatial information for the formulation, implementation and evaluation of European Union policies. It intends to set the legal framework for the gradual creation of a spatial information infrastructure. INSPIRE will initially focus on the environmental policy needs but will as a cross-sectoral initiative gradually be extended to other sectors such as agriculture and transportation, in order to let other interested Commission services participate.

The INSPIRE initiative intends to trigger the creation of a European spatial information infrastructure that delivers integrated spatial information services to the users. These services shall allow the users to identify and access spatial or geographical information from a wide range of sources, from the local level to the global level, in an inter-operable way for a variety of uses. The target users of INSPIRE include policy-makers, planners and managers at the European, national and local level and the citizens and their organisations. Possible services are the visualisation of information layers, overlay of information from different sources, spatial and temporal analysis, and alike.

The spatial information infrastructure addresses both technical and non-technical issues, ranging from technical standards and protocols, organisational issues, data policy issues including data access policy and the creation and maintenance of geographical information for a wide range of themes starting with the environmental sector.

The INSPIRE implementation will follow a step-wise approach, starting with unlocking the potential of existing spatial data and spatial data infrastructures and then gradually harmonising data and information services allowing eventually the seamless integration of systems and datasets at different levels into a coherent European spatial data infrastructure.

The first step will focus on the harmonisation of documenting existing datasets (metadata) and on the necessary tools to make this documentation accessible. Harmonization is defined as providing access to spatial data through network services in a representation that allows for combining it with other harmonised data in a coherent way by using a common set of data product specifications. This includes agreements about coordinate reference systems, classification systems, application schemas, and other components (INSPIRE Drafting Team 2007).

The second step will primarily aim at providing common ways to access the spatial datasets themselves allowing easy analysis of data on different themes coming from different sources. An example of such analysis is visual inspection of spatial relations between phenomena by the overlay of datasets.

The third step will target at the establishment of common models of the environmental objects for which spatial data is collected, such as transport networks, forests, orthoimagery This will allow the mapping of existing datasets to a common set of models, meaning the

INSPIRE Principles

The INSPIRE initiative will improve the current situation by triggering the creation of a European Spatial Data Infrastructure for the access and use of spatial information built on the basis of the following principles (INSPIRE 2011):

- Data should be collected once and maintained at the level where this can be done most effectively.
- It must be possible to combine seamlessly spatial information from different sources across Europe and share it between many users and applications.
- It must be possible for information collected at one level to be shared between all the different levels, e. g. detailed for detailed investigations, general for strategic purposes.
- Geographic information needed for good governance at all levels should be abundant and widely available under conditions that do not restrain its extensive use.
- It must be easy to discover which geographic information is available, fits the needs for a particular use and under what conditions it can be acquired and used.
- Geographic data must become easy to understand and interpret because it can be visualised within the appropriate context and selected in a user-friendly way.

start of the creation of a really harmonised spatial data infrastructure that will facilitate the combination of information of various sources and more advanced analysis work.

The fourth and last step will build upon the previous steps and concentrate on completing the common models and on providing the services to fully integrated data from various sources and various levels, from the local to the European level into coherent seamless datasets supporting the same standards and protocols. This step will allow real time access to up-to-date data across the whole of Europe.

These steps will partly be carried out in parallel, depending on user needs and degree of availability and harmonisation of existing information. All these steps involve actions of standardisation, of harmonisation and integration of data and services (Fig. 1). In this context standardisation is understood as the development of solutions for INSPIRE-components based on International Standards published by the International Organisation for Standardisation (ISO) or by the Comité Européen de Normalisation (CEN). Integration is defined as the linkage of two or more software systems by the use of a common data and method base (ISO 19132:2007).

Recognising the specific role that orthoimagery for extracting thematic information, mapping, and monitoring the environment, the related data theme has been included in Annex II of INSPIRE. Data specifications are currently being developed for 34 data themes specified in the annexes of the INSPIRE directive. These annexes are published as draft versions at INSPIRE (2011). The specifications cover all relevant issues for the harmonisation of datasets. The *Orthoimagery* data theme includes imagery from the infrared to ultraviolet region of the electromagnetic spectrum, derived from scanning of film positives and negatives, as well as digital airborne and satellite imagery.

3 Data Specification for Orthoimagery

Photographs and other images taken from airborne or space borne platforms are important means for documenting the surface of the

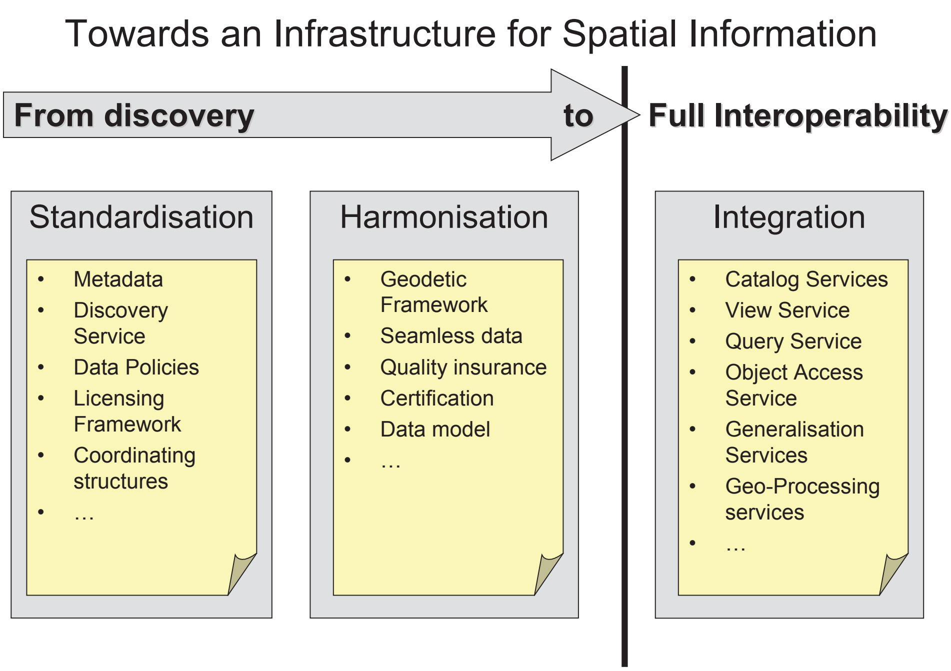

Fig. 1: Towards an Infrastructure for Spatial Information.

Earth and the state of the environment. However, these images have geometrical distortions caused by the optics and the camera/sensor tilt, as well as the differences of the elevations of the Earth's surface. Orthorectification is the process of removing these distortions resulting in a specific product: orthoimagery (Kraus 2007).

The INSPIRE data specification on orthoimagery has been prepared following the participative principle of a consensus building process. The stakeholders, based on their registration as a Spatial Data Interest Community (SDIC) or a Legally Mandated Organisation (LMO), had the opportunity to bring forward user requirements and reference materials, propose experts for the specification's development, and participate in reviewing and testing the data specifications. The Thematic Working Group responsible for the specification development was composed of experts from Belgium, Finland, France, Germany, Norway, Spain, UK, and the European Space Agency. The specification process took place according to the methodology elaborated for INSPIRE respecting the requirements and the recommendation of the INSPIRE Generic Conceptual Model. This INSPIRE Generic Conceptual Model has been developed as a baseline for the themes defined in the annexes in the INSPIRE directive and specifies the generic aspects of geometry, topology, time, thematic information, identifiers and relationships between spatial objects. As Orthoimagery is one of the themes documented in the INSPIRE annex this model applies (INSPIRE Drafting Team 2007).

Since orthoimagery can be defined as regular sampling of radiation values continuously varying in space, the grid coverage as defined in ISO 19123 *Schema for coverage geometry and functions* (ISO 19123:2005) has been selected for the spatial representation. The orthoimage coverage is the key concept of the data model that may refer to a single orthoimage or a mosaic of orthoimages. Moreover, an orthoimage coverage itself can be composed (aggregated) of other orthoimage coverages. The properties describing the geometric basis (i. e. the grid) are inherited from the Generic Conceptual Model and the ISO 19123. This allows the inclusion of technical properties such as the range and the allowed values of the coverage according to ISO 19123, the interpolation method, and the way of assigning the records to the grid points like the observed light spectrum. In fulfilling the requirement of the Directive each orthoimage coverage carries a unique identifier enabling its unambiguous identification within the INSPIRE-community. In addition, other well defined information can be attached to each orthoimage coverage, comprising name, footprint, and temporal characteristics.

Since an orthoimage coverage may consist of orthoimages that are based on images captured at different times, the *Orthoimagery* data model provides the possibility to express the data acquisition time of the images that are part of the coverage. By including the seamlines of the mosaic it is possible to address every image of the coverage and attach an individual time stamp. The feature type Seamlines informs the user which part of the orthoimage collection has been derived from which input image. It consists of a discrete coverage that returns a reference to an input image (data type *ImageSource*) for any direct position within the single polygon identifying the contribution of this image. Aggregated orthoimage coverages have to be aligned, i. e., fit to a common grid. In addition, alignment is also necessary when orthoimage coverages are integrated at the European level. In order to do so, a pan-European grid is necessary. The data specification recommends the usage of the Grid_ETRS89-GRS80, which is based on geographical coordinates. Storing orthoimagery data in geographical coordinates also helps to bridge the difficulties caused by the diverse projection systems in use within Europe. Whenever a specific projection is needed, it can be obtained by an on-the-fly transformation of the area of interest. Interoperability is further supported by harmonised metadata elements and an agreed encoding. The INSPIRE specification for orthoimagery provides a compact, purely conceptual presentation of the data theme; therefore it does not deal with file-based tiling, which is considered as a practical implementation for data storage and delivery.

Being independent of particular production methods and platforms the INSPIRE orthoimagery data specification provides an imagery base data that constitutes value not only in European, but also in local, regional and global contexts.

For the purposes of this INSPIRE data specification, orthoimagery shall include orthorectified imagery from the infrared, through the visible, to the ultraviolet region of the electromagnetic spectrum derived from:

- scanned film positives or negatives,
- digital airborne sensors (such as frame cameras or push-broom sensors),
- satellite imagery of the Earth.

The scope of the Orthoimagery data specification does not include:

- Data from the microwave, X-ray, radio or gamma ray areas of the electromagnetic spectrum,
- LIDAR data (light detection and ranging),
- Unrectified oblique aerial photography. Note: orthorectified imagery produced from oblique photography – e. g. as a mosaic – *is* included,
- Terrestrial imagery (e. g. from cameras based on the ground or on road or rail vehicles),
- Aerial video imagery. Note that orthorectified images created from video frames *is* included,
- Imagery of the sea bed from underwater sensors (only air-borne and satellite sensors are covered by the specification),
- Meteorological satellite imagery (such data is not primarily concerned with imagery of the Earth's surface).

This does not prevent data providers from delivering such datasets in conformity with this INSPIRE data specification if they feel the need to do so.

This INSPIRE data specification does not place restrictions on the spatial resolution given by the heterogeneity of data sources and the wide range of use cases across Europe. All levels of resolution are affected: the European level, the national level, the regional level and the local level. However, a minimum spatial resolution is not required. Orthoimagery data, which is a kind of raster data, is a simple form of geographic information. It consists of a set of values measuring a radiant energy, organized in a regular array of points or cells together with associated metadata and georeferencing. The *coverage* approach specified in the ISO 19123 is particularly well-suited for modelling such a data structure. Coverage is a type of feature describing the characteristics of real-world phenomena that vary over space. In contrast to other types of features, its non-spatial attributes are strongly associated with its spatial attributes (i. e. its geometry). It acts as a function to return attribute values from its range for any direct position within its spatio-temporal domain.

Since it depicts continuously-varying phenomena, an orthoimage is inherently a continuous coverage. An associated interpolation method (regular quadrilateral grid) enables the evaluation of the coverage at direct positions between the elements of its domain (e. g. points). The attribute values of an orthoimage are arranged using the geometry of a regular quadrilateral grid in two dimensions. Such a grid is a network composed of two sets of equally spaced parallel lines that intersect at right angles. The intersection points are called grid points. The areas delimited by the grid lines are called grid cells. The grid cells are rectangles.

A grid coordinate system is defined by means of the origin and the axis of the grid, that are expressed in a coordinate reference system. Grid coordinates are measured along the axes.

Furthermore, the grid of an orthoimagery coverage is geo-rectified in the sense of ISO 19123. It is related to the Earth through an affine relationship that makes a simple transformation between the grid coordinates and the coordinates in the associated Earth-based reference system. The transform parameters are determined by the location of the grid origin, the orientation of the axis and the grid spacing in each direction within the external coordinate reference system.

3.1 *Concept of mosaicking*

In this data specification, mosaicking is defined as the production process that allows the creation of a single orthoimage from several original orthorectified images. It usually involves thorough radiometric processing to give a homogeneous seamless polish to the re-

Fig. 2: Mosaicked orthoimage with seamlines (Île d'Yeu, France, scale appr. 1:68.000).

sulting mosaicked orthoimage. An example is shown in Fig. 2.

The temporal extent of a mosaic can only be stated as a time interval, because the original images are almost always acquired at different dates and times. However, a use case survey has identified a clear requirement of some user groups regarding the exact date of each pixel of the mosaic. That is the reason why the orthoimagery application schema provides an approach to spatially indicate acquisition dates through linking orthoimage pixels to the image sources temporal attributes. In practical terms, it is based on the use of the seamlines that have been created to perform mosaicking process (Fig. 2).

3.2 *Concept of tiling*

Different motivations can lead data producers to break orthoimagery data into smaller parts. This process is usually known as "tiling". However, this term may encompass different meanings depending on the abstraction level of the description. Three main levels of tiling need to be distinguished:

Firstly, tiling may be internally implemented in file formats (e. g. tiled TIFF). By rearranging image content into roughly square tiles instead of horizontally-wide strips, this method improves performances for accessing and processing high-resolution images. Since it basically reflects the storage structure of data, it does not appear in the application schema which is restricted to the conceptual level. Secondly, high-resolution orthoimages covering broad territories represent large volumes of data that can often not be stored reasonably in a single image file. Data producers usually cut them out into separate individual files to facilitate their storage, distribution and use. The most common tiling scheme used in orthoimagery is a simple rectangular grid where tiles edge-match without image overlaps or gaps (Fig. 3a). However, it is sometimes required that the individual tiles overlap with their neighbours to ensure a certain spatial continuity when handling them (Fig. 3b). The tiling scheme may also have a less regular geometry with a varying density of tiles (Fig. 3c).

This file-based data structure is artificial and has no real logical meaning on its own even though it is usually based on grid elements. Therefore it is addressed in the encoding part of this data specification.

Finally, large orthoimages can also be divided into subsets that have a thematic meaning as they describe logical structures (e. g. mapsheets, administrative units like regions or districts, etc.). Unlike the previous case, this type of file-independent tiling is fully within the scope of the conceptual model. But pragmatically, an aggregation (a reverse view on tiling) may offer more possibilities and should increase data harmonization. So, a collection of orthoimage coverages can be aggregated to make up a larger single coverage. This has the advantages that:

- The input orthoimages may just partially contribute to the aggregated coverage.
- Consequently, the input orthoimages may spatially overlap whenever necessary.

This mechanism is called "orthoimage aggregation" and also covered by the data model.

3.3 *Data structure*

A first data structure level is provided through the concept of coverage. In addition, the Orthoimagery application schema offers a second level that consists of grouping of coverages themselves in another logical structure. In other words, subsets from several homogeneous orthoimage coverages can be combined so that they build a new orthoimage coverage. The aggregated coverage does not hold directly its own pixel values. It just makes reference to its input coverages, thereby avoiding data duplication. The range set of the coverage is computed on the fly by a service or an application when requested by users.

For applicability, input and aggregated orthoimage coverages shall be part of the same Orthoimagery dataset (Fig. 4).

This mechanism is fully recursive so that an orthoimage coverage can itself be a composition of already-aggregated orthoimage coverages. The data structure is defined in a UML data model that graphically explains the structure and the content of the orthoimagery data specification including all feature types attributes and associations between the features (Fig. 5).

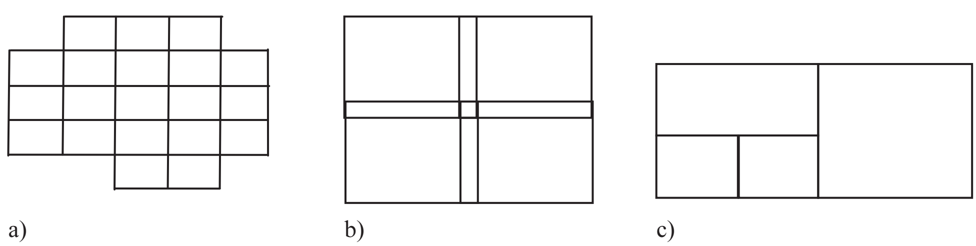

Fig. 3: Various configurations of tiling schemes, e. g. in support of different map-series. a) Simple grid with edge-matching tiles, b) Overlapping tiles, c) Varying density of tiles.

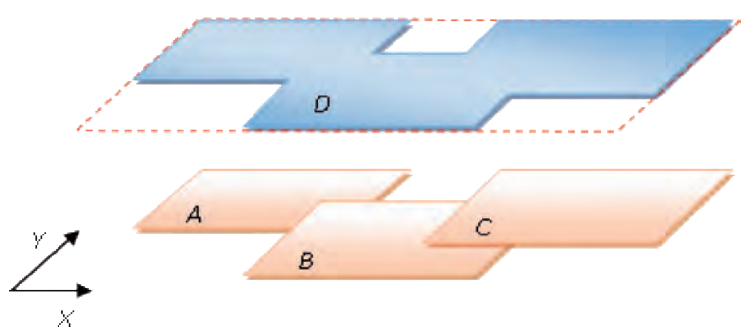

Fig. 4: Orthoimage aggregation principle: overlapping orthoimage coverages A, B and C compose the aggregated orthoimage coverage D, the bounding box of which is dotted.

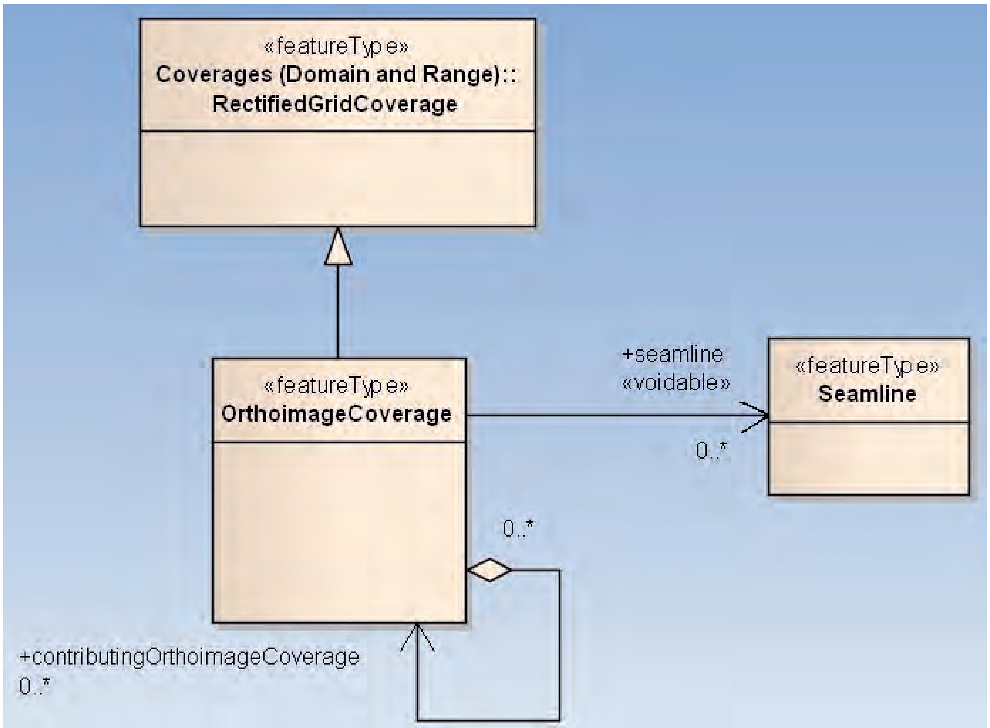

Fig. 5: UML class diagram: class Orthoimagery-Overview, *Orthoimagery* application schema.

3.4 *Feature type OrthoimageCoverage*

The feature type *OrthoimageCoverage* is the core element of the *Orthoimagery* application schema. It is defined by the INSPIRE Directive as "geo-referenced image data of the Earth's surface, from either satellite or airborne sensors". It may be derived from one single input image acquired by a sensor or from different input images that have been mosaicked together.

The class *OrthoimageCoverage* specializes the type RectifiedGridCoverage and inherits properties necessary to process the coverage. The type RectifiedGridCoverage is defined in the INSPIRE Generic Conceptual Model. The original definition can be found in the ISO 19123. A RectifiedGridCoverage is a continuous quadrilateral grid coverage. This is coverage with a rectangular grid pattern and an uninterrupted coverage of the Earth's surface – like an orthophoto. The attributes *domainSet* and *rangeType* describe the geometry and the range of the coverage. These elements are explained in ISO 19123 for coverages. A further attribute named *RangeSet* contains the feature attributes values. In the case of orthophotos they denote the colour and grey values of each pixel. Finally, the *coverageFunction* explains how to assign the records to the points of the grid according to ISO 19123. For a more detailed description of these inherited attributes, see the section 9.9.4 of the GCM [DS-D2.5] (Generic Conceptual Model). The *domainExtent* and *interpolationType (*regular quadrilateral grid) attributes stemming from ISO 19123 complete the description of the coverage characteristics.

4 Next steps

All INSPIRE data specifications will be part of the INSPIRE implementing rules which covers all mandatory elements to be delivered by the data providers. Implementing rules are legal acts which have to be implemented by the EU member states. Technical details of the data specification will be moved to the Technical Guidance Documents. Although these guidance documents are not part of the legal framework their requirements and recommendation should be also considered in order to achieve interoperability of data in Europe. A review process has been launched to allow stakeholders to submit comments to the drafts in order to achieve reasonable requirements for implementation (INSPIRE 2011). The review process ended at the end of October 2011. The implementing rules as well as the technical guidance documents for all data themes will be ready by the mid of 2012.

References

INSPIRE Homepage, 2011: http://inspire.jrc.ec.europa.eu/ (6.8.2011).

INSPIRE Directive, 2007: Directive 2007/2/EC of the European Parliament and of the Council of 14 March 2007 establishing an Infrastructure for Spatial Information in the European Community (INSPIRE). – Official Journal of the European Union, http://eur-lex.europa.eu/JOHtml.do?uri=OJ:L:2007:108:SOM:EN:HTML, **L108** (50) (6.8.2011).

INSPIRE Drafting Team 2007: Data Specifications – Deliverable D2.5: Generic Conceptual Model. – http://inspire.jrc.ec.europa.eu/reports/ImplementingRules/inspireDataspecD2_5v2.0.pdf (15.9.2011)

ISO 19123, 2005: Geographic information – Schema for coverage geometry and functions. – International Organization for Standardization, ISO Central Secretariat, Geneva, Switzerland.

ISO 19130, 2010: Geographic information – Imagery sensor models for geopositioning. – International Organization for Standardization, ISO Central Secretariat, Geneva, Switzerland.

ISO 19132, 2007: Geographic information – Location-based services – Reference model. – www.iso.ch (15.9.2011)

Kraus, K., 2007: Photogrammetry: geometry from images and laser scans. – Translated by Ian Harley and Stephen Kyle. – 459 p., de Gruyter, Berlin & New York.

Address of the Author:
Dr. Markus Seifert, Landesamt für Vermessung und Geoinformation, D-80538 München, Germany, e-mail: markus.seifert@lvg.bayern.de

Manuskript eingereicht: Juli 2011
Angenommen: September 2011

Berichte von Veranstaltungen

53. Photogrammetrische Woche, 5.–9. September 2011, Stuttgart

Multiray Photogrammetry Meets Advanced LIDAR: Unter diesem Motto stand die 53. Photogrammetrische Woche (PhoWo) 2011 und bot ein spannendes Forum, auf dem gestritten wurde, welches der beiden Verfahren bei der detaillierten dreidimensionalen Objektrekonstruktion die Nase vorn hat. Ein Höhepunkt war sicher die mit exzellenten Protagonisten beider Seiten besetzte Podiumsdiskussion am Donnerstag.

Die Schwerpunktthemen dieses Jahres waren

- Weiterentwicklung digitaler Luftbildkameras
- Erzeugung von Punktwolken und deren Verarbeitung
- Schritte zur erweiterten Realität in 3D-Welten

Die PhoWo wird im zweijährigen Rhythmus veranstaltet. In diesem Jahr konnten die Veranstalter etwa 340 Gäste aus rund 45 Ländern (ohne Veranstalter) begrüßen. Dieses sind für Photogrammetrie und Fernerkundung beeindruckende Zahlen. Ein weiteres herausstechendes Merkmal war wie auch schon in der Vergangenheit ein Programm ohne Parallelvorträge. Das einheitlich in englischer Sprache gehaltene Symposium war auch diesjahr wieder ausgezeichnet organisiert. Den Veranstaltern gebührt ein herzlicher Glückwunsch.

Als Auftakt zu den Fachvorträgen sprach Allan Carswell. Er ist der Gründer der kanadischen Firma Optech Inc. und gab einen großartigen Überblick über LIDAR-Anwendungen gestern und heute, beispielsweise bei der Wassertiefenbestimmung bis 20 m Tiefe und der Analyse der Marsatmosphäre mit einem Optech-Gerät auf einem Mars-Rover.

Am Ende des ersten Vormittags sprach Susanne Becker zur automatisierten Vervollständigung von LOD3-Gebäudemodellen im Fall von lückenhaften Ausgangsdaten, z. B. bei Verdeckungen.

OpenPhowo-Partner

Die OpenPhowo-Partner haben einen wesentlichen Anteil an der Attraktivität der PhoWo. Die traditionellen Gerätevorführungen an den Nachmittagen bieten einen direkten Kontakt zu den Geräteherstellern und einen unmittelbaren Vergleich der Systeme, welchen es sonst nur selten gibt. Die spannendste Frage aber betraf die Verortung der neuen Firmengruppen nach der Konsolidierung der Firmenlandschaft im vergangenen Jahr, denn die PhoWo bot einen der ersten großen öffentlichen Auftritte in neuer Konstellation.

Die OpenPhowo-Partner waren im einzelnen Hexagon Geosystems in Heerbrugg, Trimble Germany Geospatial Division in Stuttgart, Ingenieurgesellschaft für Interfaces (IGI) in Kreuztal, Vexcel Imaging/Microsoft in Graz und BAE Systems als JuniorOpen-Phowo-Partner.

Hexagon Geosystems besteht unter anderem aus den früheren Firmen Z/I Imaging und Leica Geosystems und war in Stuttgart durch Jack Ickes, vertreten. Vorgestellt wurden die ADS 80 mit dem zugehörigen Softwarepaket XPro (Zeilenkamera), die neue Z/I DMC II mit einem speziellen für Luftbildanwendungen von DALSA entwickelten Flächenarray (140, 230 und 250 MPixel) und die Leica RCD 30 (Fläche, Mittelformat, modularer Aufbau). Die Präsentation von Hexagon gestalteten Ruedi Wagner und Klaus Neumann. Trimble Germany Geospatial Division besteht unter anderem aus den früheren Firmen INPHO and Definiens. Ralph D. Humberg zeigte Neuerungen in der Software. Hubert Minten stellte für die Firma IGI u.a. den RailMapper vor, ein schienengebundenes Messsystem zur effizienten Bestimmung von Lichtraumprofilen. Das System ist aus dem StreetMapper entstanden und basiert auf IGIs AEROcontrol/TERRA-control. Vexcel Imaging/Microsoft stellte das neue Flaggschiff der UltraCam-Familie vor, nämlich die UltraCam Eagle (Fläche, 260 MPixel). Für Vexcel sprach Michael Gruber.

Podiumsdiskussion: Graham, Dold, Carswell, Fritsch, Haala, Hirschmüller, Hyyppä

Podiumsdiskussion

Das Thema der Podiumsdiskussion entsprach dem Motto der PhoWo, *Multiray Photogrammetry Meets Advanced LIDAR*. Zur Runde gehörten ALLAN CARSWELL, Optech, LEWIS GRAHAM, GeoCue, HEIKO HIRSCHMÜLLER, DLR, JÜRGEN DOLD, Hexagon Geosystems, NORBERT HAALA, ifp Stuttgart und JUHA HYYPPÄ, Finnish Geodetic Institute. Die Leitung hatte DIETER FRITSCH.

Noch während der letzten Photogrammetrischen Woche 2009 erlebten die Besucher eine sehr kontroverse Diskussion über die Bedeutung von LIDAR Punktwolken im Vergleich zu den mit bildbasierten Verfahren erzeugten dichten Punktwolken. In diesem Jahr bestand Konsens im Podium darüber, dass beide Verfahren nicht nur ihre Daseinsberechtigung haben, sondern vielmehr die Chance einer gegenseitigen Fusion bieten.

Carl Pulfrich Preis

Der Carl Pulfrich Preis wurde 1968 von der Firma Carl Zeiss, Oberkochen, gestiftet. Carl Pulfrich hatte die Photogrammetrische Woche 1909 ins Leben gerufen, damals unter dem Titel *Ferienkurs zur Stereophotogrammetrie*. Mit großer Freude haben die Veranstalter der PhoWo die Zusage des Firmennachfolgers, Hexagon Geosystems, entgegengenommen, den Preis auch weiterhin zu stiften. In diesem Jahr wurde er an HEIKO HIRSCHMÜLLER für die Entwicklung des Semi-Global Matching verliehen.

Carl Pulfrich Preisträger HEIKO HIRSCHMÜLLER (rechts) mit JACK ICKES, Hexagon Geosystems

1. Schwerpunkt: Weiterentwicklung digitaler Luftbildkameras

Der Themenkomplex *Weiterentwicklung digitaler Luftbildkameras* wurde mit einem Leitvortrag von MICHAEL CRAMER unter dem provokanten Titel *Geometry perfect – Radiometry unkown* eingeleitet.

Vor dem Hintergrund der zu erwartenden 80-100 GNSS Satelliten gab BERND EISFELLER einen Überblick über die weltweit wichtigsten Systeme zur Genauigkeitssteigerung der

GNSS-Positionsbestimmung. Zwei daran anschließende Vorträge behandelten den Einsatz von UAVs (Unmanned Aerial Vehicles). Werner Mayr stellte eine Blom-Firmenlösung vor. Henri Eisenbeiss bilanzierte das heutige Potenzial unter Berücksichtigung der verfügbaren Plattformen und Navigationskomponenten.

Jens Kremer zeigte danach die IGI-Lösung zur Kartierung von Hochspannungsleitungen.

Ein weiteres Thema waren die Höhenmodelle. Marco Weber demonstrierte das Genauigkeitspotenzial des weltweiten Höhenmodells auf der Basis des Satellitenpaares TerraSAR-X und TanDEM-X. Konrad Schindler erläuterte die Genauigkeitssteigerung von Höhenmodellen durch den Einsatz von Methoden der Datenfusion, beispielsweise bei der Verknüpfung von existierenden Höhenmodellen mit neuen Messdaten.

2. Schwerpunkt: Erzeugung von Punktwolken und deren Verarbeitung

Der Themenkomplex *Erzeugung von Punktwolken und deren Verarbeitung* wurde mit dem Leitvortrag von Heiko Hirschmüller gestartet. Das von ihm entwickelte Verfahren des Semi-Global Matching hat die automatische Bildauswertung auf eine völlig neue Grundlage gestellt, da dabei nicht mehr über kleine Bildflächen interpoliert werden muss, sondern jedes einzelne Pixel einen Objektpunkt im Raum liefern kann. Damit sind die erzeugten Punktwolken dichter als diejenigen, die von LIDAR-Messungen her bekannt sind. Darauf aufbauend erläuterte Norbert Haala Filterverfahren bei hoher Bildüberlappung (multiple Stereopaare, multiray photogrammetry) zur weiteren Genauigkeitssteigerung des erzeugten Höhenmodells. Tobias Heuchel stellte Weiterentwicklungen in Match-T DSM, dem Trimble-Softwarepaket zur Höhenmodellerzeugung, vor.

Mit LIDAR-Verfahren beschäftigten sich vier Beiträge. Juha Hyyppä begann mit einer Darstellung des State-of-the-Art beim Laserscanning basierend auf den Erfahrungen am Finish Geodetic Institute und verwies auf die nächste Gerätegeneration, z.B. hyperspektrale Laserscanner. Andreas Ullrich schlug eine Klassifikation von Full-Waveform Laserscannern vor, eines Instrumententyps, der unter anderem von Riegl in Horn (Österreich) gebaut wird. Lewis Graham schlug ein Verfahren zur Integration von Punktwolken unterschiedlicher Herkunft vor, z. B. von Flugzeugen und Fahrzeugen aufgenommenen. Ronald Roth erläuterte das Verfahren zur Verdichtung von Laserpunktwolken, das im Leica ALS70 verwendet wird.

3. Schwerpunkt: Schritte zur erweiterten Realität in 3D-Welten

Auf den dritten Themenkomplex *Schritte zur erweiterten Realität in 3D-Welten* wurden die Besucher mit dem Leitvortrag von Jan-Michael Frahm, einem Fachmann für Computer Vision, eingestimmt. Er stellte Crowd Sourcing in den Mittelpunkt und zeigte, dass es schon heute riesige Bildsammlungen frei zugänglich im Internet gibt, die mit geeigneten Tools verarbeitet wertvolle Produkte erzeugen lassen würden, beispielsweise zur Tourismusförderung, für den Denkmalschutz und für die innere Sicherheit, wenn die Konzepte ausgereift und in betriebsbereite Systeme umgesetzt wären. Lyn Wilson stellte eine virtuelle 3D-Rekonstruktion der Rosslyn Chapel in Schottland vor, und zwar mit Innen- und Außenansicht. Bart Beers präsentierte ein Aufnahmeverfahren für Panoramabilder aus einem bis zu 80 km/h schnell fahrenden Auto. Der Einsatz von UAVs für den Aufbau von 3D-Modellen war Thema des Beitrags von Christoph Strecha. Florian Siegert überzeugte mit seinem Verfahren zum Aufbau von hoch aufgelösten 3D Landschaftsmodellen und deren schneller Darstellung im Internet. Die Vortragsfolge schloss mit einer Untersuchung zum Einsatz von low-cost Geräten für die Erzeugung von sehr dichten Punktwolken, vorgetragen von Dieter Fritsch. Dabei wurden Smartphones, Amateurkameras, einfache GPS-Empfänger und ähnliche Systeme diskutiert.

Rahmenprogramm

Wie gewohnt bot die PhoWo ein großartiges Rahmenprogramm. Am Montag luden die Veranstalter zu einem Empfang im Foyer des großen Hörsaals ein. Am Dienstag waren die

Gruppenphoto 53. Photogrammetrische Woche 2011

PhoWo-Teilnehmer Gäste im Stuttgarter Rathaus und wurden von KARLHEINZ JÄGER, dem Leiter des Stadtmessungsamtes Stuttgart als Vertreter der Stadt, begrüßt. Den Höhepunkt bildete das festliche Dinner am Donnerstag. Es fand in gemütlicher Atmosphäre bei Dixiland und schwäbischem Wein in der Alten Kelter in Fellbach statt.

WOLFGANG KRESSE, Neubrandenburg

Persönliches

Hans-Karsten Meier zum Gedächtnis

Am 5. August 2011 verstarb unerwartet im 86. Lebensjahr Prof. Dr.-Ing. HANS-KARSTEN MEIER, Ehrenmitglied der Deutschen Gesellschaft für Photogrammetrie, Fernerkundung und Geoinformation und auch der britischen Remote Sensing and Photogrammetry Society. Nur zwei Tage bevor er nach einer gut verlaufenden zweiten Hüftoperation aus der Rehabilitation mit Optimismus nach Hause zurückkehren wollte, war er am frühen Morgen friedlich eingeschlafen. Ein engerer Familien- und Freundeskreis war eingeladen und am 12. August zum Itzelberger Friedhof seiner Heimatgemeinde Königsbronn gekommen, um „in liebevoller Verehrung“ von einem Ehemann, Vater, Großvater und ehemaligen Kollegen und Freund Abschied zu nehmen.

Der Verstorbene war den älteren Lesern der PFG mit seiner unverwechselbaren Art des Humors und der Diskussionsfreudigkeit sehr vertraut und den etwas jüngeren unter uns noch bekannt, da er auch nach seinem schrittweisen Rückzug aus dem Berufsleben Mitte der 1980er Jahre sein Engagement für unser

Berufsfeld fortsetzte. Seine Verdienste für die Photogrammetrie sind in dieser Zeitschrift mehrfach und ausführlich gewürdigt worden, so 1986, 1990, 1995, und 2000. Deshalb sollen hier nur die wichtigsten Meilensteine und Tätigkeiten seines Lebens wiederholt werden.

Am 10. Oktober 1925 geboren, wuchs H.-K. Meier in Cuxhaven auf und musste noch als Schüler in den Krieg ziehen, so dass er erst nach dem Abitur 1948/49 das Vermessungsstudium in Hannover aufnehmen konnte, zu einer Zeit, als die Studienbedingungen noch alles andere als wieder normal zu bezeichnen waren. Nach dem Diplom Ostern 1953 wurde er Assistent bei Richard Finsterwalder in München und promovierte bereits nach zwei Jahren über Lotabweichungen im Hochgebirge. Im Juli 1955 holte ihn Kurt Schwidefsky, damals Leiter der Bildmess-Abteilung, zu Carl Zeiss nach Oberkochen. Keine andere Persönlichkeit hat die Entwicklung von Luftbildmesskammern nach dem Krieg so sehr beeinflusst und vorangetrieben wie Meier. Die ständige Verbesserung von Bildgeometrie und Abbildungsqualität, auch im Hinblick auf größere Bildwinkel und Colorfilme, stand dabei im Vordergrund und schlug sich u. a. in seinen wissenschaftlichen Veröffentlichungen nieder. Die Entwicklung des Präzisionskomparators PSK und des Orthoprojektors Gigas-Zeiss wurde ebenfalls primär von ihm geprägt.

Als technischer Leiter der Abteilung für Geodäsie und Photogrammetrie ab November 1968 musste er seine geliebte wissenschaftliche und labormäßige Arbeit jüngeren Kollegen überlassen und sich auf die Führungsaufgaben konzentrieren. Es gelang ihm, die erforderlichen strategischen Entscheidungen der 1970er Jahre erfolgreich zu treffen: den Ausbau der elektronischen Tachymeter bei „Geo", den Einstieg in die analytischen Systeme bei „Bms" und die Komplettierung der Kleinreihenbildner für die Aufklärung. Ab Februar 1981 übernahm Hans-Karsten Meier, zusammen mit Karlheinz Vogel, die unternehmerische Gesamtverantwortung für den Geschäftsbereich Vermessung, also auch für Vertrieb und wirtschaftlichen Erfolg. Neben dieser Führungsaufgabe blieb H.-K. Meier als Wissenschaftlicher weiterhin der Fachwelt verbunden. Von 1969 bis 1987 leitete er zusammen mit Friedrich Ackermann die von Universität und Zeiss gemeinsam veranstaltete Photogrammetrische Woche. Seit 1972 mit einem Lehrauftrag betraut, wurde er 1978 an der Universität Stuttgart zum Honorarprofessor ernannt. Die Mitarbeit in Gremien von u. a. DIN/ISO, FIM, DLR, ESA, ITC und für die DGPF belegen seinen begehrten Sachverstand, der sich darüber hinaus in über 100 Veröffentlichungen niederschlug. Diese Anerkennung drückte sich auch in verschiedenen Auszeichnungen aus, u. a. der Albrecht-Meydenbauer-Medaille und den beiden eingangs erwähnten Ehrenmitgliedschaften.

Im April 1986 hatte er sich entschlossen, freiwillig sein berufliches Engagement schrittweise zurückzufahren, und mit dem 63. Geburtstag trat „Mei", wie er von den Kollegen genannt wurde, endgültig in den so genannten Ruhestand. Dennoch engagierte er sich weiterhin für die Normungsarbeit und erfüllte sich darüber hinaus einen lang gehegten Traum: nachdem er bisher in den Urlauben seiner Segelleidenschaft auf dem Wasser gefrönt hatte, erwarb er die Privatpilotenlizenz. Und es war ihm noch bis vor wenigen Jahren vergönnt, sein langjähriges Hobby mit einem eigenen Motorsegler nun auch auf die ihm vertraute dritte Dimension auszuweiten.

Alle die ihn kannten, schätzten seinen Humor, seine Diskussionsfreude, seinen gesunden Menschenverstand und seine treffenden Kommentare zum Zeitgeschehen. Wir trauern mit seiner Ehefrau und den Familien seiner zwei Söhne und werden uns immer angenehm und mit einem Schmunzeln an den Kollegen Hans-Karsten Meier erinnern.

Dierk Hobbie, Königsbronn

Hochschulnachrichten

Martin-Luther-Universität Halle-Wittenberg

Herr Dipl.-Geogr. Christian Götze promovierte am 16.12.2010 am Institut für Geowissenschaften (Fachgebiet Geofernerkundung und Kartographie) der Martin-Luther-Universität Halle-Wittenberg mit der Arbeit „Detektion von Schwermetallkontaminationen in den Elb- und Muldeauen mittels Parametrisierung des spektralen Verhaltens der Vegetation" zum Dr. rer. nat.

1. Gutachter: Prof. Dr. Cornelia Glässer, Martin-Luther-Universität Halle-Wittenberg.
2. Gutachter: Prof. Dr. Gunter Menz, Rheinische Friedrich-Wilhelms-Universität Bonn.

Kurzfassung: Die natürlichen Auenökosysteme unterliegen einer hohen Dynamik durch die Hochwasserereignisse. In intensiv genutzten Flusseinzugsgebieten werden diese Ökosysteme erheblich anthropogen beeinflusst. Zusätzlich zu vielfältigen Nährstoffeinträgen durch Siedlungen und Landwirtschaft unterliegen die Einzugsgebiete von Elbe und Mulde hohen Stoffeinträgen, die von Altindustrie und Altbergbau verursacht werden und hohe Schwermetallgehalte in den Auen verursachen. Die in den Böden akkumulierten Schwermetalle gelangen über die Wurzeln letztendlich in die Pflanze. Ziel der Arbeit ist es, mit Hilfe von spektrometrischen Labor- und Feldmessungen den Einfluss der ökotoxikologischen Effekte der Böden auf die Auenvegetation mittels der spektralen Eigenschaften abzuleiten.

Die Ergebnisse der vorliegenden Arbeit basieren auf einer dreijährigen Gefäßversuchsreihe zur Entwicklung einer neuen Methode zur Bestimmung von Schwermetallstress bei Auenpflanzen und der Trennung von Schwermetallstress von anderen Stressoren. In der Versuchsstation des Helmholtz-Zentrums für Umweltforschung (UFZ) Leipzig-Halle in Bad Lauchstädt wurden in einem standardisierten Gefäßversuch die spektralen Reflektionseigenschaften ausgewählter typischer Pflanzenarten auf drei unterschiedlich Schwermetall belasteten Böden innerhalb der phänologischen Phase der Auenvegetation untersucht. Ziel war es, in Abhängigkeit vom Kontaminationsgrad Schwermetallstress bzw. -schädigungen der Vegetation mittels spektrometrischer Messungen zu detektieren und zu parametrisieren. Dabei wurden durch standardisierte Bewässerung und Nährstoffzufuhr andere natürliche Einflussfaktoren ausgeschlossen, um die Zusammenhänge zwischen dem spektralen Verhalten und der Schwermetallkontamination spezifisch zu ermitteln. Mit verschiedenen Methoden wie Vegetationsindizes, Red-Edge Position und Continuum Removal wurden die gemessenen Spektraldaten der Vegetation normiert, um das Potenzial der Methoden zur Detektion von Schwermetallstress an den Auenpflanzen zu untersuchen. Die Ergebnisse der Arbeit zeigen, dass der Einfluss von Schwermetallen im Boden und deren Transfer in die Pflanze in bestimmten phänologischen Phasen charakteristische Veränderungen im Spektralsignal verursacht. Mit Hilfe eines entwickelten Algorithmus zur Parametrisierung der Spektralkurve zeigten sich signifikante Beziehungen zu den Schwermetallbelastungen. Die neu entwickelte Methode CR1725 zeigte hohe Korrelationen zum Schwermetallgehalt und gleichzeitig niedrige Korrelationen zu den untersuchten Pflanzenparametern wie Nährstoff- und Chlorophyllgehalt.

Die Übertragbarkeit der Methode auf hyperspektrale Fernerkundungsdaten des Sensors Hymap zur Ausweisung räumlich differenzierter Belastungsareale innerhalb der Aue schloss sich an. Im Ergebnis erfolgte eine Gefährdungsabschätzung für das Gebiet der Muldeaue anhand eines Schwellwertverfahrens, das sich als robustes Verfahren zur flächendeckenden Ausweisung belasteter bzw. kontaminierter Auenstandorte erwies.

Fachhochschule Mainz

Im Rahmen eines kooperativen Promotionsverfahrens mit der Universität Burgund legte

Herr Ashish Karmacharya M.Sc., wissenschaftlicher Mitarbeiter am Institut für Raumbezogene Informations- und Messtechnik (i3mainz) der FH Mainz, am 30.6.2011 in Dijon mit der Arbeit *"Introduction of a spatial layer in the Semantic Web framework: a proposition through the Web platform ArchaeoKM"* die Dissertationsprüfung zum PhD ab.

1. Gutachter: Prof. Dr. Franck Marzani, Laboratoire Electronique, Information et Image (Le2i), Université de Bourgogne.
2. Gutachter: Prof. Dr. Frank Boochs, Institut für Raumbezogene Informations- und Messtechnik (i3mainz), Fachhochschule Mainz.
3. Gutachter: Dr. Christophe Cruz, Laboratoire Electronique, Information et Image (Le2i), Université de Bourgogne.

Kurzfassung: Database systems are an important prerequisite for the advancement of spatial technology. In addition, there has been done a significant amount of research in the field of the geospatial ontology domain in order to achieve the semantic interoperability between different data sources. Although, data interoperability is one of the main objectives of Semantic Web technologies, the potentiality of the underlying knowledge tools and techniques have not been completely identified. With the growing influence of the Semantic Web technologies towards the application based on knowledge management and intelligent systems, the geospatial application benefits from this influence. This thesis emphasizes the use of knowledge to manage spatial data within spatial information systems through the Semantic Web framework.

This research activity is carried out with the backdrop of the case study of the industrial archaeology. It sets up an ideal environment for the application of knowledge to manage the huge and heterogeneous dataset. The use of knowledge to manage the diversity of information was well executed through the application prototype named ArchaeoKM (Managing Archaeological data through Archaeological Knowledge) which is based on the Semantic Web. The ArchaeoKM framework follows the 4Ks processing steps: Knowledge Acquisition, Knowledge Management, Knowledge Visualization and Knowledge Analysis. The same processing principle of 4Ks was implemented during the spatial knowledge processing. A top level ontology was developed in order to serve as the background representation of the case study in order to adjust the spatial components. Keeping the usual procedure, the spatial knowledge processing begins with acquiring spatial signatures of the identified objects. The spatial signatures are stored within the spatial database system with proper mapping to the objects in the knowledge base. The spatial knowledge of these objects is managed through executing the spatial functions at the database level and enriching the knowledge base with the results. This spatially enriched knowledge base is used again to analyze the spatial knowledge. This research thesis benefits from the Semantic Web Rule Language in order to infer knowledge. In addition, the spatial built-ins proposed during the course add up spatial dimension to the SWRL for spatial inferences. Similarly, a spatial extension of the query language SPARQL is proposed in order to query spatial knowledge from the knowledge base.

Actually, this research thesis provides the initial steps in integrating spatial components within the Semantic Web framework. This integration process is important for both technologies. Regarding the Semantic Web, the integration of non-typical semantic information within this framework opens up doors to other data pattern making the transformation of technologies easier. Likewise, geospatial technologies and GIS systems benefits through the inclusion of knowledge in the analysis process making the analysis much closer and efficient to human interpretation.

Veranstaltungskalender

2011

7.–8. Dezember: **Wo?-Kongress 2011 – Geo-Mobility** in **Gelsenkirchen**. http://www.ikt.nrw.de/veranstaltung/

2012

23.–25. Januar: **GIS Ostrava** 2012 – Surface models for geosciences in **Ostrava**. http://gis.vsb.cz/gisostrava/

23.–26. Januar: **Defence Geospatial Intelligence** (DGI) 2012 in **London**. www.dgieurope.com

25.–26. Januar: **GIS & GDI in der Wasserwirtschaft** in **Kassel**. www.dwa.de

1.–2. Februar: 11. **Oldenburger 3D-Tage**. www.jade-hs.de/fachbereiche/bauwesen-und-geoinformation/abteilung-geoinformation/oldenburger-3d-tage/

14.–16. März: 32. Wissenschaftlich-Technische **Jahrestagung der DGPF** in **Potsdam**. http://www.dgpf.de/neu/jahrestagung/informationen.htm

28.–30. März: **GEOINFORMATIK 2012** – Mobilität und Umwelt in **Braunschweig**. http://www.geoinformatik2012.de

17.–18. April: 6th **International Satellite Navigation Forum** – NAVITCH 2012 in **Moskau**. http://eng.glonass-forum.ru

23.–27. April: **Geospatial World Forum** 2012 in **Amsterdam**. www.geospatialworldforum.org

7.–9. Mai: **GEOBIA 2012**: 4th International Conference on Geographic Object Based Image Analysis 2012 in **Rio de Janeiro**. www.inpe.br/geobia2012

8.–10. Mai: 11. **Österreichischer Geodätentag** in **Velden** am Wörthersee. www.ogt2012.at

14.–15. Juni: **8. GIS-Ausbildungstagung** in **Potsdam**. http://gis.gfz-potsdam.de/index.php?id=238

24. August – 3. September: **XXII ISPRS Congress 2012** in **Melbourne**, Australien. www.isprs2012-melbourne.org/

9.–11. Oktober: **INTERGEO 2012** und **60. Deutscher Kartographentag** und **3. Europäischer Kongress der CLGE** (Comité de Liaison des Géomètres Européens) **in Hannover**. www.intergeo.de

2013

30. April – 2. Mai: **8th International Symposium on Mobile Mapping Technology** 2013 in **Tainan**. http://conf.ncku.edu.tw/mmt2013/

25.–30. August: **26th International Cartographic Conference (ICC)** in **Dresden**. http://www.icc2013.org/

2.–6. September: **XXIVth CIPA Heritage Documentation Symposium** in **Strasbourg**. http://cipa.icomos.org

Neuerscheinungen

Christina Andrae, Christian Graul, Martin Over & Alexander Zipf, 2011: Web Portrayal Services. OpenGIS Web Map Service, Styled Layer Descriptor, Symbology Encoding und ISO 19117 Portrayal vorgestellt und erläutert. 381 Seiten, ISBN 978-3-87907-502-7, Wichmann, VDE Verlag GmbH, Berlin-Offenbach.

Vorstand der DGPF

Präsidentin

Prof. Dr. Cornelia Glässer
Martin-Luther-Universität Halle-Wittenberg, Institut für Geographie, Von-Seckendorff-Platz 4, 06120 Halle, Tel.: 0345 / 55-260 20, Fax: 0345 / 55-271 68, e-mail: praesident@dgpf.de

Vizepräsident

Prof. Dr. rer. nat. Thomas H. Kolbe
Technische Universität Berlin, Institut für Geodäsie und Geoinformationstechnik, Fachgebiet Methodik der Geoinformationstechnik, Straße des 17. Juni 135, Sekretariat H 12, 10623 Berlin, Tel.: 030 / 314-23274 oder 23205, Fax: 030 / 314-21973, e-mail: thomas.kolbe@tu-berlin.de

Sekretär

Dr.-Ing. Manfred Wiggenhagen
Leibniz Universität Hannover, Institut für Photogrammetrie und GeoInformation, Nienburger Straße 1, 30167 Hannover, Tel.: 0511 / 762 3304, Fax: 0511 / 762 2483, e-mail: sekretaer@dgpf.de

Schatzmeister

Dr.-Ing. Herbert Krauss
Rodenkirchener Straße 47, 50997 Köln, Tel.: 02233 / 22514, Fax: 032 222 / 427 178, e-mail: mh.krauss@t-online.de

Hauptschriftleiter

Prof. Dr.-Ing. Wolfgang Kresse
Hochschule Neubrandenburg, Fachbereich Landschaftsarchitektur, Geoinformatik, Geodäsie und Bauingenieurwesen, Brodaer Straße 2, 17033 Neubrandenburg, Tel.: 0395 / 5693-4106, Fax: 0395 / 5693-4999, e-mail: kresse@hs-nb.de

Beirat

Dr. rer. nat. Klaus-Ulrich Komp
EFTAS Fernerkundung, Technologietransfer GmbH, Oststraße 2-18, 48145 Münster, Tel.: 0251 / 1330-70, Fax: 0251 / 1330-733, e-mail: klaus.komp@eftas.com

Beirat

Prof. Dr.-Ing. Hans-Gerd Maas, Technische Universität Dresden, Professur für Photogrammetrie, Helmholtzstraße 10, 01062 Dresden, Tel.: 0351 / 463-32859, Fax: 0351 / 463-37266, e-mail: hans-gerd.maas@tu-dresden.de

Beirat

Prof. Dr.-Ing. Monika Sester
Leibniz Universität Hannover, Institut für Kartographie und Geoinformatik (ikg), Appelstraße 9a, 30167 Hannover, Tel.: 0511 / 762-3588, Fax: 0511 / 762-2780, e-mail: monika.sester@ikg.uni-hannover.de

Beirat

Dr.-Ing. Eckhardt Seyfert
Landesvermessung und Geobasisinformation Brandenburg, Heinrich-Mann-Allee 103, 14473 Potsdam, Tel.: 0331 / 8844-506, Fax: 0331 / 8844-126, e-mail: eckhardt.seyfert@geobasis-bb.de

Ehrenmitglieder der DGPF

Prof. Friedrich Ackermann, Stuttgart
Prof. Heinz Draheim, Karlsbad
Prof. Gerd Hildebrandt, Freiburg
Dr.-Ing. Otto Hofmann, Brunnthal
Prof. Gottfried Konecny, Hannover
Direktor Fritz Erich Krause, Münster
Dipl.-Ing. Horst Schöler, Stadtsteinach
Prof. Klaus Szangolies, Jena

Arbeitskreise der DGPF

Aus- und Weiterbildung

Dr.-Ing. Görres Grenzdörffer
Universität Rostock, Agrar- und Umweltwissenschaftliche Fakultät, Bereich: Professur Geodäsie und Geoinformatik, Justus-v.-Liebig-Weg 6, 18051 Rostock, Tel.: 0381 / 498-3206, Fax: 0381 / 498-3202, e-mail: goerres.grenzdoerffer@uni-rostock.de

Bildanalyse und Bildverstehen

Dr.-Ing. Uwe Weidner
Karlsruher Institut für Technologie, Institut für Photogrammetrie und Fernerkundung, Englerstraße 7, 76131 Karlsruhe, Tel.: 0721 / 608-43945, Fax: 0721 / 608-48450, e-mail: uwe.weidner@kit.edu

Geoinformatik

Prof. Dr. rer. nat. habil. Jürgen Döllner
Hasso-Plattner-Institut für Softwaresystemtechnik, Computer Graphics Systems, Prof.-Dr.-Helmert-Straße 2-3, 14482 Potsdam, Tel.: 0331 / 5509-170, Fax: 0331 / 5509-172, e-mail: doellner@hpi.uni-potsdam.de

Hyperspektrale Fernerkundung

Dr. Andràs Jung
SphereOptics GmbH, Remote Sensing Technology, Bergstraße 36, 88690 Uhldingen, Tel.: 07556 / 9299666, Fax: 07556 / 50108, e-mail: ajung@dgpf.de

Radarfernerkundung und Flugzeuglaserscanning

Prof. Dr.-Ing. Uwe Sörgel
Leibniz Universität Hannover, Institut für Photogrammetrie und GeoInformation, Nienburger Straße 1, 30167 Hannover, Tel.: 0511 / 762-2981, Fax: 0511 / 762-2483, e-mail: soergel@ipi.uni-hannover.de, www.ipi.uni-hannover.de/us.html

Auswertung von Fernerkundungsdaten

Dr. habil. Horst Weichelt
RapidEye AG, Molkenmarkt 30, 14776 Brandenburg a.d. Havel, Tel.: 03381 / 8904-311, Fax: 03381 / 8904-101, e-mail: dgpf-akfe@h-weichelt.de

Standardisierung und Qualitätssicherung

Dipl.-Ing. Sven Baltrusch
Landesamt für Innere Verwaltung Mecklenburg-Vorpommern, Amt für Geoinformation, Vermessung und Katasterwesen, Lübecker Straße 289, 19059 Schwerin, Tel.: 0385 / 588-56322, e-mail: sven.baltrusch@laiv-mv.de

Optische 3D-Messtechnik

Prof. Dipl.-Ing. Thomas Kersten
HafenCity Universität Hamburg, Labor für Photogrammetrie & Laserscanning, Hebebrandstraße 1, 22297 Hamburg, Tel.: 040 / 428-27 5343, Fax: 040 / 428-27 5359, e-mail: thomas.kersten@hcu-hamburg.de, www.hcu-hamburg.de/geomatik/kersten

Dr.-Ing. Danilo Schneider
Technische Universität Dresden, Institut für Photogrammetrie & Fernerkundung, Helmholtzstraße 10, 01062 Dresden, Tel.: 0351 / 463-33144, Fax: 0351 / 463-37266, e-mail: danilo.schneider@tu-dresden.de, www.danilo-schneider.de

Fernerkundung in der Geologie

Dr. Hans-Ulrich Wetzel
GeoForschungsZentrum Potsdam (GFZ), PB 1.5, Telegrafenberg, 14473 Potsdam, Tel.: 0331 / 288-1194, Fax: 0331 / 288-1192, e-mail: wetz@gfz-potsdam.de

Dr. Friedrich Kühn
Bundesanstalt für Geowissenschaften und Rohstoffe, Stilleweg 2 ,30655 Hannover, Tel.: 0511 / 643-3007, Fax: 0511 / 643-3664, e-mail: friedrich.kuehn@bgr.de

Sensoren und Plattformen

Prof. Dr. Norbert Haala
Universität Stuttgart, Institut für Photogrammetrie, Geschwister-Scholl-Straße 24d, 70174 Stuttgart, Tel.: 0711 / 685-83383, Fax: 0711 / 685-83297, email: norbert.haala@ifp.uni-stuttgart.de

3D-Stadtmodelle

Dipl.-Ing. Bettina Petzold
Landesbetrieb Forst Baden-Württemberg, Geschäftsbereich FGeo, Bertoldstraße 43, 79098 Freiburg, Tel.: 0761 / 208-1339, e-mail: bettina.petzold@rpf.bwl.de, www.forstbw.de

Dipl.-Ing. Ekkehard Matthias
Freie und Hansestadt Hamburg, Landesbetrieb Geoinformation und Vermessung, Sachsenkamp 4, 20097 Hamburg, Tel.: 040 / 428-26-5750, Fax: 040 / 428-26-5966, e-mail: ekkehard.matthias@gv.hamburg.de, www.geo-info.hamburg.de

Berichterstatter für ISPRS und CIPA

Kommission I – Image Data Acquisition – Sensors and Platforms

Dr.-Ing. Franz Kurz
D-82230 Oberpfaffenhofen
e-mail: franz.kurz@dlr.de

Kommission II – Theory and Concepts of Spatial Information Science

Prof. Dr.-Ing. Monika Sester
D-30167 Hannover
e-mail: monika.sester@ikg.uni-hannover.de

Kommission III – Photogrammetric Computer Vision and Image Analysis

Prof. Dr.-Ing. Stefan Hinz
D-76128 Karlsruhe
e-mail: stefan.hinz@kit.edu

Kommission IV – Geodatabases and Digital Mapping

Dr.-Ing. Volker Walter
D-70174 Stuttgart
e-mail: volker.walter@ifp.uni-stuttgart.de

Kommission V – Close-Range Sensing: Analysis and Applications

Dr.-Ing. Danilo Schneider
D-01062 Dresden
e-mail: danilo.schneider@tu-dresden.de

Kommission VI – Education and Outreach

Dipl.-Inf. Gerhard König
D-10623 Berlin
e-mail: gerhard.koenig@tu-berlin.de

Kommission VII – Thematic Processing, Modeling and Analysis of Remotely Sensed Data

Dr.-Ing. Uwe Weidner
D-76128 Karlsruhe
e-mail: uwe.weidner@kit.edu

Kommission VIII – Remote Sensing Applications and Policies

Prof. Dr. Irmgard Niemeyer
D-09599 Freiberg
e-mail: irmgard.niemeyer@freiberg.de

CIPA – Internationales Komitee für Architekturphotogrammetrie

Prof. Dr.-Ing. Michael Scherer
D-44780 Bochum, e-mail: michael.scherer@rub.de

Gutachter der PFG im Jahr 2011

Der Wert einer wissenschaftlichen Zeitschrift hängt wesentlich von der Qualität der Gutachten ab. Die Schriftleiter der PFG möchten sich hiermit bei den Gutachtern des Jahres 2011 herzlich bedanken, die neben dem Editorial Board ihre Arbeitszeit der Begutachtung der PFG-Artikel gewidmet haben:

- Clemens Atzberger, Wien, Österreich
- Sven Baltrusch, Schwerin
- Emmanuel Baltsavias, Zürich, Schweiz
- Ellen Banzhaf, Leipzig
- Lutz Bischoff, Greven
- Christian Briese, Wien, Österreich
- Heinz Brüggemann, Remagen
- Tilman Bucher, Berlin
- Matthias Butenuth, München
- Christopher Conrad, Würzburg
- Michael Cramer, Stuttgart
- Martin Drauschke, Neubiberg
- Henri Eisenbeiss, Zürich, Schweiz
- Roland Götze, Bonn
- Gerhard Gröger, Bonn
- Norbert Haala, Stuttgart
- Volker Hochschild, Tübingen
- Michael Hovenbitzer, Frankfurt/Main
- Viktor Kaufmann, Graz, Österreich
- Fredie Kern, Mainz
- Birgit Kleinschmit, Berlin
- Tobia Lakes, Berlin
- Ioannis Manakos, Chania, Griechenland
- Ulrich Michel, Heidelberg
- Matthias Möller, Berlin
- Jeremy Morley, Nottingham, Großbritannien
- Stephan Nebiker, Muttenz, Schweiz
- Maik Netzband, Bochum
- Klaus Neumann, Aalen
- Konstantinos Nikolakopoulos, Acharnae, Griechenland
- Norbert Pfeifer, Wien, Österreich
- Heinz-Jürgen Przybilla, Bochum
- Camillo Ressl, Wien, Österreich
- Ribana Roscher, Bonn
- Carl-Thomas Schneider, Braunschweig
- Danilo Schneider, Dresden
- Hannes Taubenböck, Oberpfaffenhofen
- Thomas Vögtle, Karlsruhe
- Björn Waske, Bonn
- Uwe Weidner, Karlsruhe
- Manfred Wiggenhagen, Hannover
- Bernhard Wrobel, Bonn
- Chunsun Zhang, Melbourne, Australien

Daneben geht ein besonderer Dank an Ulrich Michel und Manfred Ehlers für die Organisation der Begutachtung für das PFG-Heft 4/2011.

Zum Titelbild

Hochgenaue True-Orthobilder und Oberflächenmodelle einer modularen Luftbildkamera (Modular Airborne Camera System – MACS) am Beispiel Berlin-Adlershof

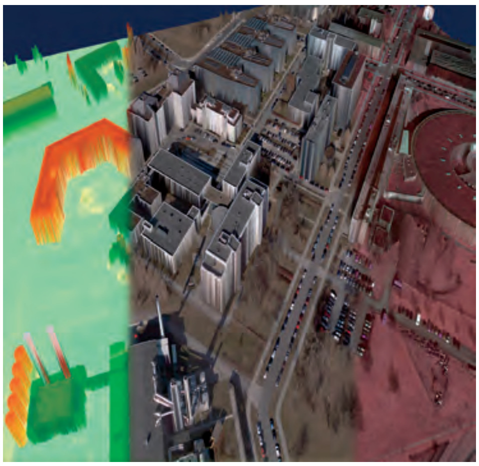

Das Titelbild zeigt den Standort des Deutschen Zentrums für Luft- und Raumfahrt e.V. (DLR) am Wissenschafts- und Technologiestandort Berlin-Adlershof. Es handelt sich um eine 2,5D Ansicht ohne Seitenfassaden. Dafür wurde ein Digitales Oberflächenmodell mit drei verschiedenen Bildinformationen texturiert: Einer Farbkodierung der Höhenstufen, True-Orthobildern in Echtfarben (RGB) und und einem geringer aufgelösten Farbinfrarotbild (CIR).

Aufgenommen wurden die Bilddaten mit einem modularen Luftbildkamerasystem (MACS), welches in der Einrichtung Optische Informationssysteme des DLR auf Basis von Industriekameramodulen und Industrieoptiken entwickelt und in verschiedenen Ausbaustufen seit 2009 zur Erhebung experimenteller Luftbilddaten verwendet wird.

Zielstellung der MACS-Entwicklung war die einfache und kostengünstige Erzeugung von Bilddatensätzen mit Bodenauflösungen im Bereich weniger Zentimeter, die sich zu hochgenauen photogrammetrischen Produkten bis hin zu 3D-Punktwolken verarbeiten lassen. Mit den Daten des Kamerasystems sollen die dafür notwendigen photogrammetrischen Verfahren demonstriert und weiterentwickelt werden. Besonderer Wert wurde auf eine hohe Geschwindigkeit der Datenverarbeitung in den Kameramodulen gelegt. Die damit erzielbaren hohen Überlappungen und geringen Bewegungsunschärfen sind Voraussetzung für exakte und dichte 3D-Modellierungen auch aus schnellfliegenden Trägerflugzeugen sowie aus geringen Flughöhen.

Die Daten wurden im März 2011 auf einer stabilisierten Plattform aus 700 m Flughöhe bei einer Fluggeschwindigkeit von 200 km/h erhoben. Es wurden 7 Flugstreifen geflogen und Bilddaten mit einer GSD von 13 cm (CIR-Kamera-Modul) und 9 cm (RGB-Kamera-Module) aufgenommen. Die Überlappung der Bilder betrug dabei ungefähr 98% längs und 78% quer zur Flugrichtung.

Die gesamte Prozessierung (Postprozessierung der Navigationsdaten, Aerotriangulation, Semi-Global Matching und True-Orthobilderstellung) erfolgte am DLR. Durch die schnelle Bildfolge werden sichttote Räume vermieden. Insbesondere in urbanen Räumen stehen damit auch für enge Sichtgeometrien genügend Bilder zur Bildzuordnung zur Verfügung.

Die MACS kann aufgrund ihrer kompakten Bauweise und ihres geringen Gewichts in kleinen Flugzeugen und in Außenbehältern eingebaut werden. Auch eine Konfiguration als schrägblickendes System wurde schon erprobt und erfolgreich ausgewertet.

Dipl.-Geol. Frank Lehmann
Abteilungsleiter Sensorkonzepte und Anwendungen, Einrichtung Optische Informationssysteme am Institut für Robotik und Mechatronik, Deutsches Zentrum für Luft- und Raumfahrt, Rutherfordstr. 2, D-12489 Berlin, Tel.: +49-30-67055-425, Fax: +49-30-67055-385, e-mail: frank.lehmann@dlr.de, www.dlr.de/os/

Korporative Mitglieder

Firmen
AEROWEST GmbH
AICON 3D Systems GmbH
Alpha Luftbild GmbH
aphos Leipzig AG
Becker GeoInfo GmbH
Bernhard Harzer Verlag GmbH
Blom Deutschland GmbH
Brockmann Consult
bsf swissphoto
Büro Immekus
CGI Systems GmbH
con terra GmbH
DELPHI IMM GmbH
Deutsches Bergbau-Museum
EFTAS Fernerkundung Technologietransfer GmbH
ESG Elektroniksystem- und Logistik-GmbH
ESRI Geoinformatik GmbH
EUROPEAN SPACE IMAGING
Eurosense GmbH
fokus GmbH
g.on experience gmbh
GAF GmbH
GeoCad GmbH
GeoCart Herten GmbH
GeoContent GmbH
Geoinform. & Photogr. Engin. Dr. Kruck & Co. GbR
geoplana Ingenieurgesellschaft mbH
GEOSYSTEMS GmbH
GGS - Büro für Geotechnik, Geoinformatik, Service
Hansa Luftbild AG
IGI - Ingenieur-Gesellschaft für Interfaces mbH
ILV Ing.-büro für Luftbildausw. und Vermessung
Imetric 3D GmbH
Infoterra GmbH
INVERS - Industrievermessung & Systeme
ITT Visual Information Solutions Germany
J. Linsinger ZT-GmbH
Jena-Optronik GmbH
KAZ Bildmess GmbH
Leica Geosystems GmbH
Luftbilddatenbank-Würzburg
Messbildstelle GmbH
Microsoft Photogrammetry
MILAN Geoservice GmbH
PHOENICS GmbH
PMS - Photo Mess Systeme AG
RIEGL Laser Measurement Systems GmbH
RWE Power AG, Geobasisdaten/Photogrammetrie
technet GmbH
TerraVista Umweltdaten GmbH
TRIGIS Vermessung + Geoinformatik GmbH
Trimble Germany GmbH
trimetric 3D Service GmbH
Wichmann, VDE Verlag GmbH
Z/I Imaging Ltd.

Behörden
Amt für Geoinformationswesen der Bundeswehr
Bayerische Landesanstalt für Wald und Forstwirtschaft
Bundesamt für Kartographie und Geodäsie
Bundesmin. für Ernäh., Landw. u. Verbraucherschutz
DB Netz AG
Hess. LA für Bodenmanagement und Geoinformation
Innenministerium NRW, Gruppe Vermessungswesen
Inst. für Umwelt- und Zukunftsforschung
LA für Geoinformation u. Landentw., Baden-Württem.
LA für Vermessung und Geoinformation, Bayern
LB Geoinformation und Vermessung, Hamburg
LB f. Küstenschutz, Nationalpark u. Meeresschutz, SH
Landesvermessung und Geobasisinformation Nieders.
Märkischer Kreis, Vermessungs- und Katasteramt
Regierungspräs. Tübingen, Abt. 8 Forstdirektion
Regionalverband Ruhr
Staatsbetrieb Sachsenforst Pirna
Stadt Bocholt, Fachbereich 31
Stadt Düsseldorf, Vermessungs- und Katasteramt

Stadt Köln, Amt für Liegensch., Verm. und Kataster
Stadt Wuppertal, Verm., Katasteramt und Geodaten
Thüringer LA für Vermessung und Geoinformation

Hochschulen
BTU Cottbus, Lehrstuhl für Vermessungskunde
FH Frankfurt a.M., FB 1, Studiengang Geoinformation
FH Mainz, Inst. f. Raumbez. Inform.- und Messtechn.
FH Oldenburg, Inst. für Angew. Photogr. und Geoinf.
HCU HafenCity Universität Hamburg, Geomatik
HfT Stuttgart, Vermessung und Geoinformatik
HS Bochum, FB Vermessung und Geoinformatik
HS Karlsruhe, FB Geoinformationswesen
HTW Dresden, FB Vermessungswesen/Kartographie
Karlsruher Institut für Technologie, KIT, Inst. für Photogrammetrie und Fernerkundung
MLU Halle, FG Geofernerkundung
Ruhr-Uni Bochum, Geographisches Institut
RWTH Aachen, Geodätisches Institut
TU Bergak. Freiberg, Inst. f. Markscheid. u. Geodäsie
TU Berlin, Computer Vision & Remote Sensing
TU Berlin, Inst. für Geodäsie und Geoinformationstechnik
TU Braunschweig, Inst. für Geodäsie und Photogr.
TU Clausthal, Inst. für Geotechnik und Markscheidew.
TU Darmstadt, Inst. für Photogrammetrie und Kartogr.
TU Dresden, Inst. für Photogrammetrie und Fernerk.
TU München, FG Photogrammetrie und Fernerk.
TU Wien, Inst. für Photogrammetrie und Fernerk.
Uni Bonn, Inst. für Photogrammetrie
Uni Göttingen, Inst. für Waldinv. und Waldwachstum
LUH Hannover, Inst. für Kartogr. und Geoinformatik
LUH Hannover, Inst. für Photogrammetrie und GeoInf.
Uni Heidelberg, IWR Interdis. Zentr. f. Wiss. Rechnen
Uni Kassel, FB Ökologische Agrarwissenschaften
Uni Kiel, Geographisches Institut
Uni Stuttgart, Inst. für Photogrammetrie
Uni Würzburg, Geographisches Institut
Uni zu Köln, Geographisches Institut

PFG – Jahrgang 2011, Heft 1 – 6
Inhaltsverzeichnis Jahrgang 2011

Originalbeiträge, alphabetisch nach Autoren

Aus Wissenschaft und Technik

Berichte und Mitteilungen

Berichte von Veranstaltungen

Kurzfassungen der ausgezeichneten Arbeiten des Karl Kraus-Nachwuchsförderpreises 2011

Berichte der Arbeitskreise der DGPF

Mitteilungen der DGPF

Persönliches

TECHNISCHE UNIVERSITÄT DARMSTADT

Am Fachbereich Bauingenieurwesen und Geodäsie der Technischen Universität Darmstadt ist zum Sommersemester 2012 eine

Universitätsprofessur (W3) für Fernerkundung und Bildanalyse/Remote Sensing and Image Analysis

(Kenn-Nr.: 418)

zu besetzen.

Der/die Inhaber/in dieser Stelle soll insbesondere bei der Ausbildung von Bau- und Umweltingenieuren, Geodäten und Geowissenschaftlern mitwirken. Die Bewerberin/der Bewerber ist durch hervorragende Forschungsleistung auf mindestens einem der Teilgebiete von Fernerkundung und Bildanalyse ausgewiesen.

Schwerpunkt sollte die Forschung im Bereich von satellitengestützten Methoden (z. B. SAR, INSAR), hyperspektralen Bilddaten und die Aspekte der Datenfusion mit anderen Raum- und Geodaten sein. Nachgewiesene ingenieurwissenschaftliche Expertise in der Kombination und Integration dieser Teilgebiete ist erwünscht.

Die Stelleninhaberin/der Stelleninhaber wird sich an den Lehraufgaben der Bachelor- und Masterstudiengänge des Fachbereichs Bauingenieurwesen und Geodäsie sowie fachbereichsübergreifender Studiengänge beteiligen.

Zudem wird von der zukünftigen Stelleninhaberin/dem zukünftigen Stelleninhaber die Fähigkeit und Bereitschaft zur interdisziplinären Zusammenarbeit und die Mitarbeit in der universitären Selbstverwaltung erwartet.

Neben einer hervorragenden Befähigung zu eigenständiger wissenschaftlicher Arbeit, nachgewiesen durch eine qualifizierte Promotion, Habilitation oder habilitationsäquivalente Leistungen, wird eine entsprechende pädagogische didaktische Eignung vorausgesetzt. Wünschenswert sind Erfahrungen in der Einwerbung von Drittmitteln und eine internationale Vernetzung.

Die Einstellung erfolgt im außertariflichen Angestelltenverhältnis mit einer qualifikationsabhängigen Vergütung in Anlehnung an die W-Besoldung. Diese wird zwischen Bewerber/in und Hochschulleitung verhandelt. Professorinnen und Professoren, die bereits in einem Beamtenverhältnis stehen, können in einem solchen weiterbeschäftigt werden. Es gelten ferner die Einstellungsvoraussetzungen der §§ 61 und 62 Hessisches Hochschulgesetz.

Die Technische Universität Darmstadt strebt eine Erhöhung des Anteils der Frauen am Personal an und fordert deshalb besonders Frauen auf, sich zu bewerben. Schwerbehinderte werden bei gleicher Eignung bevorzugt.

Bewerbungen sind mit den üblichen Unterlagen, insbesondere Lebenslauf, Schriftenverzeichnis, Übersicht über die bisherige Lehrtätigkeit (inklusive Lehrevaluationen) und Darstellung wissenschaftlicher Aktivitäten unter Angabe der u. g. Kenn-Nummer zu senden an den Dekan des Fachbereichs Bauingenieurwesen und Geodäsie, Technische Universität Darmstadt, Petersenstraße 13, 64287 Darmstadt.

Bewerbungsfrist: 15.01.2012